MULTIPLEXING OPTOGENETIC SYSTEMS IN YEAST FOR THE DYNAMIC CONTROL OF BIOLOGICAL BEHAVIOR

by

Zachary P Harmer

A dissertation submitted in partial fulfillment of the requirements for the degree of

Doctor of Philosophy

(Cellular and Molecular Biology)

at the

UNIVERSITY OF WISCONSIN-MADISON

2023

Date of final oral examination: 12/05/2023

The dissertation is approved by the following members of the Final Examination Committee:

Megan N. McClean, Associate Professor, Biomedical Engineering

Victor M. Zavala, Professor, Chemical and Biological Engineering

Ophelia Venturelli, Associate Professor, Biochemistry

Lindsay Kalan, Assistant Professor, Medical Microbiology & Immunology

Nancy Keller, Professor, Medical Microbiology & Immunology

© Copyright by Zachary P Harmer 2023

ALL RIGHTS RESERVED

DEDICATION

For Lily, Jonas, Mae, and Nathan. May you never cease to bring joy into this world.

ACKNOWLEDGMENTS

I'm very grateful for the help and support of fellow McClean lab members. In particular, Neydis Moreno and Kevin Stindt provided feedback on many manuscripts and Stephanie Geller taught me how to use the yeast modular cloning toolkit. Althys Cao has been great to help with molecular cloning and performing experiments. I appreciate my committee taking the time to attend my committee meetings and for providing me with valuable feedback on the direction of my project through its twists and turns. I'm grateful Victor Zavala was willing to join my committee (after another committee member had to leave due to family circumstances) and collaborate on modeling optogenetic systems and that David Cole was willing to help with Python programming. Eric Young and Vincent Noireaux were stellar instructors at the Cold Springs Harbor Laboratory Synthetic Biology course and taught me many things about cell-free systems and DNA assembly. I'm grateful to David Schwartz and Louise Pape for leading the Genomic Sciences Training Program and for their enthusiasm about genomics technologies. Amit Nimunkar and Claire Mitchell were tremendously helpful in adapting our illumination devices to shake. I appreciate Hanns-Martin Schmidt, Thomas Hohener, and Eric Young for seeing value in my research and wanting to collaborate. Megan McClean has been a phenomenal advisor and I appreciate all of the help and guidance she has been willing to give, as well as for providing funding for my research, helping to patent it, and allowing me to travel to conferences.

ABSTRACT

Optogenetic systems use genetically encoded light-sensitive proteins to control cellular behavior. Light is an ideal inducer for studying how biological networks are connected and function because it can be dynamically and precisely controlled in both space and time. A wide array of optogenetic tools have been developed for transcriptional programming and genetic engineering. Many of the optogenetic systems commonly used in fungal or mammalian cells respond to similar light wavelengths, limiting the number of optogenetic systems that can be used simultaneously. However, differences in sensitivity and reversion time between the underlying light-sensitive proteins can be leveraged to multiplex optogenetic systems responsive to the same wavelength of light. I developed Lustro, a high-throughput method for screening how optogenetic systems respond to different light induction programs using the model organism Saccharomyces cerevisiae. I used Lustro to compare the activation of several different blue light-sensitive optogenetic systems and found conditions that preferentially activate one optogenetic system over the other and vice versa. Because this multiplexed light-control system independently regulates the expression of multiple genes in a spatially and temporally precise manner, it can be used for high-throughput optimization of multiple nodes in bioproduction pathways. More broadly, it can be applied to any situation where dynamically controlling several different biological outcomes with a limited number of inducers is desired.

TABLE OF CONTENTS

| DEDICATION | 1 |
|--|-----|
| ACKNOWLEDGMENTS | ii |
| ABSTRACT | iii |
| TABLE OF CONTENTS | iv |
| LIST OF ABBREVIATIONS | X |
| CHAPTER ONE: OPTOGENETIC SYSTEMS FOR DYNAMIC MULTIPLEXED OF BIOLOGICAL ACTIVITY | |
| Abstract: | 1 |
| Introduction: | 2 |
| Control of gene expression | 3 |
| Optogenetic control is limited by wavelength: | 6 |
| Multiplexing using dynamic light patterns | 7 |
| Outstanding challenges for multiplexing optogenetic systems | 10 |
| Acknowledgments | 11 |
| Author Contributions | 11 |
| Conflict of Interest | 11 |
| References | 12 |
| CHAPTER TWO: LUSTRO: HIGH-THROUGHPUT OPTOGENETIC EXPERIM ENABLED BY AUTOMATION AND A YEAST OPTOGENETIC TOOLKIT | |
| Abstract | 16 |
| Introduction | 17 |
| Results and Discussion | 18 |

| Integration of laboratory automation and light stimulation for high-through optogenetics | - |
|---|----|
| Combining optoPlate programming with automation allows for high-resolutime-course experiments | |
| A yeast optogenetic toolkit (yOTK) combined with Lustro allows for rapid prototy and testing of optogenetic systems | |
| Combining the yOTK and Lustro to generate an optimized Magnet-based s | |
| Conclusion | 31 |
| Materials and Methods | 32 |
| Strains, media, and culture conditions | 32 |
| optoPlate configuration and calibration | 33 |
| Automated characterization of optogenetic systems on the Tecan Fluent Automation Workstation and Spark plate reader | 34 |
| Data analysis | 35 |
| Materials Availability | 35 |
| Supporting Information | 35 |
| Acknowledgments | 35 |
| Author Contributions | 36 |
| Conflict of Interest | 36 |
| References | 36 |
| PTER THREE: THE YEAST OPTOGENETIC TOOLKIT (yOTK) FOR TOTEMPORAL CONTROL OF GENE EXPRESSION IN BUDDING YEAST | 41 |
| Abstract | 41 |
| Introduction | 42 |
| Materials | 43 |

| General cloning | 43 |
|---|----|
| Generation of new parts | 44 |
| Golden Gate assembly | 44 |
| Transformation and screening of yeast | 44 |
| Optogenetic screening of yeast | 46 |
| Methods | 46 |
| Selection of light-sensitive proteins | 46 |
| Selection of standard parts and vectors | 47 |
| Assembly and integration of multigene cassettes | 48 |
| Generation of parts | 49 |
| Cloning of cassette plasmids | 50 |
| Multigene assembly | 52 |
| Yeast transformation | 53 |
| Screening and validation of optogenetic tools | 55 |
| Illumination with optoPlate | 56 |
| Screening via plate reader | 56 |
| Scanning light intensity and dynamics | 57 |
| Notes | 59 |
| References | 62 |
| CHAPTER FOUR: DYNAMIC MULTIPLEXED CONTROL AND MODELING OF OPTOGENETIC SYSTEMS USING THE HIGH-THROUGHPUT OPTOGENETIC PLATFORM LUSTRO | 69 |
| Abstract: | |
| Introduction: | |
| | |

| | Results and Discussion: | . 73 |
|------|--|------|
| | Characterization of Optogenetic Transcription Factors Using Lustro | . 73 |
| | Sequential Activation of Optogenetic Systems | . 76 |
| | Multiplexed Control for Switching Between Optogenetic TFs | . 77 |
| | Response dynamics are insensitive to activation domain strength | . 79 |
| | Predicting System Behavior Using Machine Learning | . 82 |
| | Bayesian Optimization for Maximizing Switching | . 83 |
| | Conclusion: | . 85 |
| | Methods: | . 87 |
| | Strain Construction and Culture Conditions | . 87 |
| | Lustro | . 88 |
| | Machine Learning Model | . 89 |
| | Bayesian Inference and Uncertainty Quantification | . 89 |
| | Experimental Design using Bayesian Optimization | . 90 |
| | Materials Availability | . 91 |
| | Supporting Information | . 91 |
| | Acknowledgments | . 91 |
| | Author Contributions | . 92 |
| | Conflict of Interest | . 92 |
| | References: | . 92 |
| СНАР | TER FIVE: FUTURE DIRECTIONS | . 98 |
| | Conclusion: | . 98 |
| | Challenges and Future Directions: | . 99 |
| | | |

| | References: | 102 |
|-------|--|-----|
| | NDIX A: HIGH-THROUGHPUT OPTOGENETICS EXPERIMENTS IN YEAST UTOMATED PLATFORM LUSTRO | |
| | SUMMARY: | 106 |
| | ABSTRACT: | 106 |
| | INTRODUCTION: | 107 |
| | PROTOCOL: | 108 |
| | REPRESENTATIVE RESULTS: | 114 |
| | FIGURE AND TABLE LEGENDS: | 115 |
| | DISCUSSION: | 120 |
| | ACKNOWLEDGMENTS: | 123 |
| | DISCLOSURES: | 123 |
| | REFERENCES: | 123 |
| LITOS | NDIX B: ENHANCING HIGH-THROUGHPUT OPTOGENETICS: INTEGRATION WITH LUSTRO ENABLES SIMULTANEOUS LIGHT STIMULATION AND ING | |
| | Abstract: | |
| | Introduction: | |
| | Results: | |
| | Discussion: | |
| | | |
| | Methods: | |
| | Integration of LITOS with Lustro: | 132 |
| | Comparative Growth Analysis: | 133 |
| | Temperature Measurements: | 133 |
| | Materials Availability | 134 |

| Acknowledgments | 134 |
|----------------------|-----|
| Author Contributions | 134 |
| Conflict of Interest | 134 |
| References: | 134 |

LIST OF ABBREVIATIONS

TF Transcription factor

AD Activation domain

DBD DNA-binding domain

GOI Gene of interest

MoClo Modular cloning

RGA Robotic gripper arm

yOTK Yeast optogenetic toolkit

NN Neural network

AUC Area under the curve

SC Synthetic complete media

GG Golden gate assembly

OD Optical density

YPD Yeast peptone dextrose media

CHAPTER ONE: OPTOGENETIC SYSTEMS FOR DYNAMIC MULTIPLEXED CONTROL OF BIOLOGICAL ACTIVITY

Zachary P Harmer¹ and Megan N McClean^{1,2,*}

- Department of Biomedical Engineering, University of Wisconsin-Madison, Madison, Wisconsin 53706, United States
- ² University of Wisconsin Carbone Cancer Center, University of Wisconsin School of Medicine and Public Health, Madison, Wisconsin 53706, United States

Email: mmcclean@wisc.edu

In preparation for *Trends in Biotechnology*

Abstract:

Optogenetics offers a potent means to precisely regulate biological processes. Light-induced protein conformational changes can be used to change protein binding or localization, which can be used to control gene expression or cell signaling. A powerful optogenetic tool is the ability to control gene expression through optogenetic transcription factors (TFs). However, most optogenetic systems respond to blue light, which presents a key obstacle in independently controlling multiple different biological outcomes. Taking advantage of kinetic differences between optogenetic systems, such as different response times, deactivation times, and light sensitivity, can be leveraged to surmount this limitation. In order to measure and model these response kinetics to find the useful space for multiplexing, it is necessary to clone many optogenetic constructs into the same biological context and perform high-throughput screening on them with a range of light-pulsing conditions. Addressing this gap promises to unlock

enhanced control and versatility in optogenetics, heralding a new era of spatiotemporal precision in gene expression for transformative biological research and therapeutic interventions.

Introduction:

The ability to exert precise control over cellular behavior is critical for developing a comprehensive understanding of complex biological processes. Optogenetics empowers researchers to attain this control through light pulses, the timing and location of which can be readily (and cheaply) controlled[1–3]. Optogenetics has transformed our understanding of cellular processes and holds immense potential for applications ranging from fundamental research to bioproduction to therapeutic interventions. Central to optogenetics are natural light-sensitive proteins, found in a diverse array of organisms, including plants, bacteria, and animals. These photoreceptors, such as microbial opsins and plant phytochromes, serve as the basis for engineering light-sensing modules that can be integrated into various cellular contexts to allow orthogonal control[4.5]. Understanding the molecular mechanisms underlying light-induced conformational changes in these proteins has been pivotal in the development of optogenetic tools.

By strategically manipulating protein binding, localization, and conformation, regulation of gene expression and rewiring of cell signaling pathways can be controlled in a spatially and temporally precise manner. For example, an optogenetic LOV2 domain was used to engineer a tool, CLASP, that can ferry protein cargo, such as transcription factors, in and out of the nucleus to dynamically control gene expression[6,7]. The optical heterodimerizer pair CRY2/CIB1 has been used to control membrane localization of a Rho GTPase to disrupt the directional growth of the fungal human pathogen *Candida albicans*[8]. The optogenetic protein VVD has been used to

make the split TF (transcription factor) GAVPO, which has been used to control gene expression in neurons[9–11].

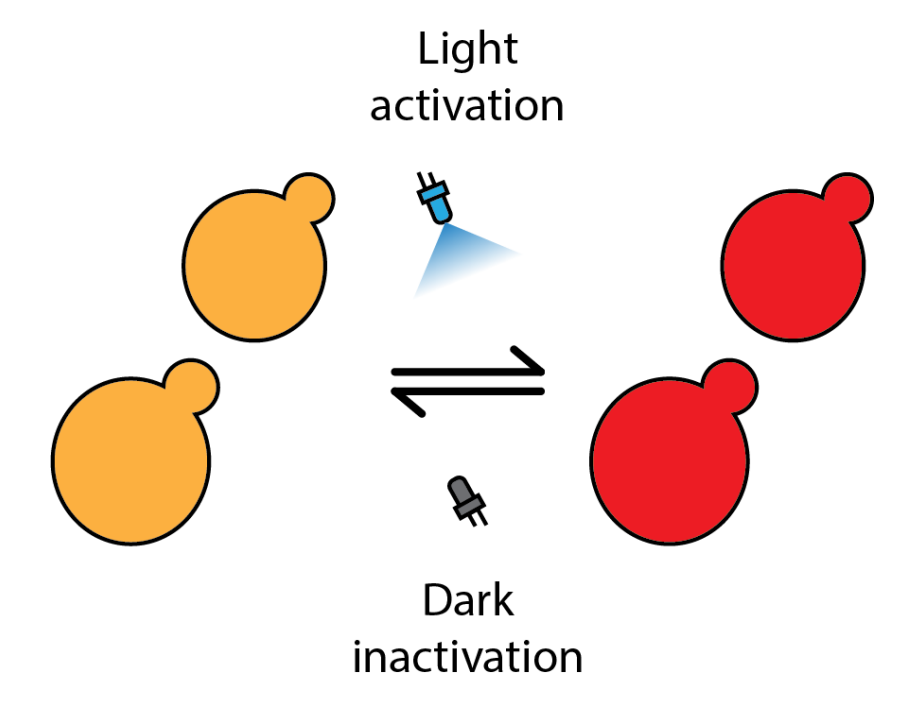


Figure 1. In optogenetics, light is used to induce a change of state in cells. In the sample optogenetic system depicted here, blue light-sensitive optogenetic TFs in yeast are activated by blue light induction, causing them to express a protein that turns the cell red. After being left in the dark, the system will eventually become inactivated and the cell will begin to return to its original state.

Control of gene expression

Cells continually respond to external stimuli, adjusting metabolism, exports, shape, growth, mating, and more, by adjusting the expression of different genes. The ability to control gene expression using a precise and dynamic medium like light affords synthetic control over these many cellular processes. Due to their high importance, many optogenetic TFs have been developed to regulate these behaviors by controlling gene expression, offering unprecedented insights into cellular behavior. Optogenetic TFs hold great promise in bioproduction, the

development of engineered living materials, therapeutic interventions, and improving understanding of disease models.

This optogenetic gene expression control is often done through split TFs, where light-induced binding is used to reconstitute TF activity (see Table 1)[5,12,13]. Single-component split TFs use identical proteins that bind in pairs (homodimerize) to activate gene expression when induced. Two-component split TFs use two different proteins that bind each other when induced with light to recruit an activation domain (AD) to a DNA-binding domain (DBD), activating the gene of interest. Split TFs have found applications in diverse biological contexts, from directing cell fate determination and differentiation to orchestrating complex developmental processes and tissue patterning. While there are many optogenetic tools and many reviews about them, this review focuses on split TFs as gene expression can be used to regulate many biological processes and split TFs can be used as a modular framework to understand how to improve control of optogenetic systems generally.

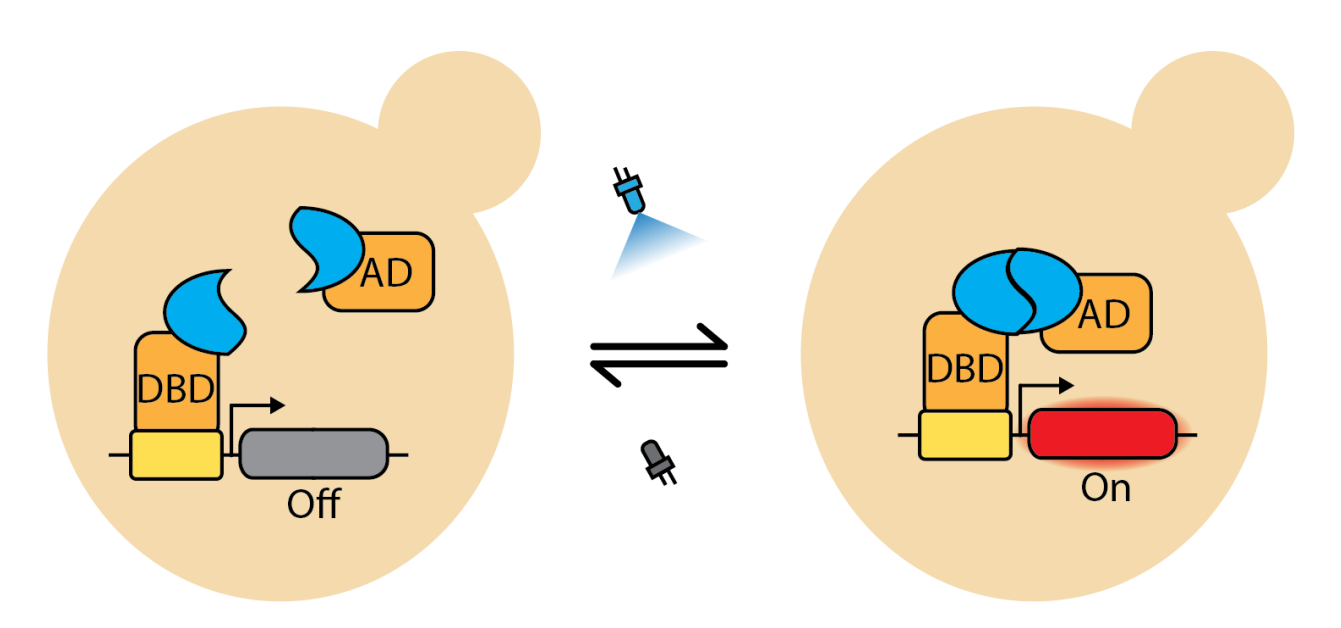


Figure 2. Depiction of an optogenetic two-component split TF in yeast. An optical heterodimerizer pair (blue) has each protein in the pair bound to an activation domain

(AD) or DNA-binding domain (DBD). Upon blue light induction, the proteins in the optical dimerizer pair activate and bind each other. This recruits the AD to the DBD, resulting in expression of the protein of interest (here depicted as generating red fluorescence). Figure not drawn to scale.

| Optogenetic System | Wavelength | Туре | Cofactor | Sources | Notes |
|------------------------|--------------|--------------------------|---------------|----------------|---|
| CRY2/CIB1 | Blue | Two-component | FAD | [14–16] | High signal, medium signal, long reversion, fast reversion, homooligomerization mutants |
| VVD/WDTC1 (FUN-LOV) | Blue | Two-component | FMN or FAD | [17] | |
| GAVPO (VVD) | Blue | Single- component | FMN or FAD | [9–11] | Low temp (28°C) and high temp (37°C) variants |
| Magnets (VVD) | Blue | Two-component | FMN or FAD | [13,18– 21] | Strong signal, fast reversion mutants |
| EL222 | Blue | Single- component | FMN | [22,23] | Fast, medium, slow reversion mutants |
| PixD/PixE | Blue | Two-component, octameric | FMN or FAD | [24] | |
| TULIP | Blue | Two-component | FMN | [25] | |
| PhyB/PIF | Red/infrared | Two-component | РСВ | [26,27] | |

| CcaS/CcaR | Red/green | Two-component | РСВ | [3,28,29] | Only applied in bacteria and plants |
|-----------|-------------|-------------------|------|-----------|-------------------------------------|
| BICYCL | Red/green | Two- component | РСВ | [30] | |
| UVR8/COP1 | Ultraviolet | Two- component | None | [27,31] | |

Table 1. Optogenetic systems used for split TFs. A comprehensive list is maintained at optobase.org[32].

Optogenetic control is limited by wavelength:

Most optogenetic switches, including split TFs, are blue light-sensitive (Figure 3)[30,33]. This wavelength sensitivity is due to the chemistry of the underlying light-sensitive proteins and the properties of the bound cofactor. The predominance of blue light-responsive optogenetic systems limits simultaneous control over multiple optogenetic systems, posing challenges for multiplexing control over multiple biological processes[23,33] (described below). These blue light-sensitive switches, including LOV domains, cryptochromes, and BLUF domains (PixD/PixE), bind FMN or FAD as a cofactor[14,24,34]. Red light-sensitive phytochromes bind PCB[35], and the UV-sensitive UVR8 does not require a cofactor[36]. Cobalamin-binding domains respond to green light, but only homotetramerization systems have been described to date. Multiplexed control strategies can be used to overcome this single-wavelength dependence to allow for simultaneous control of multiple biological systems.

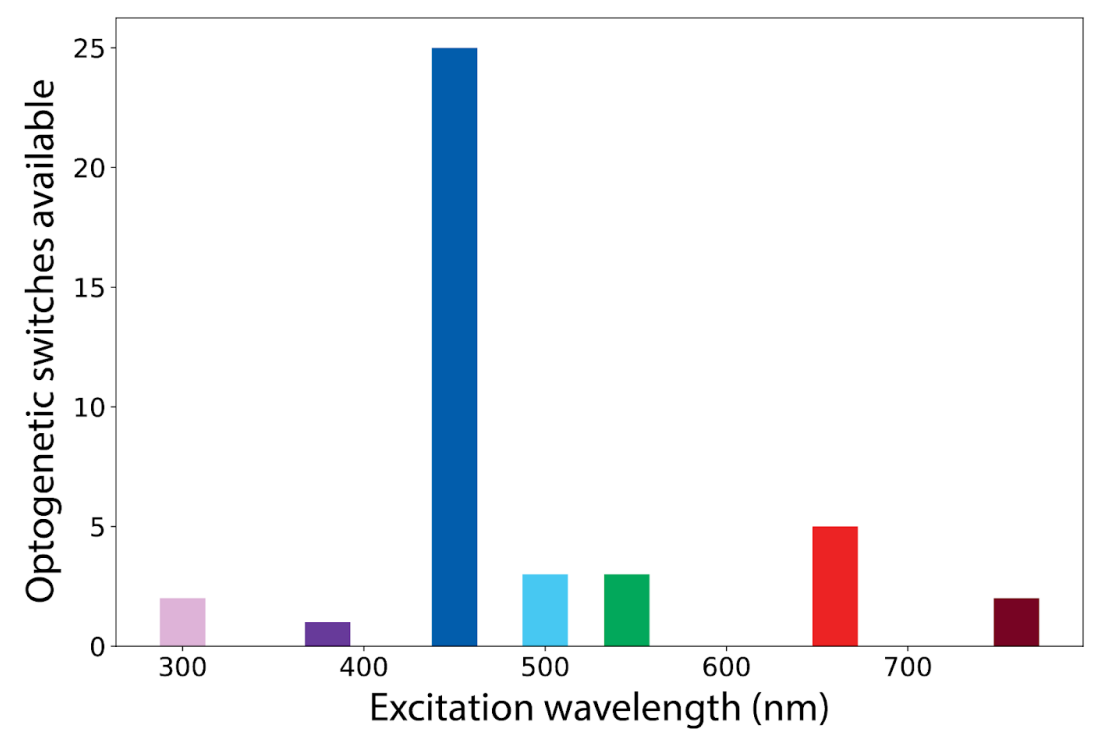
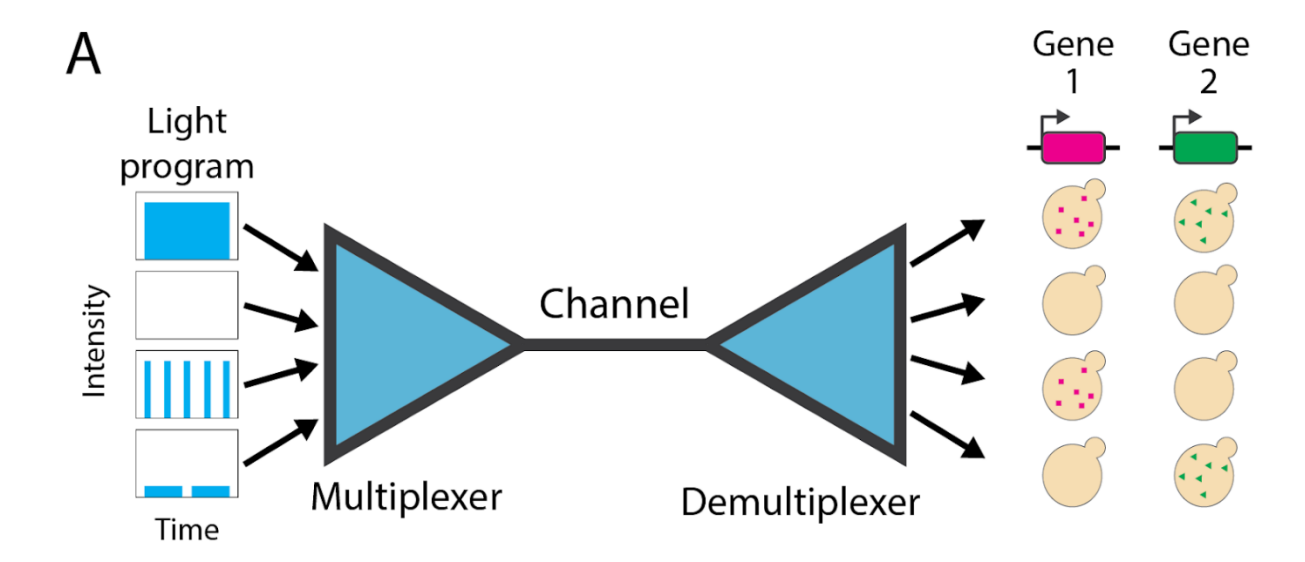


Figure 3. Distribution of optogenetic switches by excitation wavelength in the curated optogenetics database, optobase.org[32]. Modes of action vary, but blue light-responsive systems prevail.

In addition, blue light-responsive systems have some advantages in terms of chromophore over the others, particularly the red light-responsive systems. The blue light cofactors, FMN and FAD, are readily available in yeast and mammalian cells[37]. However, the red light cofactor PCB must be synthesized or exogenously added to media[35], increasing cost and experimental burden. Blue light systems also work more reliably than red light systems. Thus, using blue light for simultaneous control over multiple biological processes would be preferable[23].

Multiplexing using dynamic light patterns

In communications, multiplexing is taking different inputs, feeding them through the same channel, then demultiplexing the signal at the end to the respective outputs. The two strategies for multiplexing control over optogenetic systems are orthogonal multiplexing (where different wavelengths of light are utilized to stimulate different optogenetic systems responsive to those wavelengths) and dynamic multiplexing (where different light pulsing programs are used to activate different optogenetic systems by different amounts). Tabor et al. demonstrated orthogonal multiplexed control of red and green light-responsive optogenetic systems [3,28]. Benzinger et al. described a dynamic method for multiplexing, taking advantage of long and short reversion times in EL222 and cryptochrome variants to generate a feed-forward control loop in yeast[23]. One strategy to achieve dynamic multiplexed control over optogenetic systems responsive to the same wavelength of light is to take advantage of the differences in response kinetics between optogenetic systems. Optogenetic systems have different light sensitivities, light activation times, and dark reversion times. As such, varying light pulsing programs can activate different optogenetic systems by different amounts, even when the total light dose remains the same. These differences in preferential activation can be used to activate one optogenetic system more than another, or vice versa, allowing for multiplexed control.



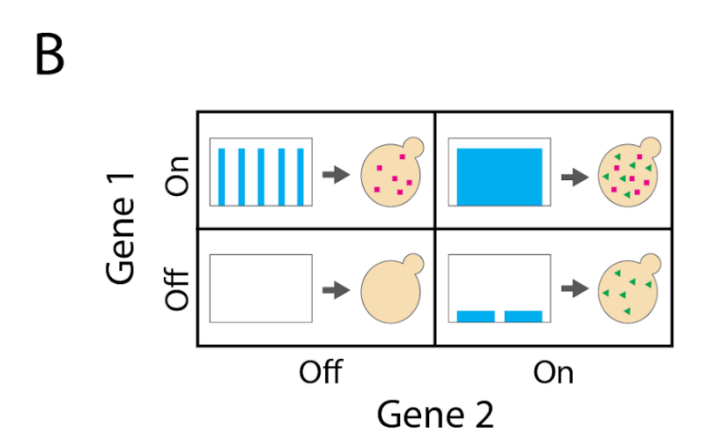


Figure 4. Schematic representation of multiplexing control over two biological systems using different blue light-pulsing programs. (A) Different light programs with varying blue light intensity and pulsing patterns over time lead to different activation patterns of two different blue light-responsive optogenetic systems, producing red or green reporters. The multiplexer chooses the light program, the channel is the medium of blue light, and the demultiplexer is the response pattern of the optogenetic systems. (B) The four light patterns used in (A) can be represented as four distinct states in a binary logic matrix. Different light programs are used to independently toggle two different optogenetic systems on or off, simultaneously controlling production of both the red and green reporters.

Because multiplexing control over optogenetic systems enables the simultaneous manipulation of multiple components within a biological system, it facilitates precise adjustments where different levels of control or stimulation may be needed. This can be used for developing a comprehensive understanding of complex, multifaceted biological systems. The

exploration of some biological effects, such as synergistic effects, is difficult and timeconsuming to achieve using single-component control, and would be faster and simpler using
multiplexed control. Multiplexed control supports dynamic adaptation to changing conditions
and optimization of efficient resource utilization, accelerating research and reducing costs.

Additionally, multiplexing using only one wavelength of light maximizes the use of light
wavelengths, freeing others for fluorescence detection. Ultimately, the ability to multiplex
control over optogenetic systems empowers researchers and engineers to achieve a higher degree
of precision and versatility in manipulating biological processes, with broad implications for
scientific discovery and biotechnological and medical applications. Comparing response kinetics
of optogenetic systems to find conditions for multiplexing can be done using optogenetic split
TFs.

Outstanding challenges for multiplexing optogenetic systems

Achieving multiplexed control of optogenetic systems demands careful selection of systems with compatible differences in response kinetics and consideration of experimental conditions. In order to determine which systems and conditions are compatible for multiplexing, it is necessary to compare different optogenetic systems side-by-side and to have a high-throughput method for characterizing them. Modularity and control of gene expression make optogenetic split TFs a great means to explore space for multiplexing. Gene expression in living cells is straightforward to detect, for example, by using expression of fluorescent protein reporters for readout. Control of gene expression is also very relevant to a variety of biological applications, including therapeutics and industrial bioproduction. The simple architecture of split TFs makes comparing different systems accessible and amenable to construction with

hierarchical DNA assembly techniques, such as the yeast optogenetic toolkit (yOTK)[12,13,38]. Comparing the response level of different optogenetic systems to different light pulsing programs can be performed in a high-throughput manner with access to automated techniques, such as Lustro[13,39] (described in Chapter 2). These high-throughput data sets can then be used for building machine learning models to identify conditions for optimizing different objective functions of gene expression control. This thesis details a strategy for assembling optogenetic constructs and characterizing them to identify conditions for dynamic multiplexing of optogenetic systems for control of biological behavior.

Acknowledgments

This work was supported by National Institutes of Health grant R35GM128873 and National Science Foundation grant 2045493 (awarded to M.N.M.). Megan Nicole McClean, PhD, holds a Career Award at the Scientific Interface from the Burroughs Wellcome Fund. Z.P.H. was supported by an NHGRI training grant to the Genomic Sciences Training Program 5T32HG002760. We acknowledge fruitful discussions with McClean lab members.

Author Contributions

Z.P.H. and M.N.M conceived of the review, Z.P.H. wrote the original draft of the manuscript, and Z.P.H. and M.N.M wrote, reviewed, and edited the final manuscript.

Conflict of Interest

The authors declare no competing interests.

References

- 1. Lan, T.-H. *et al.* (2022) Optogenetics for transcriptional programming and genetic engineering. *Trends in Genetics* 38, 1253–1270
- 2. Pérez, A.L.A. *et al.* (2022) Optogenetic strategies for the control of gene expression in yeasts. *Biotechnology Advances* 54, 107839
- 3. Olson, E.J. and Tabor, J.J. (2014) Optogenetic characterization methods overcome key challenges in synthetic and systems biology. *Nat Chem Biol* 10, 502–511
- 4. Joshi, J. *et al.* (2020) Optogenetics: Background, Methodological Advances and Potential Applications for Cardiovascular Research and Medicine. *Frontiers in Bioengineering and Biotechnology* 7
- 5. Polesskaya, O. *et al.* (2018) Optogenetic regulation of transcription. *BMC Neurosci* 19, 12
- 6. Chen, S.Y. *et al.* (2020) Optogenetic Control Reveals Differential Promoter Interpretation of Transcription Factor Nuclear Translocation Dynamics. *Cell Syst* 11, 336-353.e24
- 7. Sweeney, K. and McClean, M.N. (2022) Transcription Factor Localization Dynamics and DNA Binding Drive Distinct Promoter InterpretationsbioRxiv, 2022.08.30.505887
- 8. Silva, P.M. *et al.* (2019) Secretory Vesicle Clustering in Fungal Filamentous Cells Does Not Require Directional Growth. *Cell Reports* 28, 2231-2245.e5
- 9. Ma, Z. *et al.* (2013) Fine tuning the LightOn light-switchable transgene expression system. *Biochemical and Biophysical Research Communications* 440, 419–423
- 10. Zárate, R.V. *et al.* (2021) Optimization of the Light-On system in a lentiviral platform to a light-controlled expression of genes in neurons. *Electronic Journal of Biotechnology* 51, 50–57
- 11. Qian, Y. *et al.* (2023) A Single-Component Optogenetic Gal4-UAS System Allows Stringent Control of Gene Expression in Zebrafish and Drosophila. *ACS Synth. Biol.* 12, 664–671

- 12. An-adirekkun, J. (My) *et al.* (2020) A yeast optogenetic toolkit (yOTK) for gene expression control in Saccharomyces cerevisiae. *Biotechnology and Bioengineering* 117, 886–893
- 13. Harmer, Z.P. and McClean, M.N. (2023) Lustro: High-Throughput Optogenetic Experiments Enabled by Automation and a Yeast Optogenetic Toolkit. *ACS Synth. Biol.* DOI: 10.1021/acssynbio.3c00215
- 14. Kennedy, M.J. *et al.* (2010) Rapid blue-light–mediated induction of protein interactions in living cells. *Nat Methods* 7, 973–975
- 15. Pathak, G.P. *et al.* (2014) Benchmarking of Optical Dimerizer Systems. *ACS Synth Biol* 3, 832–838
- 16. Taslimi, A. *et al.* (2016) Optimized second generation CRY2/CIB dimerizers and photoactivatable Cre recombinase. *Nat Chem Biol* 12, 425–430
- 17. Salinas, F. *et al.* (2018) Fungal Light-Oxygen-Voltage Domains for Optogenetic Control of Gene Expression and Flocculation in Yeast. *mBio* 9
- 18. Kawano, F. *et al.* (2015) Engineered pairs of distinct photoswitches for optogenetic control of cellular proteins. *Nat Commun* 6, 6256
- 19. Benedetti, L. *et al.* (2020) Optimized Vivid-derived Magnets photodimerizers for subcellular optogenetics in mammalian cells. *eLife* 9, e63230
- 20. Baumschlager, A. *et al.* (2022) Enhancing the performance of Magnets photosensors through directed evolutionbioRxiv, 2022.11.14.516313
- 21. di Pietro, F. *et al.* (2021) Rapid and robust optogenetic control of gene expression in Drosophila. *Developmental Cell* 56, 3393-3404.e7
- 22. Benzinger, D. and Khammash, M. (2018) Pulsatile inputs achieve tunable attenuation of gene expression variability and graded multi-gene regulation. *Nat Commun* 9, 3521
- 23. Benzinger, D. *et al.* (2022) Synthetic gene networks recapitulate dynamic signal decoding and differential gene expression. *Cell Syst* 13, 353-364.e6

- 24. Masuda, S. *et al.* (2013) Blue Light-Mediated Manipulation of Transcription Factor Activity In Vivo. *ACS Chem. Biol.* 8, 2649–2653
- 25. Strickland, D. *et al.* (2012) TULIPs: tunable, light-controlled interacting protein tags for cell biology. *Nat Methods* 9, 379–384
- 26. Shimizu-Sato, S. *et al.* (2002) A light-switchable gene promoter system. *Nat Biotechnol* 20, 1041–1044
- 27. Müller, K. *et al.* (2013) A red/far-red light-responsive bi-stable toggle switch to control gene expression in mammalian cells. *Nucleic Acids Res* 41, e77
- 28. Tabor, J.J. *et al.* (2011) Multichromatic control of gene expression in Escherichia coli. *J Mol Biol* 405, 315–324
- 29. Larsen, B. *et al.* (2023) Highlighter: An optogenetic system for high-resolution gene expression control in plants. *PLoS Biol* 21, e3002303
- 30. Jang, J. *et al.* (2023) Engineering of bidirectional, cyanobacteriochrome-based light-inducible dimers (BICYCL)s. *Nat Methods* 20, 432–441
- 31. Crefcoeur, R.P. *et al.* (2013) Ultraviolet-B-mediated induction of protein–protein interactions in mammalian cells. *Nat Commun* 4, 1779
- 32. Kolar, K. *et al.* (2018) OptoBase: A Web Platform for Molecular Optogenetics. *ACS Synth Biol* 7, 1825–1828
- 33. Dwijayanti, A. et al. (2022) Toward Multiplexed Optogenetic Circuits. Frontiers in Bioengineering and Biotechnology 9
- 34. Pudasaini, A. *et al.* (2015) LOV-based optogenetic devices: light-driven modules to impart photoregulated control of cellular signaling. *Frontiers in Molecular Biosciences* 2
- 35. Uda, Y. *et al.* (2017) Efficient synthesis of phycocyanobilin in mammalian cells for optogenetic control of cell signaling. *Proc Natl Acad Sci U S A* 114, 11962–11967
- 36. Jenkins, G.I. (2014) The UV-B Photoreceptor UVR8: From Structure to Physiology. Plant Cell 26, 21–37

- 37. Hühner, J. *et al.* (2015) Quantification of riboflavin, flavin mononucleotide, and flavin adenine dinucleotide in mammalian model cells by CE with LED-induced fluorescence detection.

 Electrophoresis 36, 518–525
- 38. Lee, M.E. *et al.* (2015) A Highly Characterized Yeast Toolkit for Modular, Multipart Assembly. *ACS Synth. Biol.* 4, 975–986
- 39. Harmer, Z.P. and McClean, M.N. (2023) High-Throughput Optogenetics Experiments in Yeast Using the Automated Platform Lustro. *JoVE (Journal of Visualized Experiments)* DOI: 10.3791/65686

CHAPTER TWO: LUSTRO: HIGH-THROUGHPUT OPTOGENETIC EXPERIMENTS ENABLED BY AUTOMATION AND A YEAST OPTOGENETIC TOOLKIT

Zachary P Harmer1 and Megan N McClean1,2,*

- 1 Department of Biomedical Engineering, University of Wisconsin-Madison, Madison, Wisconsin 53706, USA
- 2 University of Wisconsin Carbone Cancer Center, University of Wisconsin School of Medicine and Public Health, Madison, Wisconsin 53706, USA

*Email: mmcclean@wisc.edu

Published in ACS Synthetic Biology

Abstract

Optogenetic systems use genetically encoded light-sensitive proteins to control cellular processes. This provides the potential to orthogonally control cells with light, however these systems require many design-build-test cycles to achieve a functional design and multiple illumination variables need to be laboriously tuned for optimal stimulation. We combine laboratory automation and a modular cloning scheme to enable high-throughput construction and characterization of optogenetic split transcription factors in *Saccharomyces cerevisiae*. We expand the yeast optogenetic toolkit to include variants of the cryptochromes and Enhanced Magnets, incorporate these light-sensitive dimerizers into split transcription factors, and automate illumination and measurement of cultures in a 96-well microplate format for high-throughput characterization. We use this approach to rationally design and test an optimized Enhanced Magnet transcription factor with improved light-sensitive gene expression. This

approach is generalizable to high-throughput characterization of optogenetic systems across a range of biological systems and applications.

Keywords: optogenetics, automation, MoClo, yeast, high throughput, synthetic transcription factors

Introduction

Optogenetics is a powerful technique that allows for dynamic, spatial, and temporal control over cellular behavior using light. Optogenetics leverages light-sensitive proteins, taking advantage of light responsive changes in protein conformation to actuate processes inside the cell. Such tools have been used to activate specific signaling pathways. repress and activate transcription. control protein localization. And induce protein degradation. A common approach is to control a process of interest by fusing effectors to light-activated heteroor homodimerizers to generate activity through proximity. For example, light-sensitive split transcription factors (TFs) are frequently generated by fusing one protein of an optical heterodimerizer pair to a DNA-binding domain (DBD) and the other to an activation domain (AD). This allows expression of the gene of interest (GOI) to be activated by inducing dimerization (and reconstitution) of the split TF using light.

One of the challenges of using optogenetics is that both prototyping a construct for a given application, as well as identifying appropriate illumination conditions, represent significant bottlenecks. To generate a functional optogenetic construct, many factors need to be tuned and tested including expression levels, linker lengths, and choice of components. A cloning toolkit can be used to rapidly develop prototype constructs, and a yeast optogenetic toolkit was recently developed. but it contains a relatively small fraction of the existing repertoire of light-sensitive

proteins. In addition, once constructs are created, a high-throughput method is needed to characterize their function and activity in response to light. Bioreactor-based techniques have been developed that allow real-time measurement of light-sensitive cultures but they have limited throughput. Several tools allow for individual programming of LEDs in a microwell plate format such as the LPAs, optoPlate, and LITOS and enable higher throughput light-stimulation. However, these approaches still lack a method for high-throughput and rapid measurement of the optogenetic system response. The recent optoPlateReader partially solves this problem, but requires the use of many biological replicates to obtain reliable data and lacks access to liquid handling capabilities, important for performing certain assays or long-term experiments.

To accelerate optogenetic prototyping, in this work we use laboratory automation to enable high-throughput screening and characterization of optogenetic systems with frequent and reliable measurements. This enables more rapid optimization and subsequent application of optogenetic systems. We dub this technique Lustro, after the Latin verb signifying movement, surveying, and illumination. We couple this laboratory automation technique for high-throughput optogenetics stimulation and readout with a modular cloning (MoClo) toolkit to build and characterize a library of split transcription factors in the important biotechnology model organism budding yeast, or *Saccharomyces cerevisiae*.

Results and Discussion

Integration of laboratory automation and light stimulation for high-throughput optogenetics

In order to increase testing throughput and reliability we developed an automated platform, Lustro, for screening and characterizing optogenetic systems. Lustro comprises an illumination device, a shaking device, and a plate reader integrated into a Tecan Fluent Automated Workstation (Figure 1a). A Robotic Gripper Arm (RGA) is able to move a microwell plate between these devices according to a programmed schedule. In our experiments, S. cerevisiae cultures are diluted into a 96-well plate with conditions measured in triplicate (Figure S1). This plate is placed on the illumination device (an optoPlate) for 26.5 minutes to receive light induction by individually programmable LEDs. The Robotic Gripper Arm then moves the plate to the shaking device to shake at 1000 rpm for 60 seconds to resuspend the yeast cells. This ensures accurate and consistent measurements of a homogenous culture and improves growth conditions. The plate is then moved to the plate reader to measure optical density and fluorescence before being moved back to the illumination device. The cycle is repeated in 30minute intervals. Due to its size and weight, the optoPlate could not be incorporated onto the small plate shaker. We therefore shook cells intermittently, which led to a small but measurable lag in growth (Figure S2).

We demonstrated that the Lustro platform can be used to measure the activity of optogenetic split TFs (Figure 1b). These split TFs utilize the Gal4 DNA-binding domain (GAL4DBD) and Gal4 activation domain (Gal4AD) to drive expression of the fluorescent reporter mScarlet-I¹² (hereafter referred to as mScarlet) from the pGAL1 promoter under light induction. This signal is readily measured by the plate reader. We induced a strain carrying a split transcription factor based on an optogenetic heterodimerizer pair (the cryptochrome CRY2PHR and its binding partner CIB1¹²) (Figure 1c) and compared it to a non-fluorescent

strain (negative), a strain with only the reporter construct (pGAL1-mScarlet), and a strain with constitutive expression of the fluorescent reporter (pRPL18B-mScarlet).

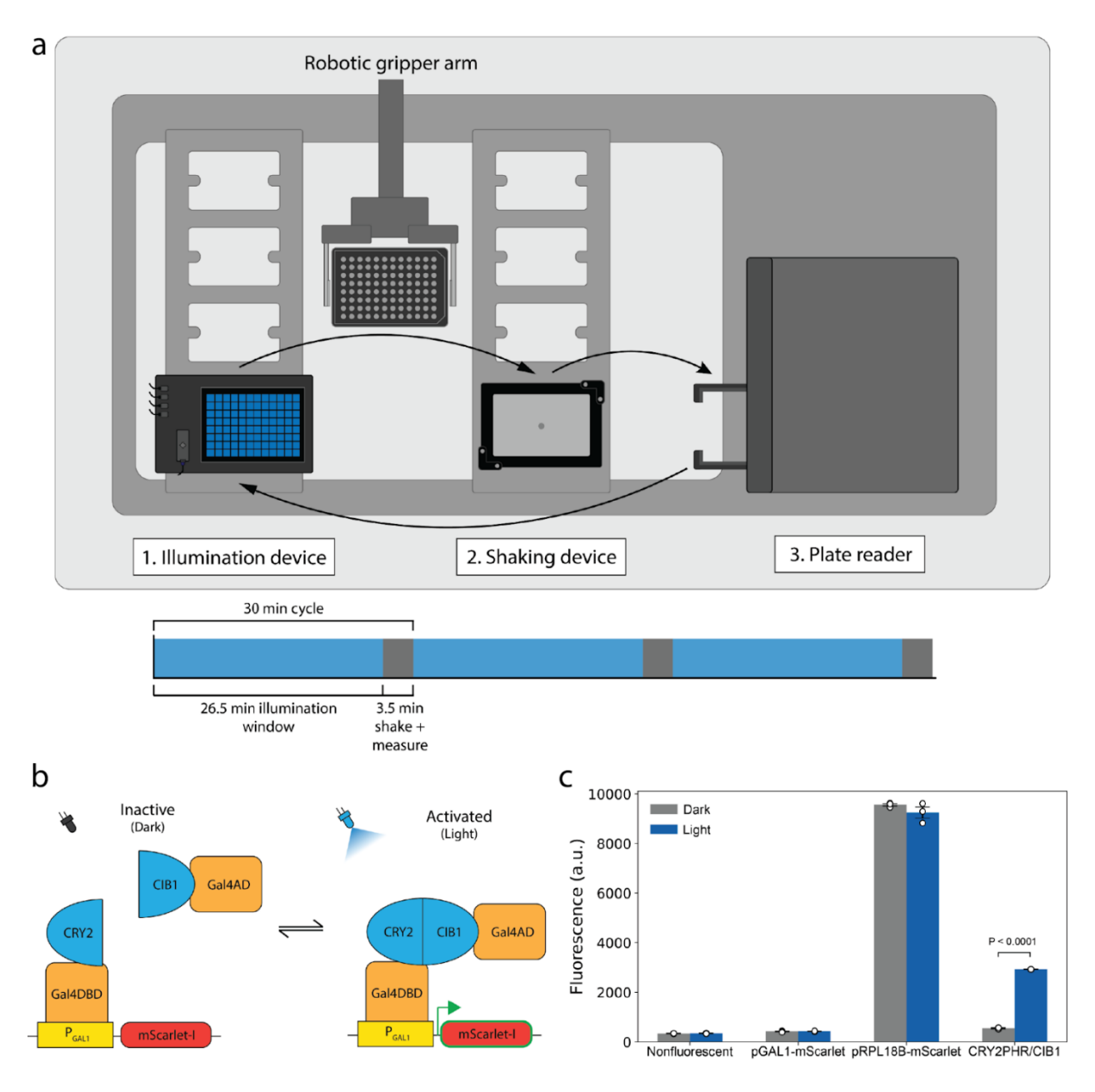


Figure 1. (a) The automated platform, Lustro. The Robotic Gripper Arm transfers microwell plates between the illumination device, shaking device, and plate reader. (b) Optogenetic split TF with CRY2 and CIB1 as the optical dimerizer pair. When Gal4AD is recruited to Gal4DBD (bound to pGAL1), expression of the gene of interest (mScarlet) is induced. (c) mScarlet fluorescence driven by induction of the CRY2PHR/CIB1 TF (p=0.000039, t-statistic=160, paired Student's t-test), with non-fluorescent (negative) cells, a

non-inducing control with only the reporter construct, and mScarlet under constitutive (pRPL18B) expression. Measurements were taken every 30 minutes and raw fluorescence values are shown for the light and dark conditions 10 hours into induction.

Combining optoPlate programming with automation allows for highresolution time-course experiments

A powerful advantage of Lustro is the ability to easily record output over time (Figure 2). This can reveal dynamic changes which would not be observed using a single end point measurement. We measured gene expression (using the fluorescent reporter) induced by a split TF (consisting of a cryptochrome variant, CRY2(535), andCIB1)²² every 30 minutes for 16 hours (Figure 2). Measurements reveal behavior of the optogenetic system in response to different light induction programs as the cell culture reaches saturation (compare to OD measurements in Figure S3).

In preliminary experiments, we created strains using mRuby2²⁰²⁰ as a fluorescent reporter (later replaced with mScarlet). However, a strain with mRuby2 under constitutive expression (pRPL18B) was unexpectedly found to temporarily exhibit higher fluorescence following light induction (Figure S4). This effect did not depend on co-expression of an optogenetic system. We were able to observe the kinetics of this photoactivated effect by using the automated platform, which we would not have been able to observe by taking single measurements at a delayed endpoint. The short sampling time (3.5 minutes to shake and measure a plate) and the ability to program illumination means that measurements can be taken with even finer timescale resolution if duplicate wells are used and illumination patterns are staggered. We used this approach to measure the timescale of the decay rate of the mRuby2 photoactivated effect. A strain constitutively expressing mRuby2 (pRPL18B-mRuby2) was induced with blue light and the timing of the light switching off between duplicate wells was staggered by 5-minute intervals so

that measurements recorded on 30-minute intervals could show finer granularity (Figure S4b). These measurements were combined and fit to an exponential decay curve (Figure S4c) and the half-life of this photosensitive effect was found to be 26.5 minutes. While frustrating for measuring the response of blue-light stimulated optogenetic systems, this effect could potentially be leveraged for other applications. For instance, to track protein movement and localization by stimulating mRuby2 in a defined location and observing the change and movement of the photosensitive fluorescence effect.

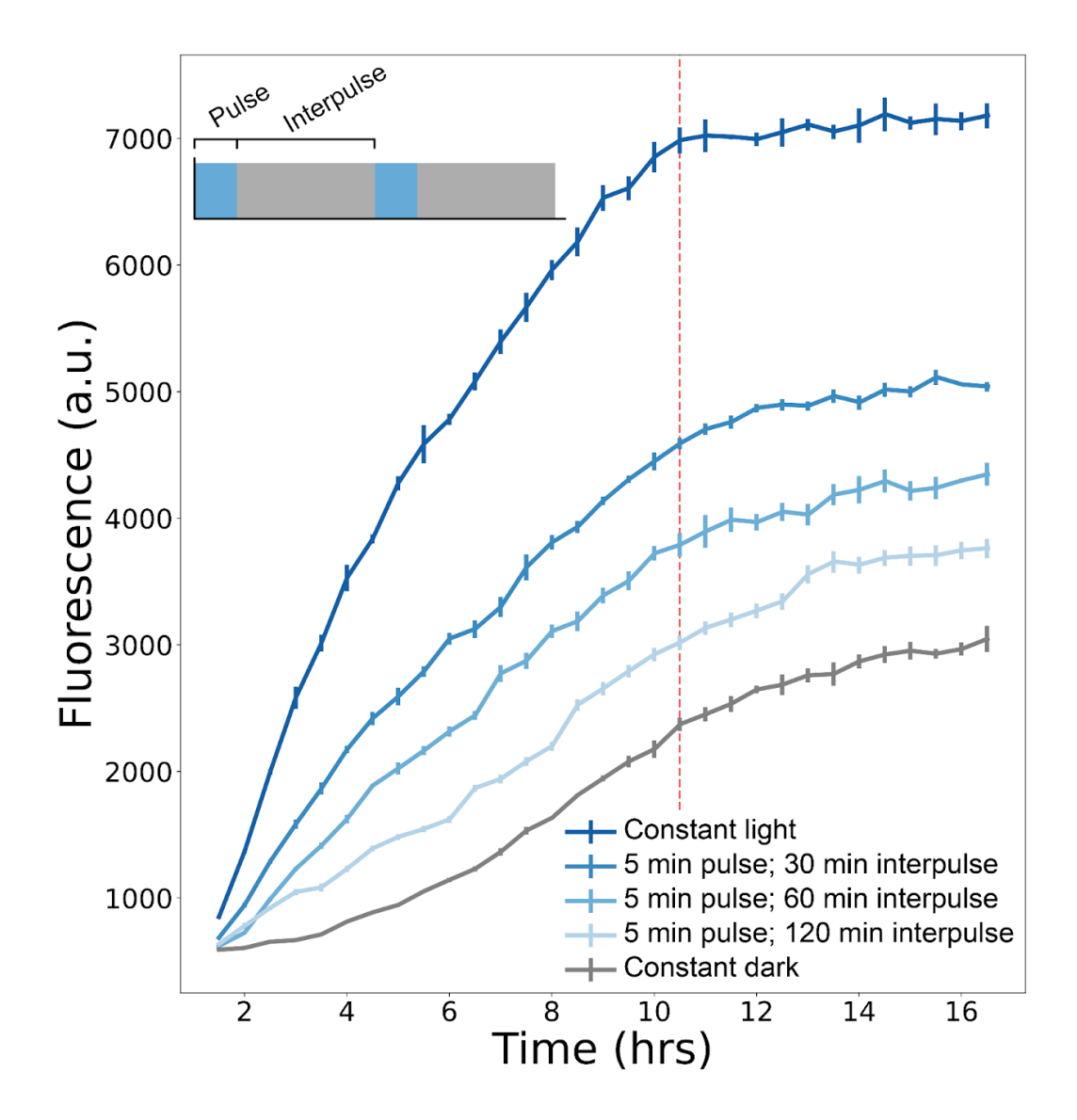


Figure 2. Induction of a CRY2(535)/CIB1 split TF strain over time by different light regimes. Each intermediate induction regime shown has a 5-minute pulse of light followed by an interval of darkness (the interpulse) as indicated on the figure legend for the duration of light induction (shown on the horizontal axis). The red vertical line indicates when the cultures reach saturation (Figure S3).

A yeast optogenetic toolkit (yOTK) combined with Lustro allows for rapid prototyping and testing of optogenetic systems

Optogenetic split transcription factors can, in theory, be built from any pair of optically dimerizing proteins. However, these proteins have different properties, including their light sensitivity, photocycle kinetics, as well as their sensitivity to protein fusion and context. In order to compare how different optical dimerizers tune the activity of optogenetic split TFs, we introduced new light-sensitive dimerizers as parts into the yeast optogenetic toolkit (yOTK) 229.30. We specifically introduced several different cryptochrome³⁵ variants (CRY2FL/CIB1¹⁹, CRY2PHR/CIB1¹⁹, CRY2(535)/CIB1²²) and Enhanced Magnets (eMags) (eMagA/eMagB, eMagAF/eMagBF)²⁶, selected to have different photocycle kinetics between light and dark states and light sensitivity (Table 1; see Table S3 for full list of plasmids generated in this work). Using the toolkit, these optical dimerizer pairs are cloned into the same cellular context (Figure 3a) using Golden Gate assembly to rapidly and reliably assemble individual "part" plasmids into "cassette" plasmids (Figure S5) containing split TFs that use the Gal4 activation domain (Gal4AD), the Gal4 DNA-binding domain (Gal4DBD), with the GAL1 promoter (pGAL1) driving expression of the fluorescent protein mScarlet. Cassettes containing the individual TF components (DBD, AD, or pGAL1) are further assembled into "multigene" plasmids for transformation into yeast.

| Dimerizer variant | Binding partner | Description | | |
|----------------------|-----------------------------|----------------------------|--|--|
| eMagA | eMagB, eMagBF, or eMagBM | Enhanced magnet dimerizer® | | |

| eMagAF | eMagB, eMagBF, or eMagBM | Enhanced magnet dimerizer with faster kinetics ³⁶ |
|-----------|-----------------------------|--|
| eMagB | eMagA or eMagAF | Enhanced magnet dimerizer ³² |
| eMagBF | eMagA or eMagAF | Enhanced magnet dimerizer with faster kinetics ³⁶ |
| eMagBM | eMagA or eMagAF | Enhanced magnet dimerizer with slower kinetics (Figure 4) |
| CRY2FL | CIB1 | Full length CRY2 ¹⁹ |
| CRY2PHR | CIB1 | CRY2 truncation (residues 1-498 of CRY2) ¹⁹ |
| CRY2(535) | CIB1 | CRY2 truncation (residues 1-535 of CRY2)32 |

Table 1. Optogenetic parts added to the yeast MoClo toolkit in this work. Additional plasmid information in Table S3.

We used Lustro to test various induction programs and screen several colonies from each construct transformation. Different transformants of the same construct were found to have variable fold-change gene expression response to induction (Figure 3b). We hypothesize these differences are due to copy number integration variation, as has been seen previously. Lustro allows for 46 transformants to be screened in each 96-well plate (light and dark conditions of each transformant alongside blank and negative controls, see Figure S1), providing a robust and reliable method for identifying transformants with desired traits. For purposes of comparing the effects of different promoters and optical dimerizers, the lowest fold-change transformants were assumed to be single-copy integrations and selected. The transformants exhibiting a higher light-induced gene expression level, presumably due to multiple integrations, might be preferred for some applications and merit further exploration in a future study.

Tuning relative expression levels of the two components in split TF optogenetic systems is important for optimizing their activity. We used the yeast optogenetic toolkit to develop

strains with the DBD and AD components under different strength promoters and rapidly tested the strains with the Lustro automated platform. We generated light-inducible split TF strains with optical dimerizer eMagA and eMagB components²⁶ under constitutive expression of low, medium, and high strength promoters (Figure 3c). Using Lustro, all construct transformants were screened and tested in two days. The strains use pRPL18B as the low promoter, pHHF1 as the medium, and pTEF1 as the high, based on characterizations done by Lee, et al 2015²⁶.

We reasoned that excess expression levels of the DBD component relative to the AD component expression levels would result in suboptimal activation as there are limited binding sites in the genome and unbound DBD could sequester the AD component away from the DNA without providing gene expression activity. This effect has been seen in previous studies, which demonstrated that higher expression of the DBD component relative to the AD component suppressed light-induced gene expression. Thus, we only generated strains where the expression of the AD component is equal to or greater than the expression of the DBD component. For each expression strength of the AD component, a higher fold change in fluorescence corresponded to a lower expression strength of the DBD component, with the largest effect occurring for the AD component under highest expression and the DBD component under lowest expression (Figure 3c, lower right).

Different optical dimerizers are known to exhibit different light sensitivity 5.19.32.36.39.40. The yOTK was used to generate strains with different optical dimerizers cloned into a similar split TF context and Lustro was used to characterize the light sensitivity of these strains (Figure 3d). We found that TFs using CRY2FL and CRY2(535) exhibited similar levels of sensitivity to light intensity, while the CRY2PHR TF exhibited very high sensitivity to even low doses of constant light. CRY2PHR is a truncation of CRY2FL that exhibits both higher basal and light-induced

activity¹². CRY2(535) is an intermediate-length truncation that produces intermediate activation and background, as compared to CRY2FL and CRY2PHR¹². Comparatively, TFs using the Enhanced Magnets (detailed below) exhibited less sensitivity to low levels of light intensity. TFs using a variant of eMagA/eMagB designed to have faster photocycle kinetics, eMagAF/eMagBF¹², had a lower gene expression response than TFs using eMagA/eMagB, but similar light sensitivity. Surprisingly, a split TF using a combination of the two, eMagAF/eMagB, exhibited a much higher gene expression level (and somewhat higher light sensitivity) than TFs using either eMagA/eMagB or eMagAF/eMagBF.

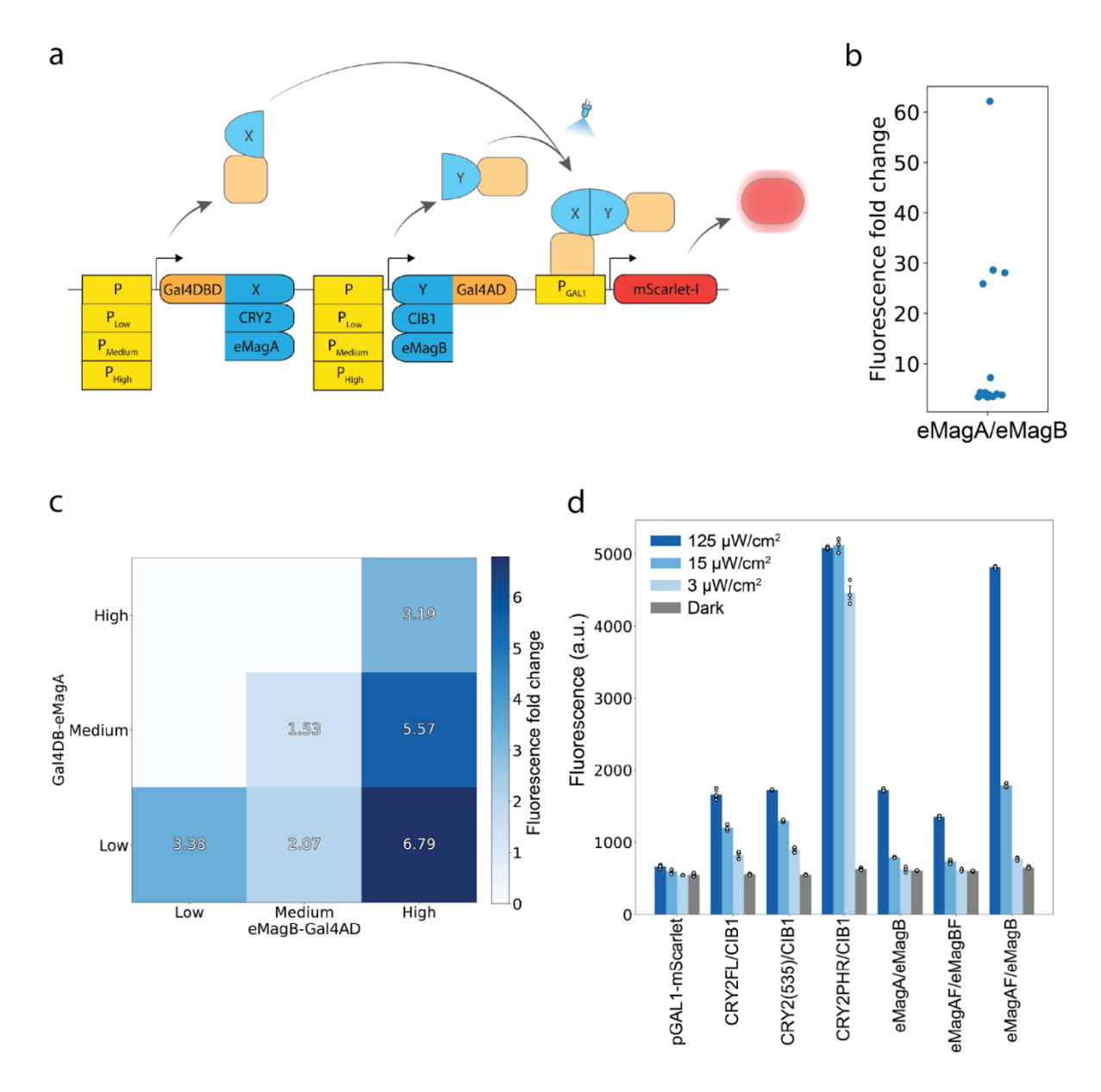


Figure 3. (a) Using the yeast optogenetic toolkit, multigene cassettes containing optical dimerizers fused to appropriate effector domains and controlled by a range of promoter strengths are created and integrated into the yeast genome. Once expressed, the light-inducible split TF induces expression of the fluorescent reporter, pGAL1-mScarlet, in a light-dependent manner. (b) Each dot represents the fold change in mScarlet fluorescence between light and dark conditions for a different transformant of the eMagA/eMagB split TF. Data shown represent averaged triplicates measured after 12 hours of light induction. (c) Heat map showing fold change in fluorescence after 12 hours of induction between light and dark conditions for eMagA/eMagB split TF strains with components expressed at different levels. Horizontal and vertical axes identify the strains with each split TF component under low (pRPL18B), medium (pHHF1), or high (pTEF1) expression. (d) Fluorescence values after 12 hours of light induction at the indicated light intensities for strains expressing split TFs using the indicated protein pairs and a reporter-only pGAL1-mScarlet control strain.

Combining the yOTK and Lustro to generate an optimized Magnet-based split TF

The original Magnet proteins were developed by introducing positively and negatively charged residues into the Ncap homodimer interface of the homodimerizer protein Vivid, a naturally occurring light-sensitive protein in *Neurospora crassa*. Subsequent mutations were introduced to reduce (pMagFast2) or increase (nMagHigh1) reversion time to the dark state. The Enhanced Magnets eMagA and eMagB developed in a later study were generated from nMagHigh1 and pMagFast2 (respectively) by introducing mutations to improve thermal stability and binding activity. To develop a version of eMagB that reverts to the dark state more slowly, we introduced these "enhanced" mutations into another Magnet protein, pMagFast1 (a slower reverting version of pMagFast2), generating an "enhanced" pMagFast1 protein, eMagBM (Figure 4a, Table S5).

We used Lustro to characterize split TFs with eMagBM and compare them to split TFs using eMagB. Induction with eMagBM-based TFs was found to be higher than induction with eMagB-based TFs as we had anticipated (Figure 4b) and was tunable by varying light pulse and interpulse duration (Figure 4c). Interestingly, induction with the Magnet-based TFs was found to continue to increase fluorescence even after cultures reached saturation at around 12 hours (data shown for eMagA/eMagBM in Figure 4c), which might be useful for high cell density bioproduction schemes. This contrasts with the activity of the CRY2/CIB1-based TFs (data shown for CRY2PHR/CIB1 in Figure 2), where fluorescence plateaus around the saturation point at 10 hours.

To further optimize the eMagA/eMagBM split TF, we cloned constructs with the components of the eMagBM-based split TF system each expressed under different promoter

strengths, as was done with the eMagA/eMagB split TF in Figure 3c. Transformants were screened as in Figure 3b to identify single-copy integrations for comparison (Figure S6). Different expression levels of the eMagA/eMagBM split TF exhibited a similar pattern to the expression levels of the eMagA/eMagB split TF shown in Figure 3c, but with a higher expression of the reporter at all component expression levels (Figure S7).

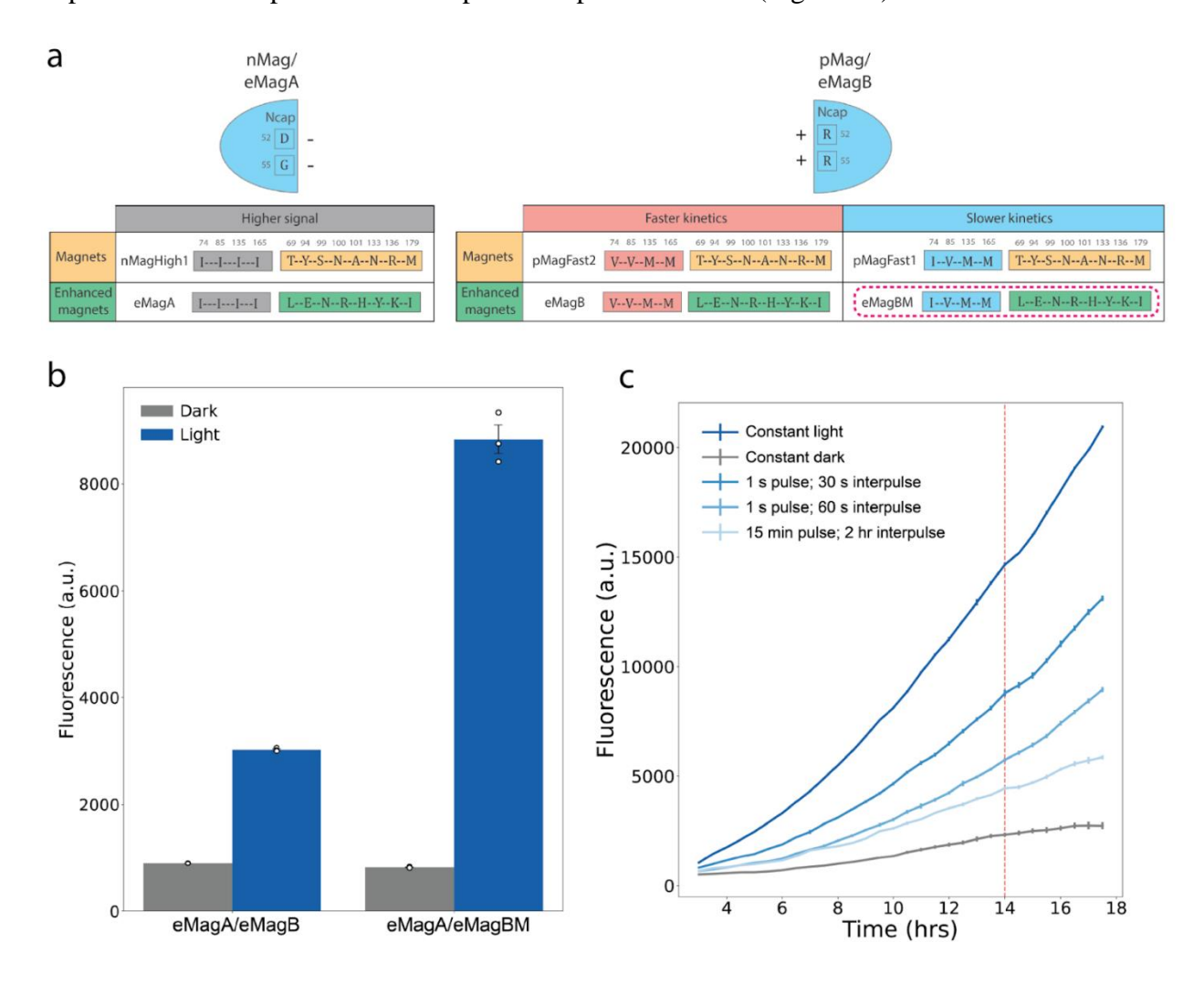


Figure 4. (a) Table showing the mutations made to design eMagBM (highlighted in pink dashed line). Mutation of residue 74 to I was associated with slower kinetics in pMag. See Table S5 for full sequences. (b) Fluorescence values are shown after 12 hours of continuous light induction between light and dark samples of strains with eMagB- or eMagBM-based split TFs. Fluorescence with the eMagA/eMagB split TF system increases 3.4-fold under light induction and fluorescence of the eMagA/eMagBM split TF system increases 10.8-fold. All split TF components are expressed under pRPL18B. (c) Fluorescence is shown for

the eMagA/eMagBM TF strain under different induction regimes that vary the pulse on and pulse off times in minutes and seconds. The vertical red line shows when the cultures reach saturation, and the horizontal axis shows time since the start of induction.

Conclusion

Optogenetics is a potent tool for the precise control of biological activity. Combining advancements in high-throughput strain construction with rapid screening creates a pipeline to improve the speed and robustness of design-build-test cycles. In this study, we developed an automated high-throughput platform for optogenetics in microwell plates, Lustro, that enables rapid screening and comparison of different optogenetic systems. With the Lustro automated platform, it is possible to quickly test and optimize different light-sensitive proteins for their desired purposes. We demonstrate that Lustro can be used for growing and inducing cells with only a small lag in growth due to shaking and temperature conditions. Lustro is able to quickly screen transformants, allowing for selection of strains with desired properties. The combination of programmed light to stagger light conditions between duplicate wells allows for rapid phenomena to be measured, as demonstrated by measuring the decay rate of mRuby2 photoactivation. We combine Lustro with a modular cloning toolkit 223.32 to create a pipeline that allows for testing and tuning the design of different optogenetic systems and comparing the response of different optogenetic systems to various light induction conditions. We use Lustro to characterize a split TF that uses a new, rationally designed Enhanced Magnets with a higher level of gene expression and expanded that cloning toolkit to include more optogenetic tools.

The Lustro platform is highly adaptable and can be generalized to work with other laboratory automation robots, illumination devices, plate readers, cell types, and optogenetic systems, including those responsive to other wavelengths of light 18.43. For example, the optoPlate could be exchanged with the LPA25, LITOS22, or optoWELL-2446. It can also be adapted to

perform any assay that can be done using a plate reader or a pipetting robot, which expands its potential applications. Laboratory automation has long been a staple in the pharmaceutical industry and genomics, as it dramatically increases throughput and frees up researchers from repetitive tasks to perform higher-level analysis 45.46. Recent years have seen an increase of automation in optogenetics experiments^{22,27}, and performing automated experiments in a microwell plate format increases throughput and allows for integration with other types of assays. The strategy of rapidly prototyping optogenetic circuit construction strategies in a microwell plate format complements other strategies for scaling up production with optogenetics24. Lustro can be further modified to facilitate automated dilutions for continuous culture applications, which is advantageous for long-term experiments. The possibility of frequent measurements allows Lustro to be adapted for cybergenetic feedback control, using real-time feedback and adjustments to alter the experimental conditions and while all of the experiments performed here used the Gal4DBD for consistency, these split TFs can be designed using other DBDs or a targetable deactivated nuclease (such as dCas9¹⁰) to allow for screening of dynamic expression changes in multiple genes, making it a valuable tool for functional genomics studies 10.24. Our automated high throughput platform Lustro offers a highly versatile and adaptable tool for rapidly screening and optimizing optogenetic systems, which will enable many new avenues of exploration into dynamic gene expression control.

Materials and Methods

Strains, media, and culture conditions

Single-construct strains were assembled by transforming NotI-digested multigene plasmids into BY4741¹⁰ Saccharomyces cerevisiae MATα HIS3D1 LEU2D0 LYS2D0 URA3D0 GAL80::KANMX GAL4::spHIS5. Transformations were performed according to an established LiAc/SS carrier DNA/PEG protocol¹⁰. Constructs were genomically integrated to reduce cell-to-cell variability. Integrations were done at the URA3 site and transformants were selected using SC-Ura dropout media.

Yeast strains were inoculated from colonies on a YPD agar³² plate into 3mL liquid SC media³² and grown overnight at 30°C, shaking. Overnight cultures were diluted to OD₇₀₀ = 0.1 in SC media. 200 μL of each culture was then added to each well of a 96-well black-wall, glass-bottom plate (Cat. #P96-1.5H-N). OD₇₀₀ was used to avoid bias from the red fluorescent mScarlet-I^{31.54}. All strains and conditions were measured in triplicate after initial transformant screening.

Cloning was carried out using a modular cloning toolkit as previously described 22232. In brief, part plasmids were constructed using BsmBI Golden Gate assembly of PCR products (primers are listed in Table S2) or gBlocks (Table S4) into the part plasmid entry vector (yTK001). Optogenetic constructs are listed in Table S5. Part plasmids were subsequently assembled into cassette plasmids using BsaI Golden Gate assembly. Cassette plasmids were assembled into multigene plasmids using BsmBI Golden Gate assembly.

optoPlate configuration and calibration

The optoPlate for light induction was constructed and calibrated according to previously published methods. Re-calibration of the optoPlate was found to be necessary for consistent illumination since the time of its initial calibration by Grødem et al (possibly due to decay of the LEDs). The optoPlate was programmed for each experiment using scripts found here:

https://github.com/mccleanlab/Optoplate-96. An intensity of 125 μ W/cm² was used for all experiments except where otherwise specified.

Automated characterization of optogenetic systems on the Tecan Fluent Automation Workstation and Spark plate reader

Automated experiments were carried out on a Tecan Fluent Automation Workstation, programmed using the Tecan Fluent Control visual interface software. The Fluent was equipped with an optoPlate²², BioShake 3000-T elm heater shaker for well plates, a Tecan Spark plate reader, and a Robotic Gripper Arm (RGA) for moving plates and plate lids. The Fluent was covered with a blackout curtain for the duration of experiments to prevent ambient light. Experiments were done using Cellvis 96-well glass bottom plates with #1.5 cover glass (Cat. # P96-1.5H-N). Plates were covered with a lid for all experiments except for those measuring the photoactivation effect of mRuby233.34. For experiments measuring the photoactivation effect of mRuby2, the plate was covered in a Breathe-Easy polyurethane sealing membrane (Diversified Biotech, BEM-1) because these conditions created a stronger light-induced fluorescent signal. Each 96-well plate with culture diluted to $OD_{100} = 0.1$ was incubated for 5 hours in the dark at 30°C, shaking, before beginning light induction. For each light induction experiment, the plate was placed on the optoPlate for 26.5 minutes at 21°C, transferred to the BioShake to shake at 1000 rpm (2 mm orbital) for 1 minute, and then transferred to the Tecan Spark plate reader to read optical density and fluorescence (with the lid temporarily removed by the Robotic Gripper Arm to ensure accurate OD readings). The plate was then transferred back to the optoPlate, and this cycle was repeated over the course of the experiment. Optical density was measured at 700 nm to avoid bias from measuring red fluorescent mScarlet-I_{31.54}. For mScarlet-I, fluorescence was measured with excitation at 563 nm and emission at 606 nm, with Z=28410, and an optical gain of 130.

Data analysis

Error bars shown represent the standard error of sample means performed in technical triplicate. Fold change shown is the raw fluorescence value of the induced strain divided by the raw fluorescence of the dark control. Exponential decay of mRuby2 photoactivation measurements (Figure S4) were fit to the decay curve y=a·e·*+c using the curve_fit function from the scipy.optimize package in Python.

Materials Availability

Key plasmids have been deposited on Addgene. For all other reagent requests, please contact the corresponding author.

Supporting Information

Additional data and schematics for the experiments described in the text, strains, plasmids, oligos, gene blocks, and optogenetic constructs used in this work

Acknowledgments

This work was supported by National Institutes of Health grant R35GM128873 and National Science Foundation grant 2045493 (awarded to M.N.M.). Megan Nicole McClean, PhD holds a Career Award at the Scientific Interface from the Burroughs Wellcome Fund. Z.P.H. was supported by an NHGRI training grant to the Genomic Sciences Training Program

5T32HG002760. We thank Amit Nimunkar and Edvard Grødem for building and modifying the optoPlate, and we thank Katrina Forest for discussions and insight on mRuby2 photoactivation. We acknowledge fruitful discussions with McClean lab members and in particular we are grateful to Neydis Moreno and Kevin Lauterjung for providing comments on the manuscript and to Stephanie Geller for providing pMM0773.

Author Contributions

Z.P.H. and M.N.M conceived of the study; Z.P.H. designed optogenetic parts, developed the Lustro platform, performed experiments, and analyzed data. M.N.M. provided funding.

Z.P.H. wrote the original draft of the manuscript and both Z.P.H. and M.N.M wrote, reviewed, and edited the final manuscript.

Conflict of Interest

The authors declare no competing interests.

References

- 1. Pérez, A. L. A. *et al.* Optogenetic strategies for the control of gene expression in yeasts. *Biotechnol. Adv.* **54**, 107839 (2022).
- 2. Lan, T.-H., He, L., Huang, Y. & Zhou, Y. Optogenetics for transcriptional programming and genetic engineering. *Trends Genet.* **38**, 1253–1270 (2022).
- 3. Olson, E. J. & Tabor, J. J. Optogenetic characterization methods overcome key challenges in synthetic and systems biology. *Nat. Chem. Biol.* **10**, 502–511 (2014).
- 4. Tan, P., He, L., Huang, Y. & Zhou, Y. Optophysiology: Illuminating cell physiology with optogenetics. *Physiol. Rev.* **102**, 1263–1325 (2022).

- Hallett, R. A., Zimmerman, S. P., Yumerefendi, H., Bear, J. E. & Kuhlman, B. Correlating in vitro and in vivo Activities of Light Inducible Dimers: a Cellular Optogenetics Guide. ACS Synth. Biol. 5, 53–64 (2016).
- Scott, T. D., Sweeney, K. & McClean, M. N. Biological signal generators: integrating synthetic biology tools and in silico control. *Curr. Opin. Syst. Biol.* 14, 58–65 (2019).
- Levskaya, A., Weiner, O. D., Lim, W. A. & Voigt, C. A. Spatiotemporal Control of Cell Signalling Using A Light-Switchable Protein Interaction. *Nature* 461, 997–1001 (2009).
- 8. Xu, Y. *et al.* Optogenetic control of chemokine receptor signal and T-cell migration. *Proc. Natl. Acad. Sci. U. S. A.* **111**, 6371–6376 (2014).
- 9. An-adirekkun, J. (My) et al. A yeast optogenetic toolkit (yOTK) for gene expression control in Saccharomyces cerevisiae. Biotechnol. Bioeng. 117, 886–893 (2020).
- Geller, S. H., Antwi, E. B., Di Ventura, B. & McClean, M. N. Optogenetic Repressors of Gene Expression in Yeasts Using Light-Controlled Nuclear Localization. *Cell. Mol. Bioeng.* 12, 511–528 (2019).
- Moreno Morales, N., Patel, M. T., Stewart, C. J., Sweeney, K. & McClean, M. N.
 Optogenetic Tools for Control of Public Goods in *Saccharomyces cerevisiae*. mSphere
 6, e00581-21 (2021).
- 12. Niopek, D. *et al.* Engineering light-inducible nuclear localization signals for precise spatiotemporal control of protein dynamics in living cells. *Nat. Commun.* **5**, 4404 (2014).
- 13. Glantz, S. T. *et al.* Directly light-regulated binding of RGS-LOV photoreceptors to anionic membrane phospholipids. *Proc. Natl. Acad. Sci.* **115**, E7720–E7727 (2018).
- 14. Yazawa, M., Sadaghiani, A. M., Hsueh, B. & Dolmetsch, R. E. Induction of protein-protein interactions in live cells using light. *Nat. Biotechnol.* **27**, 941–945 (2009).
- 15. van Bergeijk, P., Adrian, M., Hoogenraad, C. C. & Kapitein, L. C. Optogenetic control of organelle transport and positioning. *Nature* **518**, 111–114 (2015).
- Tague, N., Coriano-Ortiz, C., Sheets, M. B. & Dunlop, M. J. Light inducible protein degradation in E. coli with LOVtag. *BioRxiv Prepr. Serv. Biol.* 2023.02.25.530042 (2023) doi:10.1101/2023.02.25.530042.

- Renicke, C., Schuster, D., Usherenko, S., Essen, L.-O. & Taxis, C. A LOV2 domain-based optogenetic tool to control protein degradation and cellular function. *Chem. Biol.* 20, 619–626 (2013).
- 18. Shimizu-Sato, S., Huq, E., Tepperman, J. M. & Quail, P. H. A light-switchable gene promoter system. *Nat. Biotechnol.* **20**, 1041–1044 (2002).
- 19. Kennedy, M. J. *et al.* Rapid blue-light–mediated induction of protein interactions in living cells. *Nat. Methods* **7**, 973–975 (2010).
- 20. Milias-Argeitis, A., Rullan, M., Aoki, S. K., Buchmann, P. & Khammash, M. Automated optogenetic feedback control for precise and robust regulation of gene expression and cell growth. *Nat. Commun.* **7**, 12546 (2016).
- 21. Harrigan, P., Madhani, H. D. & El-Samad, H. Real-Time Genetic Compensation Defines the Dynamic Demands of Feedback Control. *Cell* **175**, 877-886.e10 (2018).
- 22. Bertaux, F. *et al.* Enhancing bioreactor arrays for automated measurements and reactive control with ReacSight. *Nat. Commun.* **13**, 3363 (2022).
- 23. Benisch, M., Benzinger, D., Kumar, S., Hu, H. & Khammash, M. Optogenetic closed-loop feedback control of the unfolded protein response optimizes protein production. *Metab. Eng.* (2023) doi:10.1016/j.ymben.2023.03.001.
- 24. Melendez, J. *et al.* Real-time optogenetic control of intracellular protein concentration in microbial cell cultures. *Integr. Biol.* **6**, 366–372 (2014).
- 25. Gerhardt, K. P. *et al.* An open-hardware platform for optogenetics and photobiology. *Sci. Rep.* **6**, 35363 (2016).
- 26. Bugaj, L. J. & Lim, W. A. High-throughput multicolor optogenetics in microwell plates. *Nat. Protoc.* **14**, 2205–2228 (2019).
- 27. Höhener, T. C. *et al.* LITOS: a versatile LED illumination tool for optogenetic stimulation. *Sci. Rep.* **12**, 13139 (2022).
- Datta, S. et al. High-throughput feedback-enabled optogenetic stimulation and spectroscopy in microwell plates. 2022.07.13.499906 Preprint at https://doi.org/10.1101/2022.07.13.499906 (2022).
- 29. Lee, M. E., DeLoache, W. C., Cervantes, B. & Dueber, J. E. A Highly Characterized Yeast Toolkit for Modular, Multipart Assembly. *ACS Synth. Biol.* **4**, 975–986 (2015).

- 30. Weber, E., Engler, C., Gruetzner, R., Werner, S. & Marillonnet, S. A Modular Cloning System for Standardized Assembly of Multigene Constructs. *PLOS ONE* **6**, e16765 (2011).
- 31. Bindels, D. S. *et al.* mScarlet: a bright monomeric red fluorescent protein for cellular imaging. *Nat. Methods* **14**, 53–56 (2017).
- 32. Taslimi, A. *et al.* Optimized second generation CRY2/CIB dimerizers and photoactivatable Cre recombinase. *Nat. Chem. Biol.* **12**, 425–430 (2016).
- 33. Lam, A. J. *et al.* Improving FRET dynamic range with bright green and red fluorescent proteins. *Nat. Methods* **9**, 1005–1012 (2012).
- 34. Kredel, S. *et al.* mRuby, a Bright Monomeric Red Fluorescent Protein for Labeling of Subcellular Structures. *PLOS ONE* **4**, e4391 (2009).
- 35. Liu, H. *et al.* Photoexcited CRY2 interacts with CIB1 to regulate transcription and floral initiation in Arabidopsis. *Science* **322**, 1535–1539 (2008).
- 36. Benedetti, L. *et al.* Optimized Vivid-derived Magnets photodimerizers for subcellular optogenetics in mammalian cells. *eLife* **9**, e63230 (2020).
- 37. Lee, J. H., Skowron, P. M., Rutkowska, S. M., Hong, S. S. & Kim, S. C. Sequential amplification of cloned DNA as tandem multimers using class-IIS restriction enzymes. *Genet. Anal. Biomol. Eng.* **13**, 139–145 (1996).
- 38. Sweeney, K. & McClean, M. N. Transcription Factor Localization Dynamics and DNA Binding Drive Distinct Promoter Interpretations. 2022.08.30.505887 Preprint at https://doi.org/10.1101/2022.08.30.505887 (2022).
- 39. Kawano, F., Suzuki, H., Furuya, A. & Sato, M. Engineered pairs of distinct photoswitches for optogenetic control of cellular proteins. *Nat. Commun.* **6**, 6256 (2015).
- 40. Pathak, G. P., Strickland, D., Vrana, J. D. & Tucker, C. L. Benchmarking of Optical Dimerizer Systems. *ACS Synth. Biol.* **3**, 832–838 (2014).
- 41. Schwerdtfeger, C. & Linden, H. VIVID is a flavoprotein and serves as a fungal blue light photoreceptor for photoadaptation. *EMBO J.* **22**, 4846–4855 (2003).
- 42. Zhao, E. M. *et al.* Optogenetic regulation of engineered cellular metabolism for microbial chemical production. *Nature* **555**, 683–687 (2018).

- 43. Crefcoeur, R. P., Yin, R., Ulm, R. & Halazonetis, T. D. Ultraviolet-B-mediated induction of protein–protein interactions in mammalian cells. *Nat. Commun.* **4**, 1779 (2013).
- 44. optoWELL > opto biolabs. https://optobiolabs.com/products/optowell/.
- 45. Chapman, T. Lab automation and robotics: Automation on the move. *Nature* **421**, 661–663 (2003).
- 46. Kong, F., Yuan, L., Zheng, Y. F. & Chen, W. Automatic Liquid Handling for Life Science: A Critical Review of the Current State of the Art. *SLAS Technol.* **17**, 169–185 (2012).
- 47. Gutiérrez Mena, J., Kumar, S. & Khammash, M. Dynamic cybergenetic control of bacterial co-culture composition via optogenetic feedback. *Nat. Commun.* **13**, 4808 (2022).
- 48. Milias-Argeitis, A. *et al.* In silico feedback for in vivo regulation of a gene expression circuit. *Nat. Biotechnol.* **29**, 1114–1116 (2011).
- 49. Polstein, L. R. & Gersbach, C. A. A light-inducible CRISPR/Cas9 system for control of endogenous gene activation. *Nat. Chem. Biol.* **11**, 198–200 (2015).
- 50. Baker Brachmann, C. *et al.* Designer deletion strains derived from *Saccharomyces cerevisiae* S288C: A useful set of strains and plasmids for PCR-mediated gene disruption and other applications. *Yeast* **14**, 115–132 (1998).
- 51. Gietz, R. D. & Schiestl, R. H. High-efficiency yeast transformation using the LiAc/SS carrier DNA/PEG method. *Nat. Protoc.* **2**, 31–34 (2007).
- 52. YPD media. Cold Spring Harb. Protoc. 2010, pdb.rec12315 (2010).
- 53. Synthetic Complete (SC) Medium. Cold Spring Harb. Protoc. 2016, pdb.rec090589 (2016).
- 54. Hecht, A., Endy, D., Salit, M. & Munson, M. S. When Wavelengths Collide: Bias in Cell Abundance Measurements Due to Expressed Fluorescent Proteins. *ACS Synth. Biol.* **5**, 1024–1027 (2016).
- 55. Grødem, E. O., Sweeney, K. & McClean, M. N. Automated calibration of optoPlate LEDs to reduce light dose variation in optogenetic experiments. *BioTechniques* **69**, 313–316 (2020).
- 56. Virtanen, P. *et al.* SciPy 1.0: fundamental algorithms for scientific computing in Python. *Nat. Methods* **17**, 261–272 (2020).

CHAPTER THREE: THE YEAST OPTOGENETIC TOOLKIT (yOTK) FOR SPATIOTEMPORAL CONTROL OF GENE EXPRESSION IN BUDDING YEAST

Zachary P. Harmer¹ and Megan N. McClean^{1,2,*}

¹ Department of Biomedical Engineering, University of Wisconsin-Madison, Madison, WI USA

² University of Wisconsin Carbone Cancer Center, University of Wisconsin School of Medicine and Public Health, Madison, WI USA

*Email: mmcclean@wisc.edu

Under revision at *Springer Methods for Molecular Biology*

Abstract

Optogenetic systems utilize genetically encoded light-sensitive proteins to control cellular processes such as gene expression and protein localization. Like most synthetic systems, generation of an optogenetic system with desirable properties requires multiple design-test-build cycles. A yeast optogenetic toolkit (yOTK) allows rapid assembly of optogenetic constructs using Modular Cloning, or MoClo. In this protocol, we describe how to assemble, integrate, and test optogenetic systems in the budding yeast *Saccharomyces cerevisiae*. Generating an optogenetic system requires the user to first define the structure of the final construct and identify all basic parts and vectors required for the construction strategy, including light-sensitive proteins that need to be domesticated into the toolkit. The assembly is then defined following a set of standard rules. Multigene constructs are assembled using a series of one-pot assembly steps with the identified parts and vectors and transformed into yeast. Screening of the transformants allows optogenetic systems with optimal properties to be selected.

Key words: optogenetics, yeast, modular cloning, synthetic biology, multigene constructs, biological parts

Introduction

Optogenetic systems utilize genetically encoded light-sensitive proteins to control cellular processes such as gene expression and protein localization. In the important model and industrial organism *Saccharomyces cerevisiae*, optogenetic systems have been used to control activation and repression of gene expression[1, 2], protein localization[3–5], translation[6], and intracellular and intercellular signaling activity and metabolism [7–11]. This in turn has allowed for light-based control of yeast physiology both to investigate basic biological questions[12, 13] as well as achieve optimized control of engineered metabolic pathways[14] and synthetic consortia[15].

Optogenetic systems consist of light-sensitive proteins combined with appropriate effector domains to drive the cellular process of interest in a light-induced manner. For example, fusion of an Activation Domain (AD) to one half of a light-sensitive protein-protein interaction and a DNA-Binding Domain (DBD) to the other half generates a split optogenetic chimeric transcription factor. Functional optogenetic systems require appropriate choice of light-sensitive proteins, functional arrangements of the light-sensitive components and effector domains, as well as appropriate expression levels. Thus, optogenetic systems go through many design-test-build cycles before desirable or optimal function is achieved. To facilitate rapid generation of optogenetic constructs, this protocol describes use of a yeast optogenetic toolkit which allows for Modular Cloning (MoClo) of constructs to combine and express light-sensitive proteins fused to appropriate effector domains. Modular cloning systems exist in many different organisms[16–22] and take advantage of Type IIS-based restriction enzymes and Golden Gate cloning. MoClo is a hierarchical assembly system in which transcription units are assembled from a first level containing basic "parts" (e.g. promoters, terminators, coding sequences for light-sensitive

proteins). These transcriptional units are then assembled into multigene constructs which can be transformed and integrated into the yeast genome to express all necessary elements for the optogenetic system. In this chapter, we describe how to use a yeast optogenetic toolkit[1] to make functional optogenetic systems in *Saccharomyces cerevisiae*.

Materials

General cloning

- 1. Luria-Bertani (LB) medium: 800 mL deionized water, 10 g Tryptone, 5 g NaCl, 5 g yeast extract, 15 g bacto agar (only for solid media), adjust final volume to 1 L with deionized water, sterilize by autoclaving.
- 2. Antibiotics: chloramphenicol, carbenicillin (used here instead of ampicillin), and kanamycin. Filter-sterilized stocks of Chloramphenicol are prepared at 34 mg/mL in 10 mL EtOH. Filter-sterilized stocks of kanamycin or carbenicillin are prepared at 50 mg/mL in 10 mL EtOH. Stocks are stored in 1 mL aliquots at -20°C. Dilute each stock solution 1:1000 in medium after the medium has been autoclaved and cooled to 65°C.
- 3. 1.5 mL tubes
- 50 μL aliquots DH5α chemically competent *Escherichia coli* cells (New England Biolabs)
 (or another strain of cloning competent *E. coli* cells, such as TOP10 from ThermoFisher
 Scientific)
- 5. Plasmid Miniprep Kit (e.g. QIAwave Plasmid Miniprep Kit, Qiagen; Monarch Miniprep Kit, New England Biolabs).
- 6. Water bath, 42°C
- 7. 37°C incubator

- 8. 4-4.5 mm glass plating beads (e.g. Zymo Research, ThermoFisher Scientific, New England Biolabs)
- 9. Nanodrop
- 10. UV transilluminator (optional)

Generation of new parts

- 1. DNA insert. DNA inserts can be ordered from a DNA synthesis company (e.g. Integrated DNA Technologies) as gene blocks or generated by PCR that amplifies the target sequence with desired flanking sequences. DNA to be integrated into a part vector must be flanked by part type-specific overhangs, followed by a BsaI site, followed by a BsmBI site. The BsmBI sites should generate TCGG (at the 5' end) and ACTC (at the 3' end) overhangs for assembly into the entry vector.
- 2. Part entry vector plasmid (pYTK001[19])

Golden Gate assembly

- 1. BsmBI-v2 Golden Gate Assembly Kit (New England Biolabs)
- 2. BsaI Golden Gate Assembly Kit (New England Biolabs)
- 3. 200 µL PCR tubes

Transformation and screening of yeast

Appropriate yeast strain, for example MATα HAP1+ ura3Δ0 leu2Δ0 HIS3 LYS2 TRP1
could be used for transforming constructs with the URA3 marker and URA3 homology for
integration.

- 20 U/μL NotI-HF, CutSmart Buffer (for linearizing constructs for genomic integration) (New England Biolabs)
- 3. Synthetic Complete (SC) medium: 900 mL deionized water, 6.7 g yeast nitrogen base without amino acids, and 20 g bacto agar (only for solid media). Autoclave media and cool to 65°C. Add 50 mL 20x amino acid mix (with appropriate nutrient dropped out, such as lacking uracil for SC-URA media) and 50 mL 20x glucose solution (40% w/v, autoclaved separately). Amino acid mix: dissolve1.44 g dry powder stocks (5g adenine hemisulfate, 2 g uracil, 5 g tryptophan, 2 g histidine-HCl, 2 g arginine-HCl, 2 g methionine, 3 g tyrosine, 10 g leucine, 3 g isoleucine, 10 g lysine-HCl, 5 g phenylalanine, 10 g aspartic acid, 15 g valine, 20 g threonine, 40 g serine) into 50 mL filter-sterilized deionized water at 60°C.
- 4. YPD medium: add 950 mL deionized water, 20 g bacto peptone, 10 g yeast extract (add 24 g bacto agar for solid media), and autoclave. Add 50 mL filter-sterilized 40% w/v glucose solution.
- 5. 1.0 M LiAc solution: prepare as a 1.0 M stock in deionized water and filter-sterilize.
- 50% w/v Polyethylene glycol (PEG): add 50 g PEG to 50 mL water and filter-sterilize with a
 0.45 μm filter. Store at room temperature.
- 7. TE buffer: 10 mM Tris-HCl (pH 8.0), 1.0 mM EDTA.
- 8. Single-stranded carrier DNA (ssDNA): add 200 mg of the DNA into 100 mL of TE buffer. Mix by pipetting and then on a magnetic stirrer for 2-3 hours or until fully dissolved. Aliquot DNA into 100 μL volumes and store at -20°C. Prior to use, heat ssDNA to 95°C for 10-30 minutes and cool on ice.
- LiAc SDS buffer: mix 50 μL 1 M LiAc, 25 μL filter-sterilized 10% SDS, 175 μL sterile, deionized water.

10. DNA oligos for PCR-verification of construct integration.

11. 30°C incubator

Optogenetic screening of yeast

96-well plate (black-walled, glass bottom; e.g. Cellvis 96 Well glass bottom plate with #1.5 cover glass)

Illumination device (e.g. optoPlate, LITOS, optoWELL-24)

Plate reader or flow cytometer (e.g. Tecan Spark Multimode Microplate Reader or ThermoFisher Attune NxT Flow Cytometer)

Methods

Perhaps the most important step in the generation of a functional yeast optogenetic system is planning the design of the system including which light-sensitive proteins to employ, the structure of the final construct, and the assembly strategy. This process is described below.

Selection of light-sensitive proteins

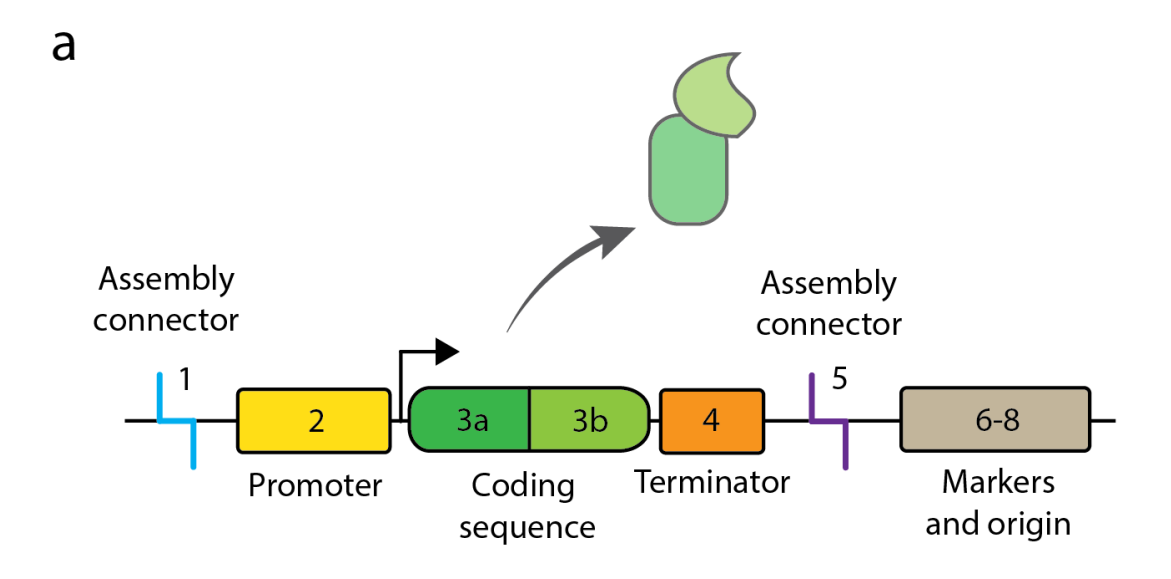
The choice of which light-sensitive proteins to use in the design of the optogenetic system is constrained by several considerations including the inherent photocycle kinetics of the light-sensitive proteins as well as which wavelengths of light can be used to stimulate the optogenetic system. For example, if the optogenetic system is to be used in combination with fluorescence microscopy this limits which wavelengths can be used to excite the light-sensitive proteins. Tolerance of the light-sensitive protein to effector fusion can also be a consideration. Optobase is a valuable resource which provides a summary of light-sensitive proteins excited by

different wavelengths of light as well as associated reference publications[23]. This database can be consulted as a started point to choose several potential light-sensitive proteins. In addition, Figueroa, et al[24] recently compiled a list of light-sensitive proteins that have already proven functional in yeast. It is often advisable to try several different designs, and even several different light-sensitive proteins and empirically test their function, which is why the ability to rapidly clone different optogenetic systems into yeast using the yeast optogenetic toolkit is so powerful.

Selection of standard parts and vectors

The yeast optogenetic toolkit, like many MoClo toolkits, is implemented as a hierarchical assembly process. Assembly of a multigene cassette, capable of integration into the yeast genome to express all aspects of the optogenetic system, requires identification of all of the basic parts needed. "Parts" are the most basic DNA sequence elements that can be assigned a function. For example, promoters, terminators, and coding sequences are all parts as are yeast marker genes and assembly connectors (Fig. 1a). An important decision is what the most basic lightsensitive part should be in the design scheme. For example, one approach is to encode the lightsensitive protein and effector domain as separate coding sequence parts (as in [2]). Alternatively, the light-sensitive protein fused to the appropriate effector domain can be encoded as a single coding sequence part (as in [1]). If a large number of light-sensitive proteins and effectors are to be screened for function in the optogenetic system, it would make sense to encode light-sensitive proteins and effectors as separate 3a and 3b parts so that different combinations can be easily assembled. These parts are then assembled into cassettes, which contain promoter and terminator elements for expression. These cassettes can be stand-alone, and contain a yeast marker and integration homology. Alternatively, if multiple cassettes are needed to express multiple

components in the optogenetic system (for example, for a split light-sensitive transcription factor, which would need at least two cassettes), cassettes can be further combined into multigene cassettes using assembly connectors (**Fig. 1b**). **Figure 1** should be consulted to design an assembly strategy. Many parts are already available [1, 2, 19] (see **Table 1**) and can be obtained from Addgene (https://www.addgene.org/Megan_McClean/).



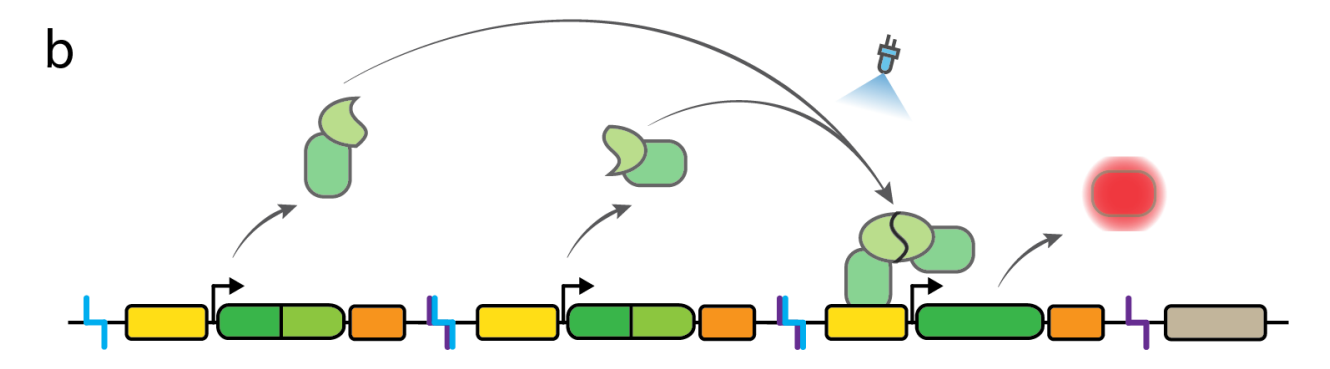


Figure 1. (a) Representative cassette plasmid formed from BsaI assembly of individual part plasmids (numbered). (b) Multigene plasmid formed from BsmBI assembly of multiple cassette plasmids. The first two cassettes express the first and second components of a two-component split optogenetic transcription factor. Light-induced dimerization of the split transcription factor induces expression of the fluorescent reporter on the third cassette.

Assembly and integration of multigene cassettes

Generation of parts

Parts plasmids consist of a DNA functional unit flanked by Type IIS restriction enzyme recognition sites that leave type-specific overhang sequences that allow appropriate assembly order during Golden Gate. While many parts exist (Table 1) if new parts are needed they can be added to the toolkit as follows:

- Set up a BsmBI Golden Gate reaction by pipetting into a 200 μL PCR tube 75 ng of the entry vector plasmid (pYTK001), the insert DNA containing the new part sequence at a 2:1 (insert:vector) molar ratio, 2 μL 10x T4 DNA Ligase Buffer, 1 μL BsmBI-v2 NEB Golden Gate Enzyme Mix, and adjusting the final volume to 20 μL with sterile, deionized water.
- 2. Thermal cycler incubation: $(42^{\circ}\text{C}, 1 \text{ min} \rightarrow 16^{\circ}\text{C}, 1 \text{ min}) \times 30 \rightarrow 60^{\circ}\text{C}, 5 \text{ min} \text{ (see Note 1)}.$
- 3. Transform Golden Gate reaction product into DH5α chemically competent *E. coli* cells (see Note 2). Thaw a tube of DH5α competent *E.coli* cells (50 μl, stored at -80°C) on ice for 5 minutes.
 - a) Add 8 μl assembly reaction product and gently mix by flicking the tube several times.
 Incubate the tube on ice for 30 minutes.
 - b) Perform a heat shock for 30 seconds at 42°C. Return the tube to ice for 2 minutes.
 - c) Add 950 µl of LB medium (or a higher nutrient medium, such as super optimal broth). Incubate at 37°C for 60 minutes with constant mixing, such as on a roller drum.
 - d) Pellet cells by centrifugation and decant the supernatant. Resuspend cells in 200 μl LB medium and plate on LB + chloramphenicol (if more even colony distribution is desired, plate 20 μl on one plate and the remaining 180 μl on a separate plate), incubating overnight at 37°C.

- 4. Transformant screening. BsmBI assembly of a part plasmid will remove sfGFP from the entry vector plasmid and replace it with the desired functional unit part insertion. Thus, *E. coli* that take up the modified plasmid will contain the gene for chloramphenicol resistance (allowing them to grow on LB + chloramphenicol plates), but will not contain sfGFP (meaning they won't fluoresce green). GFP-negative colonies should be selected for culturing (see Note 3).
- 5. GFP-negative colonies are cultured and plasmids are purified using a plasmid miniprep kit according to manufacturer instructions. Construct assembly efficiency is high for most inserts, so preparing two different colonies will typically ensure a correct plasmid is obtained.
- 6. Concentrations of purified plasmids are measured by nanodrop and the sequence of the insert and flanking restriction sites are verified by sequencing. Sanger sequencing (e.g. Functional Biosciences, GENEWIZ) from just outside the insert is a reliable method; however, due to lower costs of whole plasmid sequencing (e.g. Plasmidsaurus), this is also an option.

Cloning of cassette plasmids

Cassette plasmids contain promoter and terminator elements for expressing a desired coding sequence (and should contain part types 1-8; see Fig. 1a). They also contain machinery for replication in *E. coli* (origin and marker) and may also contain yeast markers, homology to the yeast genome, or CEN/ARS4 or 2micron elements (see Note 4). These plasmids are generated by BsaI Golden Gate assembly of the desired part plasmids into a cassette vector, such as pYTK095. If multiple cassettes are to be assembled into a multigene plasmid, they should contain the appropriate connector sequences (part types 1 and 5). For example, a cassette being

integrated into the first position of a multigene plasmid should contain the connectors ConLS and ConR1 (or for the second position, ConL1 and ConR2, and so on).

- 1. Set up a BsaI Golden Gate reaction by pipetting into into a 200 μL PCR tube 75 ng of the vector plasmid (such as pYTK095 when downstream assembly of multiple cassettes into a multigene plasmid is desired), the insert plasmids at a 2:1 (insert:vector) molar ratio, 2 μL 10x T4 DNA Ligase Buffer, 1 μL BsaI NEB Golden Gate Enzyme Mix, and adjusting the final volume to 20 μL with sterile, deionized water.
- 2. Thermal cycler incubation: $(37^{\circ}\text{C}, 5 \text{ min} \rightarrow 16^{\circ}\text{C}, 5 \text{ min}) \times 30 \rightarrow 60^{\circ}\text{C}, 5 \text{ min}$ (see Note 1).
- 3. Transform Golden Gate reaction product into DH5α chemically competent *E. coli* cells (see Note 2) as described in Generation of Parts step 3. Plate cells on LB + selection marker of vector (e.g. carbenicillin for pYTK095).
- 4. Transformant screening. BsaI assembly of a cassette plasmid will remove sfGFP from the vector plasmid and replace it with the desired functional unit part sequences. Thus, *E. coli* that take up the modified plasmid with all inserts will contain the resistance gene (allowing them to grow on, e.g., LB + carbenicillin plates), but will not contain sfGFP (meaning they won't fluoresce green). GFP-positive colonies can be readily identified by placing the plate on a UV transilluminator (see Generation of Parts step 4), allowing for selection of GFP-negative colonies for culturing.
- 5. GFP-negative colonies are cultured and plasmids are purified using a plasmid miniprep kit according to manufacturer instructions. Construct assembly efficiency is high for most sequences, so preparing two different colonies will typically ensure a correct plasmid is obtained.

6. Concentrations of purified plasmids are measured by nanodrop and the sequence of the insert and flanking restriction sites are verified by sequencing. Sanger sequencing (e.g. Functional Biosciences, GENEWIZ) from just outside the insert or whole plasmid sequencing (e.g. Plasmidsaurus) can be performed.

Multigene assembly

Cassettes can be transformed into yeast individually, or if additional transcriptional elements are required can be assembled into multigene plasmids by BsmBI assembly into a vector plasmid, such as pYTK096 (see Fig. 1b). For two-component split transcription factors, each of the two components will typically be encoded in a separate cassette of the multigene plasmid, with an optional reporter cassette also included in the multigene plasmid (see Note 5).

- Set up a BsmBI Golden Gate reaction by pipetting into a 200 μL PCR tube 75 ng of the vector plasmid (such as pYTK096 for integration at URA3), the insert plasmids at a 2:1 (insert:vector) molar ratio, 2 μL 10x T4 DNA Ligase Buffer, 1 μL BsmBI NEB Golden Gate Enzyme Mix, and adjusting the final volume to 20 μL with sterile, deionized water.
- 2. Thermal cycler incubation: $(42^{\circ}\text{C}, 5 \text{ min} \rightarrow 16^{\circ}\text{C}, 5 \text{ min}) \times 30 \rightarrow 60^{\circ}\text{C}, 5 \text{ min}$ (see Note 1).
- 3. Transform Golden Gate reaction product into DH5α chemically competent *E. coli* cells (see Note 2). As described in Generation of Parts step 3. Plate cells on LB + selection marker of vector (e.g. kanamycin for pYTK096).
- 4. Transformant screening. BsmBI assembly of a multigene plasmid will remove sfGFP from the vector plasmid and replace it with the desired cassette sequences. Thus, *E. coli* that take up the modified plasmid with all cassette inserts will contain the resistance gene (allowing them to grow on, e.g., LB + carbenicillin plates), but will not contain sfGFP (meaning they won't fluoresce green). GFP-positive colonies can be readily identified by placing the plate

- on a UV transilluminator (see Generation of Parts step 4), allowing for selection of GFP-negative colonies for culturing.
- 5. GFP-negative colonies are cultured and plasmids are purified using a plasmid miniprep kit according to manufacturer instructions. Construct assembly efficiency is high for most sequences, so preparing two different colonies will typically ensure a correct plasmid is obtained.
- 6. Concentrations of purified plasmids are measured by nanodrop and the sequence of the insert and flanking restriction sites are verified by sequencing. Sanger sequencing (e.g. Functional Biosciences, GENEWIZ) from just outside the insert or whole plasmid sequencing (e.g. Plasmidsaurus) can be performed.

Yeast transformation

- 1. NotI digestion. Multigene plasmids or cassettes designed for integration (see Note 4) can be NotI-digested and transformed into an appropriate yeast strain by mixing 500 ng plasmid with 0.5 μL NotI-HF, 1 μL 10x CutSmart buffer, adjusting the final volume to 10 μL, and incubating at 37°C for at least 15 minutes. Alternatively, plasmids with a CEN6/ARS4 or 2micron origin can be directly transformed into an appropriate yeast strain.
- 2. Yeast are transformed according to published methods[25].
 - a) Grow up a colony of the strain to be transformed in 5 mL YPD on a roller drum at 30°C overnight.
 - b) Add 500 μL of the overnight culture (or 2.5 x 10^s cells) to a 250 mL flask with 50 mL YPD. Grow in a shaking incubator for 3-5 hours (or until the cell titer is at least 2 x 10^s cells/mL).
 - c) Centrifuge cells at 3,130 g for 5 minutes and decant supernatant.

- d) Resuspend cells in 25 mL sterile water. Centrifuge again, decant supernatant, and resuspend cells in 1 mL 100mM LiAc.
- e) Transfer cell suspension to a 1.5 mL tube, centrifuge at 3,000 g, and discard the supernatant by pipetting.
- f) Add 400 μL 100 mM LiAc and resuspend cells by pipetting. Aliquot 50 mL cell mixture into 1.5 mL tubes (one for each transformation), centrifuge at 3,000 g for 2 minutes, and remove supernatant by aspiration.
- g) Add 300 μL transformation mix (240 μL PEG, 35 μL 1.0 M LiAc, 25 μL 2 mg/mL ssDNA) and 70 μL sterile water with 0.1-10 μg (see Note 6) plasmid DNA (NotI-digested if constructs are to be genomically integrated) to each cell pellet.
- h) Resuspend cells by vortex mixing. Incubate for 30 minutes at 30°C (without shaking).
- i) Perform a heat shock by placing the tubes in a water bath at 42°C for 20-25 (up to 40) minutes.
- j) Centrifuge tubes at 3,000 g for 15 seconds and discard supernatant by pipetting.
- k) If cells are being transformed with a drug selection marker (e.g., G418, clonNat, hygromycin, or 5-FOA), perform a recovery step prior to plating: resuspend the cell pellet in 1 mL YPD and incubate at 30°C for 2-18 hours. Centrifuge tubes at 3,000 g for 15 seconds and discard supernatant by pipetting. Disregard this recovery step if plating onto an amino acid deficiency selective plate.
- l) Resuspend cells in 200 μ L sterile water. To ensure single colonies, plate 150 μ L sterile water and 20 μ L cell suspension in one selection plate and the remaining 180 μ L cell suspension in a second selection plate.

- m) Spread the culture on the plates with sterile glass beads and incubate at 30°C for 2-4 days.
- 3. **gDNA preparation.** Construct integration can be verified by PCR (for optogenetic constructs that generate a readily detectable reporter, such as a fluorescent protein, this step can be omitted and transformants can be directly screened for activity as described in Generation of Parts; see Note 7). gDNA is prepared from colonies according to an established LiAc SDS protocol[26] (colony PCR can be directly performed from transformant colonies, but is generally less reliable).
 - a) Add $50 \,\mu\text{L}$ LiAc SDS buffer to a 1.5 mL tube and pick a colony by lightly touching it with a pipette tip and swirling it in the buffer.
 - b) Heat the tube to 70°C for 5 minutes and add 150 µL EtOH.
 - c) Centrifuge tube at 15,000 g for 3 minutes and aspirate the supernatant.
 - d) Resuspend the pellet in 100 µL 70% EtOH. Pellet and aspirate as before.
 - e) Resuspend pellet in 20 μL sterile deionized water. Centrifuge at 15,000 g for 30 seconds to pellet cell debris.
- 4. PCR validation of construct integration. Use 1 μL of the gDNA supernatant (from 3.3.4.3.e) for PCR. Integration of each construct should be validated using two pairs of primers (one for 5' integration and one for 3' integration). For each primer pair, one primer is designed to bind the homologous region, and one primer is designed to bind in the insert, generating, e.g., a 500 bp PCR product that can be verified by gel electrophoresis. Primer sequences for PCR verification of URA3, LEU2, and HO integrations can be found in Supplementary Table S4 of Lee et al, 2015[19].

Screening and validation of optogenetic tools

Once optogenetic systems have been transformed into yeast and integration checked by colony PCR, their functionality (i.e. response to light) should be measured (Figure 2). In this protocol, we will focus on using a commonly used open source illumination solution called the optoPlate[27]. However, many additional illumination solutions are available (see Note 8)

Illumination with optoPlate

- 1. Colonies are picked from YPD plates to test tubes with 3 mL SC media and grown overnight at 30°C on a roller drum.
- 2. Taking care to prevent light exposure of optogenetic strains (see Note 9), dilute overnight cultures to desired density (e.g. OD600 = 0.01-0.5), pipette 100-200 μL into each well of a 96-well plate (black-walled, glass bottom), and incubate for 3-5 hours at 30°C, shaking. Blank media and a non-fluorescent strain should be included as controls if a plate reader will be used for measurements. Each condition is typically performed in triplicate to ensure reliability of results (see Fig. 2a; Note 7).
- 3. Light induction is performed for the length of time desired (typically 1-16 hours; see Note10). Shaking is important for continued growth of cells.

Screening via plate reader

1. The plate reader should first be calibrated to determine the optimal measurement parameters for the desired reporter protein and well plate. This is most easily accomplished using two control strains: a strain with the desired reporter under constitutive expression and a nonfluorescent strain. The Z value (distance between the plate reader and the plate), where applicable, for each well plate is determined by measuring both strains at a range of Z values

- and determining which distance has the largest difference between the reporter and nonfluorescent controls.
- 2. For strains that produce a readily measurable output, such as a fluorescent or bioluminescent reporter, screening of activity can be readily performed in a plate reader. Cultures should be resuspended by shaking prior to measurement (e.g. 1 min shaking at 1,000 rpm with 2 mm orbital), to ensure accuracy of measurement. Inclusion of triplicate (or higher) sample numbers allows for determination of statistical significance between different illumination conditions (such as varying light intensity or duty cycle).

Scanning light intensity and dynamics

Level of gene expression can be readily controlled using light intensity and light duty cycle modulation[28]. The first experiment with a new optogenetic system should use constant illumination to determine whether the system is functioning as desired (see Note 10). Once functionality of the optogenetic system has been established, light intensity, period, and duty cycle can be optimized to achieve desired characteristics (Fig. 2b).

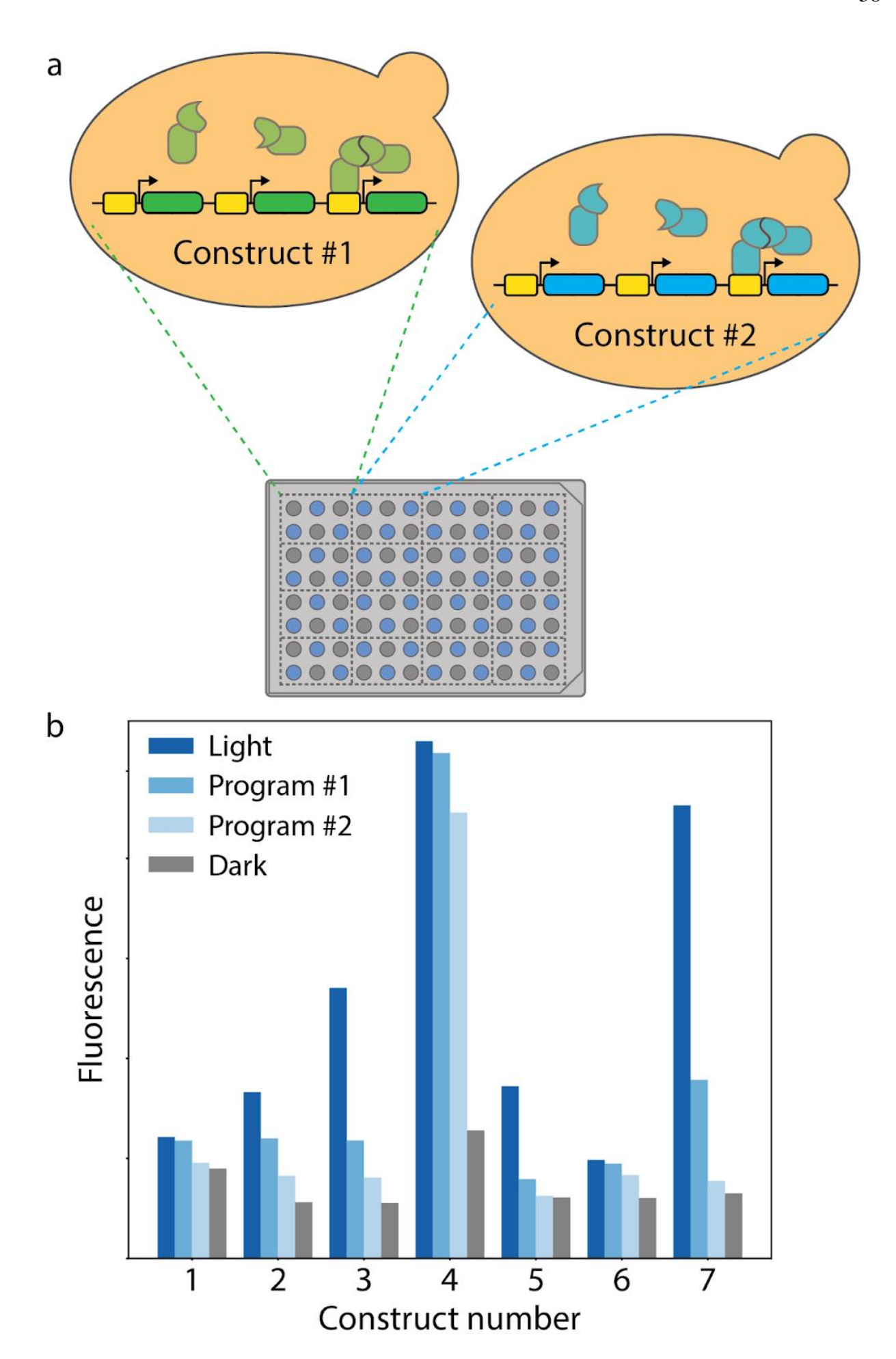


Figure 2. (a) Strains with different constructs are cultured, diluted back, and added to different sections of a 96-well plate with checkerboarded light conditions (to reduce edge effects) performed in triplicate. (b) Sample fluorescence means for each construct and light condition.

Notes

- 3. For higher efficiency Golden Gate assembly reactions (especially with multiple inserts), it is recommended to use the longer incubation time protocol: (37°C or 42°C, 5 min → 16°C, 5 min) x 30 → 60°C, 5 min. Note that the 60°C denaturation step will denature the ligase, but not most Type IIS restriction enzymes (consult enzyme denaturation temperatures from the manufacturer). This is important for cloning plasmids with internal restriction sites (such as when making a GFP-dropout vector), and the 60°C denaturation step should be skipped for such assemblies.
- DH5α is used here as an example. Other cloning competent *E. coli* strains, such as TOP10
 (ThermoFisher Scientific) may also be used, but manufacturer-recommended transformation protocols should be consulted.
- 5. GFP-positive colonies can be readily identified by briefly placing the plate on a UV transilluminator and noting which colonies fluoresce brightly (using proper safety equipment to avoid any UV exposure). Alternatively, the difference between GFP-positive and negative colonies will become more visible after 8-36 additional hours (though plates should be placed at either 4°C or 21°C after 24 hours post-plating to prevent colony overgrowth). This allows selection of GFP-negative colonies for culturing.
- 6. If cassettes are intended to be transformed individually, individual toolkit parts 6-8 can be selected (pYTK074-pYTK094). If multiple cassettes are to be assembled into a multigene plasmid, assembly vector pYTK095 can be used and the resulting transformant colonies

selected on carbenicillin media and screened for GFP dropout. Cassettes to be assembled into a multigene plasmid should be designed with appropriate connectors in mind (e.g. the cassette in the first position of a multigene plasmid should have pYTK002 ConLS and pYTK067 ConR1 in positions 1 and 5). Constructs on plasmids will exhibit greater variability in copy number, but can be maintained at higher copy numbers. Clonal populations of cells with integrated constructs will exhibit more consistent activity and don't need to be grown in selective media to prevent curing of the construct. Strains using fluorescent reporters can be used to rapidly screen the efficacy of different promoter combinations.

- 7. Expression levels for two-component split transcription factors is critical for determining level of activity[1, 29]. More optimal activity will typically be obtained if the AD component is expressed at an equal or higher level than the DBD component, as binding sites in the genome are limited and only localized AD will have the desired effect.
- 8. The amount of DNA may need to be optimized for the specific strain and construct, but 500 ng is usually sufficient to yield tens of colonies for standard strains and constructs.
- 9. For an initial screening of transformants of optogenetic construct that generate a fluorescent or bioluminescent output, transformants can be picked to wells of a 96-well plate and grown overnight at 30°C, shaking. Each culture can be diluted by the same factor. For example, 25 μL cell culture can be transferred to 175 μL SC media, mixing, then transferring 50 μL of that dilution to 150 μL SC media (once each for a light and dark control) in a 96-well plate. This plate can then be incubated in the dark at 30°C, shaking for 5 hours before beginning light induction. It is important to screen multiple transformants from each integration

- transformation as integration copy number variation can occur and can have a significant effect on the activity of the optogenetic system[29].
- 10. Various illumination platforms are available for light induction in microwell plates. The LPA[30] and optoWELL-24[31] (commercially available) are suitable for illumination in 24-well plates. The optoWELL-96[31], LITOS[32] (commercially available) and optoPlate[27] are suitable for induction in higher-capacity plates, such as 96-well plates. There are also more advanced options that allow for control of illumination in chemostat or turbidostat conditions[33–35] and could potentially allow for continuous measurement. However, these systems are not preferred for screening due to low throughput.
- 11. It is ideal to culture and prepare strains for optogenetic experiments exploring light induction response in a dark environment. For blue light sensitive optogenetic strains, red lights can be used for visibility without activating the optogenetic system. Blackout curtains can be used to protect specific areas or pieces of equipment from light, and aluminum foil can be used to cover glass windows in incubators, etc. Some optogenetic proteins, such as CRY2PHR, are highly sensitive to light[29].
- 12. Most strains and optogenetic systems will show the most measurable change in gene expression while cultures are in an exponential phase of growth. For the experimental conditions described here, this will typically occur around 5-8 hours after the start of induction (for strains lacking a significant growth defect). Determining the ideal time to induce and measure is simpler with an automated device that controls illumination and takes regular measurements, such as the optoPlateReader[36], Lustro[29, 37], or other devices[38–40]. When such a device is not available, 12 hours of constant light induction at 100 μW/cm² should allow for measurement of a fluorescent reporter in order to determine the optogenetic

system is functioning as desired. Excess light is mildly phototoxic to yeast[41] and should be avoided for more sensitive experiments.

References

- An-adirekkun J (My), Stewart CJ, Geller SH, Patel MT, Melendez J, Oakes BL, Noyes MB, McClean MN (2020) A yeast optogenetic toolkit (yOTK) for gene expression control in *Saccharomyces cerevisiae*. Biotechnol Bioeng 117:886–893. https://doi.org/10.1002/bit.27234
- Geller SH, Antwi EB, Di Ventura B, McClean MN (2019) Optogenetic Repressors of Gene Expression in Yeasts Using Light-Controlled Nuclear Localization. Cell Mol Bioeng 12:511–528. https://doi.org/10.1007/s12195-019-00598-9
- 3. Yang X, Jost AP-T, Weiner OD, Tang C (2013) A light-inducible organelle-targeting system for dynamically activating and inactivating signaling in budding yeast. Mol Biol Cell 24:2419–2430. https://doi.org/10.1091/mbc.e13-03-0126
- 4. Niopek D, Wehler P, Roensch J, Eils R, Di Ventura B (2016) Optogenetic control of nuclear protein export. Nat Commun 7:10624. https://doi.org/10.1038/ncomms10624
- Niopek D, Benzinger D, Roensch J, Draebing T, Wehler P, Eils R, Di Ventura B (2014)
 Engineering light-inducible nuclear localization signals for precise spatiotemporal control of protein dynamics in living cells. Nat Commun 5:4404.

 https://doi.org/10.1038/ncomms5404
- Lu H, Mazumder M, Jaikaran ASI, Kumar A, Leis EK, Xu X, Altmann M, Cochrane A, Woolley GA (2019) A Yeast System for Discovering Optogenetic Inhibitors of Eukaryotic Translation Initiation. ACS Synth Biol 8:744–757. https://doi.org/10.1021/acssynbio.8b00386
- 7. Rojas V, Larrondo LF (2023) Coupling Cell Communication and Optogenetics: Implementation of a Light-Inducible Intercellular System in Yeast. ACS Synth Biol 12:71–82. https://doi.org/10.1021/acssynbio.2c00338

- 8. Stewart-Ornstein J, Chen S, Bhatnagar R, Weissman JS, El-Samad H (2017) Model-guided optogenetic study of PKA signaling in budding yeast. Mol Biol Cell 28:221–227. https://doi.org/10.1091/mbc.e16-06-0354
- 9. Moreno Morales N, Patel MT, Stewart CJ, Sweeney K, McClean MN (2021) Optogenetic Tools for Control of Public Goods in *Saccharomyces cerevisiae*. mSphere 6:e00581-21. https://doi.org/10.1128/mSphere.00581-21
- Zhao EM, Suek N, Wilson MZ, Dine E, Pannucci NL, Gitai Z, Avalos JL, Toettcher JE (2019) Light-based control of metabolic flux through assembly of synthetic organelles.
 Nat Chem Biol 15:589–597. https://doi.org/10.1038/s41589-019-0284-8
- Pouzet S, Cruz-Ramón J, Le Bec M, Cordier C, Banderas A, Barral S, Castaño-Cerezo S, Lautier T, Truan G, Hersen P (2023) Optogenetic control of beta-carotene bioproduction in yeast across multiple lab-scales. Front Bioeng Biotechnol 11:1085268. https://doi.org/10.3389/fbioe.2023.1085268
- Sweeney K, McClean MN (2022) Transcription Factor Localization Dynamics and DNA
 Binding Drive Distinct Promoter Interpretations. 2022.08.30.505887
- Chen SY, Osimiri LC, Chevalier M, Bugaj LJ, Nguyen TH, Greenstein RA, Ng AH, Stewart-Ornstein J, Neves LT, El-Samad H (2020) Optogenetic Control Reveals Differential Promoter Interpretation of Transcription Factor Nuclear Translocation Dynamics. Cell Syst 11:336-353.e24. https://doi.org/10.1016/j.cels.2020.08.009
- 14. Zhao EM, Zhang Y, Mehl J, Park H, Lalwani MA, Toettcher JE, Avalos JL (2018) Optogenetic regulation of engineered cellular metabolism for microbial chemical production. Nature 555:683–687. https://doi.org/10.1038/nature26141
- 15. Aditya C, Bertaux F, Batt G, Ruess J (2021) A light tunable differentiation system for the creation and control of consortia in yeast. Nat Commun 12:5829.
 https://doi.org/10.1038/s41467-021-26129-7
- Andreou AI, Nakayama N (2018) Mobius Assembly: A versatile Golden-Gate framework towards universal DNA assembly. PLOS ONE 13:e0189892.
 https://doi.org/10.1371/journal.pone.0189892

- 17. Larroude M, Park Y-K, Soudier P, Kubiak M, Nicaud J-M, Rossignol T (2019) A modular Golden Gate toolkit for Yarrowia lipolytica synthetic biology. Microb Biotechnol 12:1249–1259. https://doi.org/10.1111/1751-7915.13427
- 18. Prielhofer R, Barrero JJ, Steuer S, Gassler T, Zahrl R, Baumann K, Sauer M, Mattanovich D, Gasser B, Marx H (2017) GoldenPiCS: a Golden Gate-derived modular cloning system for applied synthetic biology in the yeast Pichia pastoris. BMC Syst Biol 11:123. https://doi.org/10.1186/s12918-017-0492-3
- Lee ME, DeLoache WC, Cervantes B, Dueber JE (2015) A Highly Characterized Yeast Toolkit for Modular, Multipart Assembly. ACS Synth Biol 4:975–986. https://doi.org/10.1021/sb500366v
- 20. Weber E, Engler C, Gruetzner R, Werner S, Marillonnet S (2011) A Modular Cloning System for Standardized Assembly of Multigene Constructs. PLOS ONE 6:e16765. https://doi.org/10.1371/journal.pone.0016765
- Moore SJ, Lai H-E, Kelwick RJR, Chee SM, Bell DJ, Polizzi KM, Freemont PS (2016)
 EcoFlex: A Multifunctional MoClo Kit for E. coli Synthetic Biology. ACS Synth Biol
 5:1059–1069. https://doi.org/10.1021/acssynbio.6b00031
- 22. Fonseca JP, Bonny AR, Kumar GR, Ng AH, Town J, Wu QC, Aslankoohi E, Chen SY, Dods G, Harrigan P, Osimiri LC, Kistler AL, El-Samad H (2019) A Toolkit for Rapid Modular Construction of Biological Circuits in Mammalian Cells. ACS Synth Biol 8:2593–2606. https://doi.org/10.1021/acssynbio.9b00322
- Kolar K, Knobloch C, Stork H, Žnidarič M, Weber W (2018) OptoBase: A Web Platform for Molecular Optogenetics. ACS Synth Biol 7:1825–1828.
 https://doi.org/10.1021/acssynbio.8b00120
- 24. Figueroa D, Rojas V, Romero A, Larrondo LF, Salinas F (2021) The rise and shine of yeast optogenetics. Yeast Chichester Engl 38:131–146. https://doi.org/10.1002/yea.3529
- 25. Gietz RD, Schiestl RH (2007) High-efficiency yeast transformation using the LiAc/SS carrier DNA/PEG method. Nat Protoc 2:31–34. https://doi.org/10.1038/nprot.2007.13

- 26. Lõoke M, Kristjuhan K, Kristjuhan A (2011) EXTRACTION OF GENOMIC DNA FROM YEASTS FOR PCR-BASED APPLICATIONS. BioTechniques 50:325–328. https://doi.org/10.2144/000113672
- 27. Bugaj LJ, Lim WA (2019) High-throughput multicolor optogenetics in microwell plates. Nat Protoc 14:2205–2228. https://doi.org/10.1038/s41596-019-0178-y
- 28. Benzinger D, Khammash M (2018) Pulsatile inputs achieve tunable attenuation of gene expression variability and graded multi-gene regulation. Nat Commun 9:3521. https://doi.org/10.1038/s41467-018-05882-2
- 29. Harmer ZP, McClean MN (2023) Lustro: High-Throughput Optogenetic Experiments Enabled by Automation and a Yeast Optogenetic Toolkit. ACS Synth Biol. https://doi.org/10.1021/acssynbio.3c00215
- 30. Gerhardt KP, Olson EJ, Castillo-Hair SM, Hartsough LA, Landry BP, Ekness F, Yokoo R, Gomez EJ, Ramakrishnan P, Suh J, Savage DF, Tabor JJ (2016) An open-hardware platform for optogenetics and photobiology. Sci Rep 6:35363. https://doi.org/10.1038/srep35363
- 31. optoWELL > opto biolabs. https://optobiolabs.com/products/optowell/. Accessed 30 Mar 2023
- 32. Höhener TC, Landolt AE, Dessauges C, Hinderling L, Gagliardi PA, Pertz O (2022)
 LITOS: a versatile LED illumination tool for optogenetic stimulation. Sci Rep 12:13139.
 https://doi.org/10.1038/s41598-022-17312-x
- 33. Steel H, Habgood R, Kelly CL, Papachristodoulou A (2020) In situ characterisation and manipulation of biological systems with Chi.Bio. PLOS Biol 18:e3000794. https://doi.org/10.1371/journal.pbio.3000794
- 34. Wong BG, Mancuso CP, Kiriakov S, Bashor CJ, Khalil AS (2018) Precise, automated control of conditions for high-throughput growth of yeast and bacteria with eVOLVER. Nat Biotechnol 36:614–623. https://doi.org/10.1038/nbt.4151
- 35. Stewart CJ, McClean MN (2017) Design and Implementation of an Automated Illuminating, Culturing, and Sampling System for Microbial Optogenetic Applications. JoVE J Vis Exp e54894. https://doi.org/10.3791/54894

- 36. Datta S, Benman W, Gonzalez-Martinez D, Lee G, Hooper J, Qian G, Leavitt G, Salloum L, Ho G, Mhatre S, Magaraci MS, Patterson M, Mannickarottu SG, Malani S, Avalos JL, Chow BY, Bugaj LJ (2022) High-throughput feedback-enabled optogenetic stimulation and spectroscopy in microwell plates. 2022.07.13.499906
- 37. Harmer ZP, McClean MN (2023) High-Throughput Optogenetics Experiments in Yeast Using the Automated Platform Lustro. JoVE J Vis Exp e65686. https://doi.org/10.3791/65686
- 38. Melendez J, Patel M, Oakes BL, Xu P, Morton P, McClean MN (2014) Real-time optogenetic control of intracellular protein concentration in microbial cell cultures. Integr Biol 6:366–372. https://doi.org/10.1039/c3ib40102b
- 39. Bertaux F, Sosa-Carrillo S, Gross V, Fraisse A, Aditya C, Furstenheim M, Batt G (2022) Enhancing bioreactor arrays for automated measurements and reactive control with ReacSight. Nat Commun 13:3363. https://doi.org/10.1038/s41467-022-31033-9
- 40. Benisch M, Benzinger D, Kumar S, Hu H, Khammash M (2023) Optogenetic closed-loop feedback control of the unfolded protein response optimizes protein production. Metab Eng. https://doi.org/10.1016/j.ymben.2023.03.001
- 41. Robertson JB, Davis CR, Johnson CH (2013) Visible light alters yeast metabolic rhythms by inhibiting respiration. Proc Natl Acad Sci U S A 110:21130–21135. https://doi.org/10.1073/pnas.1313369110

Table 1.

| ID | Туре | Description | E coli marker | Reference |
|---------|------|-------------|------------------|-----------------------------------|
| pMM0923 | 3 | Gal4AD-CIB1 | CamR | Harmer et al. 2023 ACS Synth Biol |
| pMM1235 | 3 | mScarlet-I | CamR | Harmer et al. 2023 ACS Synth Biol |
| pMM0918 | 3a | Gal4DBD | CamR | Harmer et al. 2023 ACS Synth Biol |
| pMM1245 | 3a | eMagB | CamR | Harmer et al. 2023 ACS Synth Biol |
| pMM1246 | 3b | eMagA | CamR | Harmer et al. 2023 ACS Synth Biol |

| pMM1258 | 3a | eMagBF | CamR | Harmer et al. 2023 ACS Synth Biol |
|---------|----|-----------------------|------|---|
| pMM1259 | 3b | eMagAF | CamR | Harmer et al. 2023 ACS Synth Biol |
| pMM1260 | 3a | eMagBM | CamR | Harmer et al. 2023 ACS Synth Biol |
| pMM1247 | 3b | Gal4AD | CamR | Harmer et al. 2023 ACS Synth Biol |
| pMM0920 | 3b | CRY2(535) | CamR | Harmer et al. 2023 ACS Synth Biol |
| pMM0921 | 3b | CRY2PHR | CamR | Harmer et al. 2023 ACS Synth Biol |
| pMM0922 | 3b | CRY2FL | CamR | Harmer et al. 2023 ACS Synth Biol |
| pMM0531 | 3 | VP16-CIB1 | CamR | An-adirekkun et al. 2020 <i>Biotechnol Bioeng</i> |
| pMM0530 | 3 | Zif268DBD- CRY2PHR | CamR | An-adirekkun et al. 2020 Biotechnol Bioeng |
| pMM0529 | 3 | Zif268DBD-CRY2 | CamR | An-adirekkun et al. 2020 Biotechnol Bioeng |
| pMM769 | 3a | dCas9-NLS | CamR | Geller et al. 2019 Cell Mol Bioeng |
| pMM768 | 3b | dCas9-NLS | CamR | Geller et al. 2019 Cell Mol Bioeng |
| pMM767 | 3 | dCas9-NLS | CamR | Geller et al. 2019 Cell Mol Bioeng |
| pMM766 | 3b | dCas9-NLS-Stop | CamR | Geller et al. 2019 Cell Mol Bioeng |
| pMM765 | 3 | dCas9-NLS-Stop | CamR | Geller et al. 2019 Cell Mol Bioeng |
| pMM729 | 3 | Mxi1-dCas9 | CamR | Geller et al. 2019 Cell Mol Bioeng |
| pMM728 | 3b | Mxi1 | CamR | Geller et al. 2019 Cell Mol Bioeng |
| pMM727 | 3 | Mxi1 | CamR | Geller et al. 2019 Cell Mol Bioeng |
| pMM726 | 3a | Mxi1 | CamR | Geller et al. 2019 Cell Mol Bioeng |

| pMM725 | 4a | Linus-Mxi | CamR | Geller et al. 2019 Cell Mol Bioeng |
|--------|----|-----------|------|------------------------------------|
| pMM587 | 3b | dCas9 | CamR | Geller et al. 2019 Cell Mol Bioeng |
| pMM586 | 3 | dCas9 | CamR | Geller et al. 2019 Cell Mol Bioeng |
| pMM585 | 3a | dCas9 | CamR | Geller et al. 2019 Cell Mol Bioeng |
| pMM582 | 4a | Linus | CamR | Geller et al. 2019 Cell Mol Bioeng |

CHAPTER FOUR: DYNAMIC MULTIPLEXED CONTROL AND MODELING OF OPTOGENETIC SYSTEMS USING THE HIGH-THROUGHPUT OPTOGENETIC PLATFORM LUSTRO

Zachary P Harmer¹, Jaron C. Thompson^{2,3}, David L. Cole², Victor M. Zavala², and Megan N McClean^{1,4,*}

- Department of Biomedical Engineering, University of Wisconsin-Madison, Madison, Wisconsin 53706, United States
- ² Department of Chemical and Biological Engineering, University of Wisconsin-Madison,
 Madison, Wisconsin 53706, United States
 - ³ Department of Biochemistry, University of Wisconsin-Madison, Madison, Wisconsin 53706, United States
 - ⁴ University of Wisconsin Carbone Cancer Center, University of Wisconsin School of Medicine and Public Health, Madison, Wisconsin 53706, United States

Email: mmcclean@wisc.edu

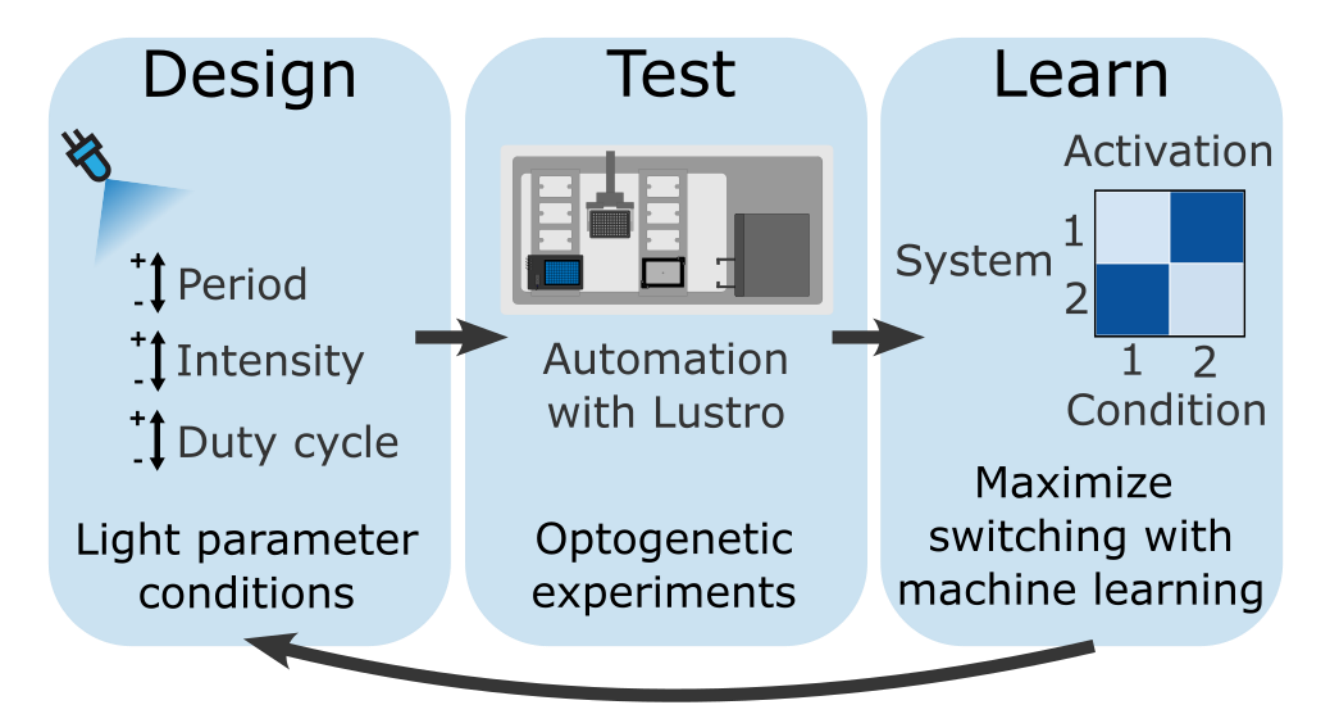
Intended for ACS Synthetic Biology

Abstract:

This paper presents an integrated framework leveraging Lustro, a powerful high-throughput optogenetics platform, and machine learning tools to enable multiplex control over blue light-sensitive optogenetic systems in budding yeast. We use Lustro to characterize a suite of optogenetic transcription factors and empirically identify conditions for dynamic multiplexed control over those optogenetic systems. Specifically, we identify conditions for sequential activation and switching between several pairs of optogenetic systems. We used the high-

throughput data generated from Lustro to build a Bayesian optimization framework that incorporates data-driven learning, uncertainty quantification, and experimental design, for enabling the prediction of system behavior and the identification of optimal conditions for simultaneous multiplexed control of blue-inducible optogenetic systems. This work lays the foundation for designing advanced synthetic biological circuits with optogenetics and has broad applications in biotechnology and functional genomics.

Keywords: optogenetics, automation, MoClo, yeast, high throughput, synthetic transcription factors, neural network, modeling, machine learning, multiplexing



Introduction:

Optogenetics is the use of light-sensitive proteins as biological effectors. Using light as an inducer has revolutionized our ability to precisely control cellular behavior. By leveraging genetically encoded light-sensitive proteins, optogenetics empowers researchers to orchestrate cellular processes with exquisite spatiotemporal precision. Optogenetic technologies have found

diverse applications, ranging from modulating gene expression, to elucidating intricate signaling pathways in, manipulating protein localization, or inducing targeted protein degradation. A significant restriction in optogenetics is the fact that most optogenetic switches are blue light-responsive. limiting the amount of biology that can be controlled simultaneously using light. One approach to overcome this restriction is dynamic multiplexing, where different light pulsing programs (of the same wavelength) are used to selectively activate different optogenetic switches. In this work, we present a strategy for taking advantage of the native differences in response kinetics of different optogenetic systems to identify conditions that allow for dynamic multiplexed control over those optogenetic systems. In order to identify these conditions, we used the previously described high-throughput automated optogenetics platform, Lustro^{1,19}. The Lustro platform employs an automation workstation equipped with a robotic gripper arm, an illumination device, a plate shaker, and a plate reader. Lustro was developed to perform automated high-throughput optogenetic experiments, collecting data over time for a wide range of light conditions. This allows us to efficiently characterize the activity of a suite of optogenetic systems in response to light programs with varying pulse intensity, period, and duty cycle.

Multiplexing involves independent and simultaneous control of multiple optogenetic systems, allowing for a higher degree of control over complex cellular functions. Benzinger and Khammash developed one strategy for dynamic multiplexed control of optogenetic systems by taking advantage of known mutants of the optogenetic system EL222 that have different response kinetics and built a falling edge detector in order to generate a different light pulse induction response profile from another optogenetic system, CRY2/CIB1, at the level of gene expression. However, many other types of dynamic multiplexed control over optogenetic

systems are possible, such as sequential activation (taking advantage of different light sensitivities between optogenetic systems) or independent switching (taking advantage of different response kinetics to control activation of different optogenetic systems). The response kinetics of optogenetics systems *in vivo* are not well understood and are difficult to measure quickly. The ability to rapidly construct and characterize optogenetic systems, coupled with data-driven modeling, presents a promising avenue to navigate this challenge, cutting down the search space to find maximally differentiated outputs for tailored multiplexing schemes.

In this work, we use the high-throughput data-generating capabilities of Lustro to characterize a set of 13 blue light-responsive optogenetic split transcription factors (TFs). Optogenetic split TFs use an optical dimerizer protein pair fused to a DNA-binding domain and an activation domain, such that light-induced dimerization of the protein pair reconstitutes the split TF and expression of the gene of interest is induced. We selected optogenetic split TFs for developing multiplexing strategies as their activity can be readily measured using a fluorescent protein reporter, control of gene expression is useful for a broad range of biological applications, and many mutants of optical dimerizers with different response kinetics are known (see Table 1). We used this high-throughput characterization to empirically identify sets of light conditions that result in different types of behavior for different blue light-sensitive optogenetic systems, allowing us to multiplex control over them using the different light pulsing patterns. We identified conditions for sequential activation, where differences in light sensitivity between optogenetic systems result in light intensities activating each optogenetic system a different amount. We also identified conditions for "switching," where one light induction program preferentially activates one optogenetic system over a second, but where switching to a second light program results in preferential activation of the second optogenetic system over the first.

We combine the high-throughput characterization with a Bayesian machine learning framework that aims to predict and optimize objectives for optogenetic control. Furthermore, we highlight the symbiotic relationship between high-throughput data collection and predictive models, showcasing how their integration can unravel the complexities of optogenetic systems, paving the way for a new era of finer cellular control and optimization.

Results and Discussion:

Characterization of Optogenetic Transcription Factors Using Lustro

Lustro² was used to characterize the expression profiles of a set of blue light-sensitive split transcription factors (see Table 1) in response to different light induction programs. These optogenetic strains drive expression of a fluorescent protein, mScarlet-In, allowing measurement of gene induction level by proxy measurement of fluorescence level. Square-wave light pulses were used to induce optogenetic strains, varying the light pulse intensity, period, and duty cycle between conditions. The response of each optogenetic system to this range of light inputs is dependent on the response kinetics (activation and reversion time) of the light-sensitive proteins as well as their native light sensitivity. Relative induction level of a strain is determined for each condition by comparing fluorescence measurements under those conditions to the fluorescence of the constant light and constant dark control conditions for that same strain. This allows comparisons of relative activation amounts to be made between strains, even when the magnitude of response of one strain differs significantly from another. While in-depth characterizations have been performed for a subset of optogenetic tools22.23, this sweep directly compares response kinetics and sensitivity of a range of optogenetic systems side-by-side in the same biological context. The maximum period used for screening light induction conditions was

limited to 4 hours (with data being compared at 10 hours into induction), as longer periods will be less relevant for many applications.

| Optical dimerizer | Binding partner | Description |
|----------------------|-----------------------------|--|
| eMagA | eMagB, eMagBF, or eMagBM | Enhanced magnet dimerizer ²⁴ |
| eMagAF | eMagB, eMagBF, or eMagBM | Enhanced magnet dimerizer with faster response kinetics ²⁴ |
| eMagB | eMagA or eMagAF | Enhanced magnet dimerizer ²⁴ |
| eMagBF | eMagA or eMagAF | Enhanced magnet dimerizer with faster response kinetics ²⁴ |
| eMagBM | eMagA or eMagAF | Enhanced magnet dimerizer with slower response kinetics ² |
| CRY2FL | CIB1 | Full length CRY2 ²² |
| CRY2PHR | CIB1 | CRY2 truncation (residues 1-498 of CRY2) ²⁵ |
| CRY2(535) | CIB1 | CRY2 truncation (residues 1-535 of CRY2) ²² |
| CRY2PHR (L348F) | CIB1 | Long-reversion mutant of CRY2PHR ²² |
| CRY2PHR (W349R) | CIB1 | Short-reversion mutant of CRY2PHR ²² |
| EL222 | N/A (homodimerizer) | Homodimerizer with fast activation and reversion response kinetics ²⁶ |
| EL222 (A79Q) | N/A (homodimerizer) | Medium-reversion mutant of EL222 ²² |
| EL222 (AQTrip) | N/A (homodimerizer) | Long-reversion mutant of EL222 ²² |

Table 1. Optogenetic split TFs characterized in this work (Figure 1). Additional plasmid information in Table S3.

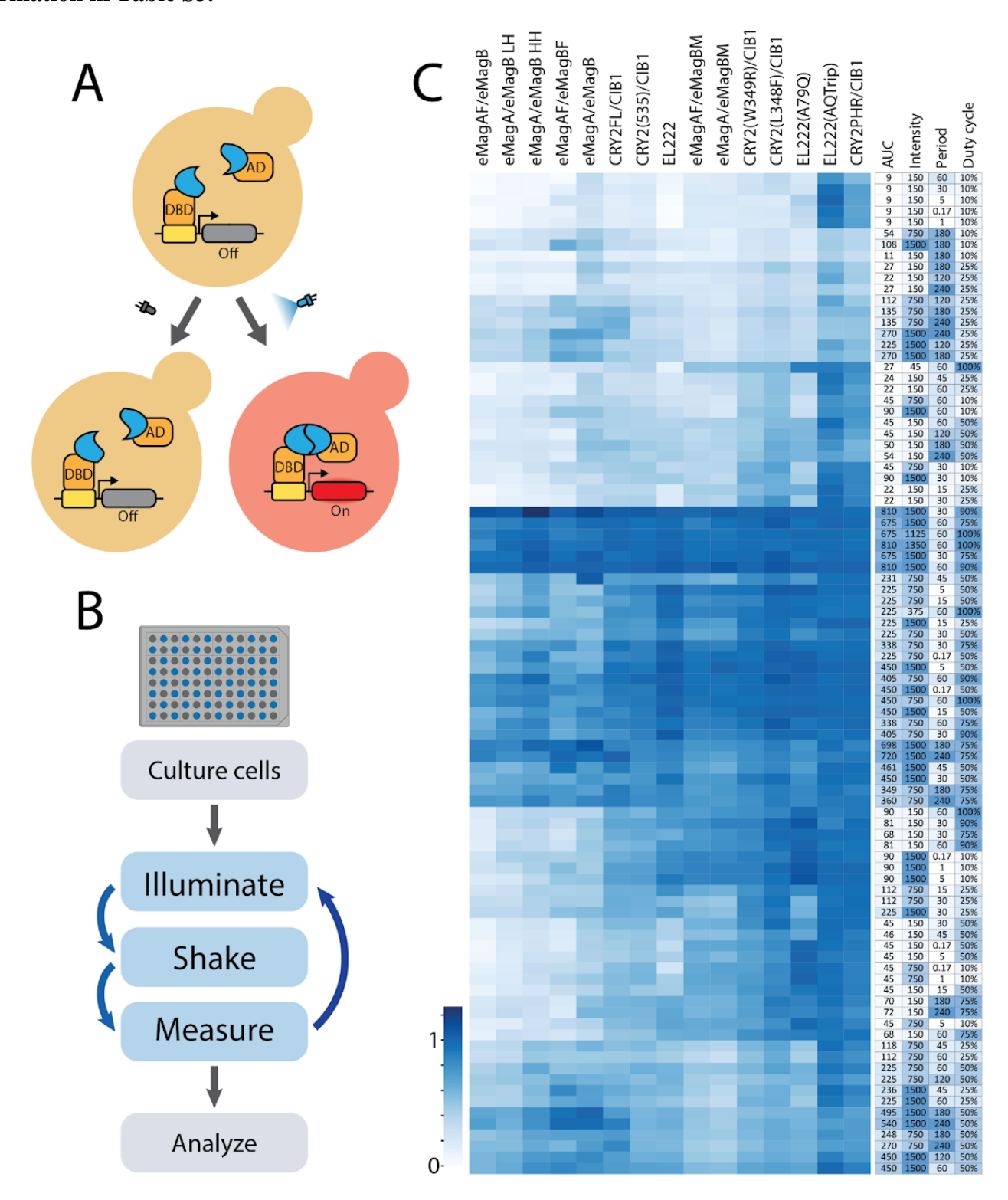


Figure 1. (A) Diagram showing activation of an optogenetic split TF. Blue light causes the split TF to dimerize, inducing expression of the gene of interest (mScarlet-I), causing red fluorescence to increase in the cell. (B) Lustro workflow.Using laboratory automation, cells are cultured in a 96-well plate and subjected to successive rounds of illumination, shaking, and measuring, every 30 minutes. Fluorescence values are measured and analyzed. (C) Lustro was used to characterize the responses of several different optogenetic split TFs to varying light pulse intensity (μW/cm²), period (min), and duty cycle (%). AUC (area under the curve) is in μW·hr/cm². Data shown are relative fluorescence levels (where the constant dark value is set to 0 and the constant light value is set to 1) collected 10 hours into light induction for the given strains. LH and HH designate relative expression levels of the two components of a split TF² (yMM1760 and yMM1761; see Table S1), used here to demonstrate that changes in relative expression levels affect the response kinetics of two-component split TFs.

Sequential Activation of Optogenetic Systems

Data from the initial scan (Figure 1) were used to identify candidates for sequential activation, where the first light program preferentially activates one optogenetic system of a pair, and the second light program activates both optogenetic systems. Sequential activation could be useful for bioproduction processes where different stages of fermentation are desired to optimize yield. CRY2(L348F)/CIB1 and eMagAF/eMagBF were identified as a candidate pair. CRY2(L348F)/CIB1 is very sensitive to light intensity and reaches a high level of activation at low light doses. eMagAF/eMagBF is less sensitive to light intensity, requiring a higher dose of light to reach maximal activation. In order to demonstrate that sequential control of blue light systems in the same strain is possible, the pair was cloned into the same strain with CRY2(L348F)/CIB1 driving expression of mScarlet-I and eMagAF/eMagBF driving expression of a second, orthogonal reporter, miRFP680^{as} (and using an orthogonal DNA-binding domain, LexA^{as}). Each strain was characterized in response to a range of light intensities using Lustro (see Figure 2).

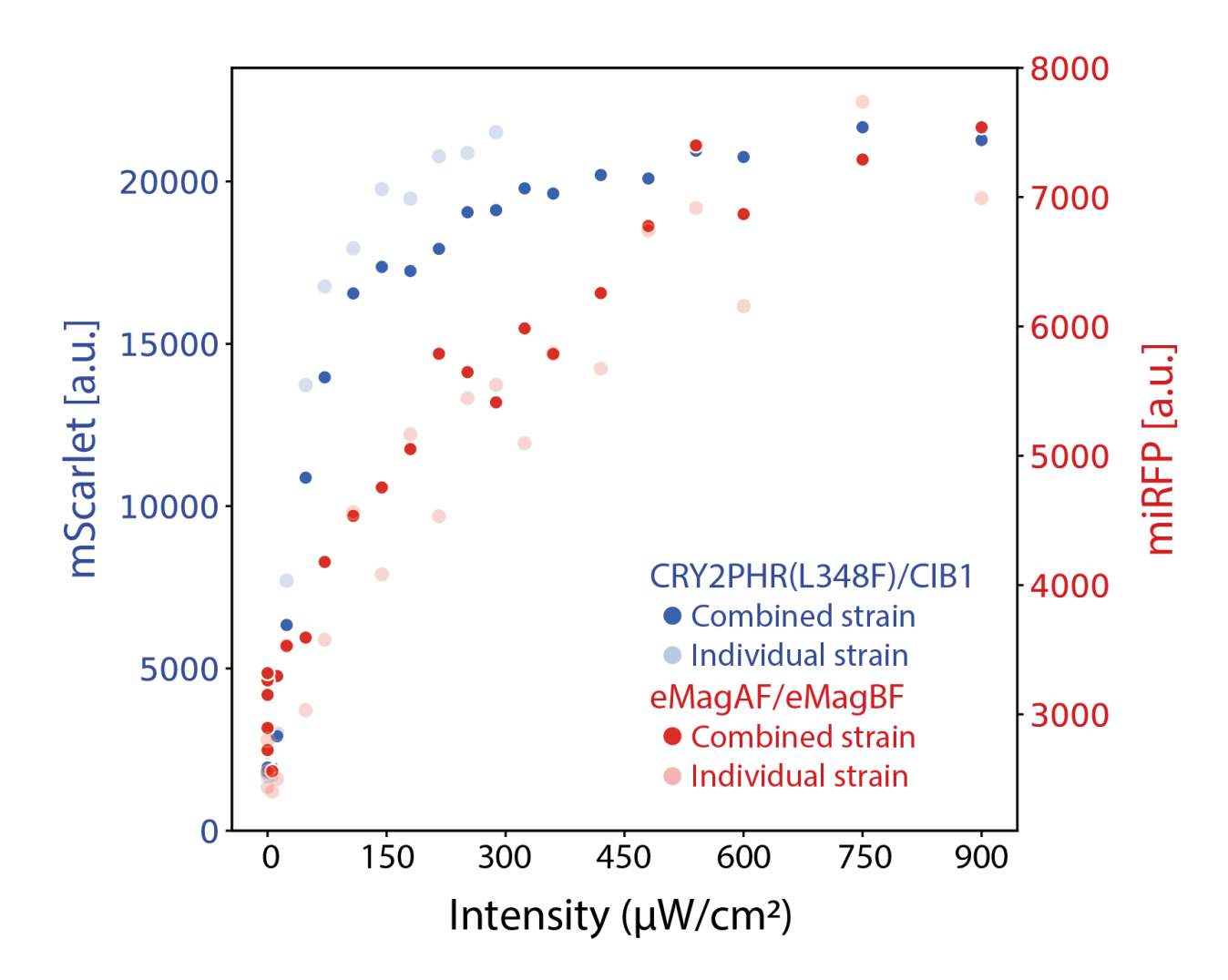


Figure 2. Sequential activation of optogenetic systems by a range of light intensities tested with Lustro. Two optogenetic systems are compared, CRY2PHR(L348F)/CIB1 and eMagAF/eMagBF, both engineered into the same strain (yMM1826; darker dots) and each in an individual strain (yMM1825 and yMM1781; lighter dots). The CRY2PHR(L348F)/CIB1 split TF drives expression of mScarlet (blue dots) and the eMagAF/eMagBF split TF drives expression of an orthogonal fluorescent reporter, miRFP680 (red dots). Values shown were measured after 10 hours of constant light induction. The CRY2PHR(L348F)/CIB1 system activates at lower light intensities than the eMagAF/eMagBF system.

Multiplexed Control for Switching Between Optogenetic TFs

We next identified candidate pairs of optogenetic systems for dynamic multiplexed control over switching states¹² (Figure 3). We took advantage of the characterization of different response kinetics (activation and reversion) and sensitivity in response to different light pulses

from the initial screen performed (see Figure 1). We empirically compared relative activation amounts between optogenetic systems and conditions in a pairwise manner to find where switching occurs. That is, where one system is activated more than another until the light pulsing condition is changed, then the second system is activated more than the first. 16 candidate pairs were further validated in technical quadruplicate (with a subset shown in Figure 3B). Additional switching pairs are found in Figure S2, as well as other interesting types of behaviors, such as where one light condition induces both strains to similar relative fluorescence or one strain of a pair that stays at similar relative activation between two light conditions while the other strain switches. These optogenetic split TFs were characterized in separate strains, as any strain pair combination that uses the same binding partners will freely interact and change the optogenetic activation profiles.

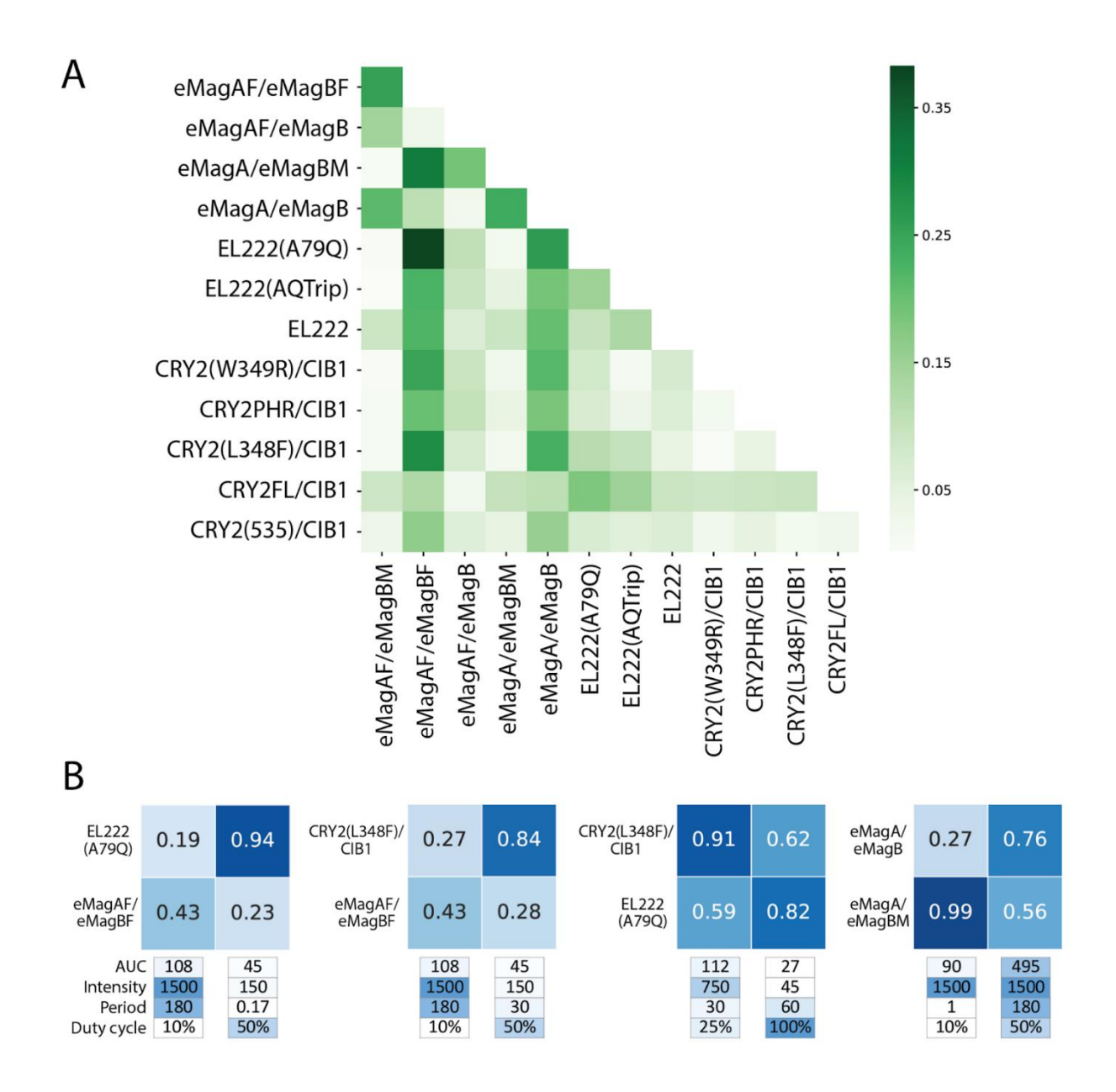


Figure 3. (A) Multiplexing potential for given optogenetic system pairs. First, pairwise differences between relative activation for all light conditions tested (Figure 1) for each pair of strains are calculated. The pair of light conditions that yields the highest product of differences for each pair of optogenetic systems is then calculated and plotted as a heat map (higher values of the product of differences are represented by darker blue squares). (B) Validation of pairs of optogenetic systems that switch relative activation amounts between two different light induction conditions. Intensity is measured in μW/cm², period in min, duty cycle by %, and AUC (area under the curve) is in μW·hr/cm². Data shown are averaged quadruplicates of relative fluorescence, recorded at 10 hours into induction. Additional examples are presented in Figure S2.

Response dynamics are insensitive to activation domain strength

While the objective functions used in this work aim to optimize relative induction levels, the scale of response of a particular optogenetic TF can be adjusted using synthetic biology techniques. Here, we demonstrate that swapping out the activation domain of a split TF can be used to tune the overall level of response of the system (Figure 4). Previous approaches integrate circuits to tune the response of an optogenetic system or generate different types of response behavior, such as OptoINVRT¹² and OptoAMP¹². Such circuits could be combined with this multiplexed control strategy to enable more types of optogenetic control and finer control of biological behavior.

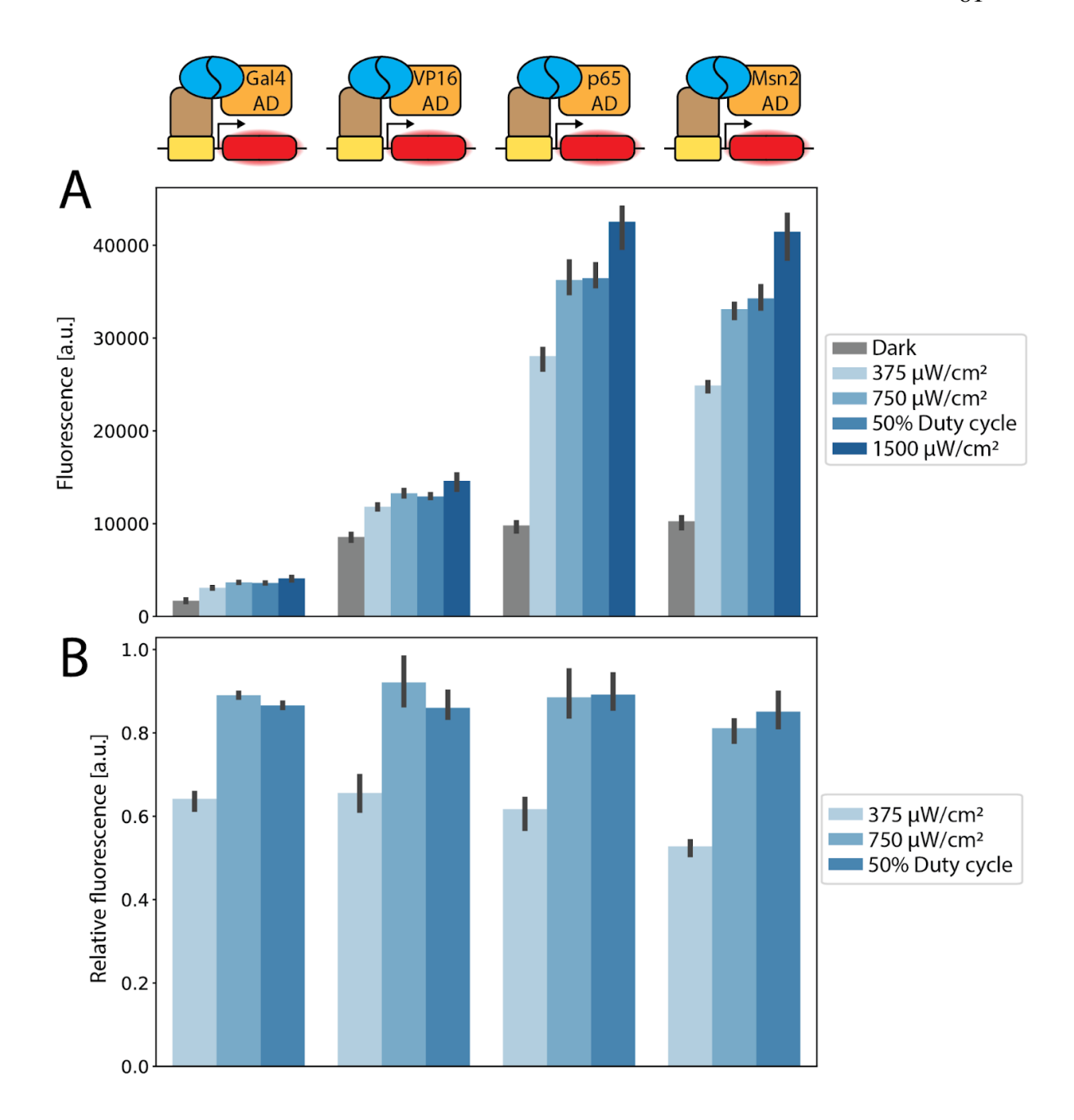


Figure 4. Activation domain swapping. (A) eMagA/eMagB split TF strains utilizing different activation domains are tested under a range of light conditions. Fluorescence values are shown after 10 hours of induction, with each condition performed in triplicate. Different activation domains exhibit widely different activation ranges, allowing for tunability of gene expression response to optogenetic induction. The 50% duty cycle condition has an intensity of 1500 $\mu W/cm^2$ and a period of 2 s. (B) Comparison of relative induction level (scaling each dark condition to 0 and each light condition to 1) for intermediate light induction conditions of each activation domain. An ANOVA test did not find a significant difference between relative activation levels between strains (p > 0.5).

Predicting System Behavior Using Machine Learning

We next sought to apply the high-throughput data collected by Lustro to generate a predictive model that would allow for selection of bespoke objective functions for various biological applications. We used a feedforward neural network (NN) to predict the relative induction of each strain given the duty cycle, intensity, and period of the light condition. To train the neural network, we used a Bayesian inference approach to determine an approximate Gaussian distribution for the parameter posterior. To evaluate model prediction performance of relative induction, we used 20-fold cross validation. This process involves dividing the data into 20 subsets, training on 19 of the subsets, and evaluating prediction performance on the held-out set. The process is repeated 20 times so that each subset is subjected to held-out testing. Prediction performance (Pearson correlation) is computed by comparing the measured relative induction to the predicted relative induction for every condition in the data set (Fig 5). The NN predicted relative induction with a Pearson correlation that ranged from 0.75 to 0.98, demonstrating that this data-driven approach provides accurate predictions of system behavior. We also highlight that the construction of this type of powerful machine learning model is enabled by the high-throughput data collection capabilities of Lustro.

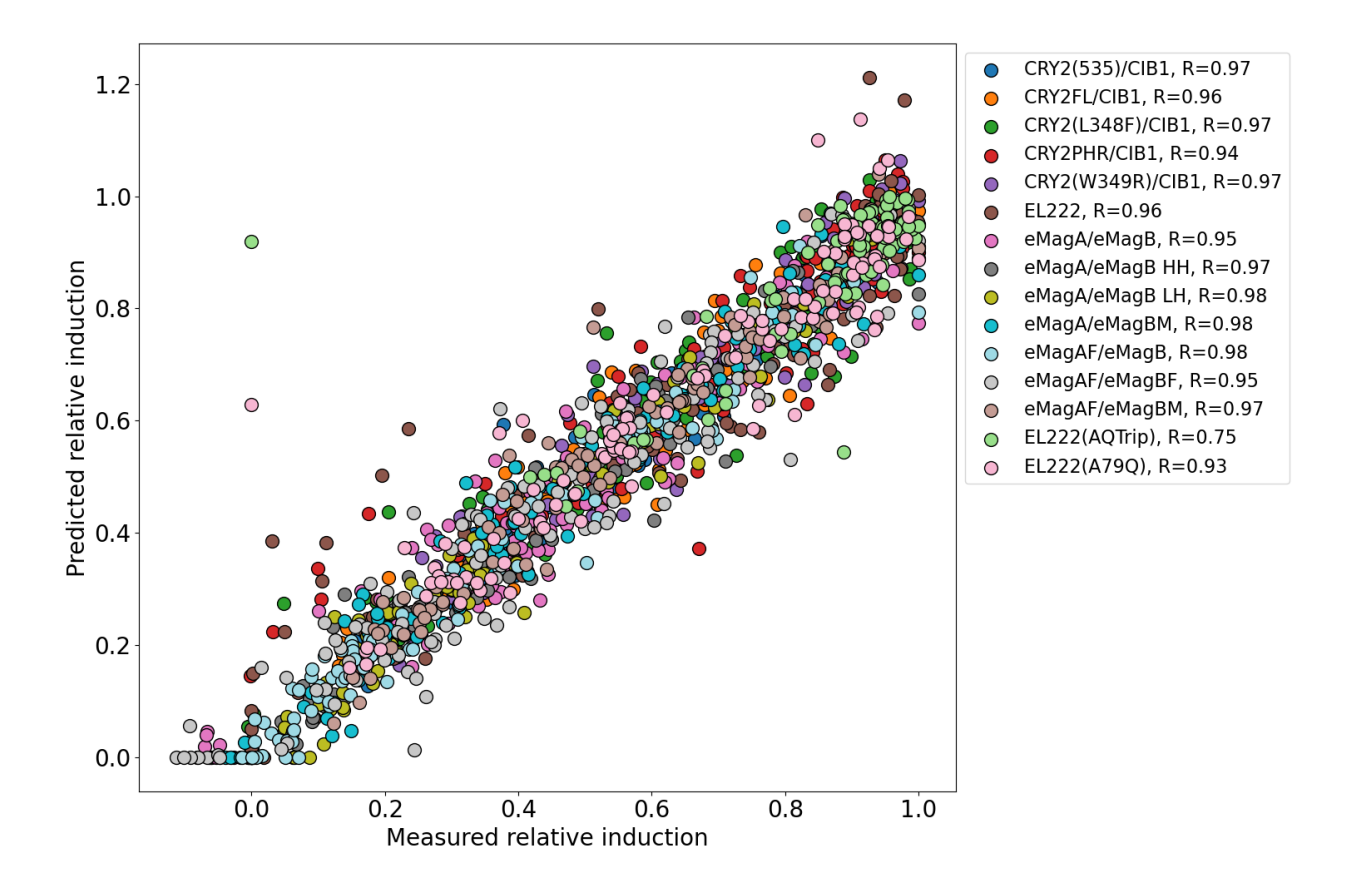


Figure 5. Prediction performance of relative induction using the machine learning model.

Bayesian Optimization for Maximizing Switching

Once trained, the NN can be used to guide the design of experiments to select pairs of light conditions that maximize predicted switching in induction levels between two optogenetic systems. We therefore define an experimental condition as a pair of light conditions applied to a pair of strains. The batch data-collection capabilities of the Lustro platform enable the use of a Bayesian optimization algorithm called Thompson sampling that selects experimental conditions predicted to maximize the difference in induction between each strain pair. We use an approximate Bayesian inference approach to infer the posterior parameter distribution of the NN. Once equipped with a posterior parameter distribution, Thompson sampling involves sampling parameter values from the posterior, and using the resulting model to identify the

condition that maximizes the objective. The process of randomly sampling from the posterior and selecting an experimental condition that optimizes the design objective can be repeated in order to design a batch of experimental conditions. To demonstrate the potential utility of this approach, we defined a design space of pairs of light conditions scanning a range of light intensities, duty cycles, and periods. We then used a NN trained on all available experimental data to predict relative induction of all strains for all conditions in the design space. We used these model predictions as a 'ground truth' dataset relating light conditions to strain induction. We then randomly selected a batch of 10 light conditions as a preliminary dataset and used this preliminary dataset to train a new NN. Using the trained model, 10 new pairs of light conditions were selected using the Thompson sampling approach to optimize an objective function defined as the negative of the product of the difference in induction levels between all pairs of strains. The set of selected light conditions and corresponding induction levels of each strain were then queried from the ground truth dataset and appended to the training data, which was then used to update the model. The process of selecting a new set of 10 pairs of light conditions was continued over 5 rounds (each round containing a batch of experiments). The overall process was repeated over 10 trials to assess the variation in the ability of the model to optimize the system. We found that when compared to random selection of light programs, the Bayesian optimization framework quickly identified combinations of light conditions that approach the maximum possible switching in relative induction levels. These results illustrate how Lustro and machine learning can be combined to quickly identify optogenetic systems with desirable switching properties.

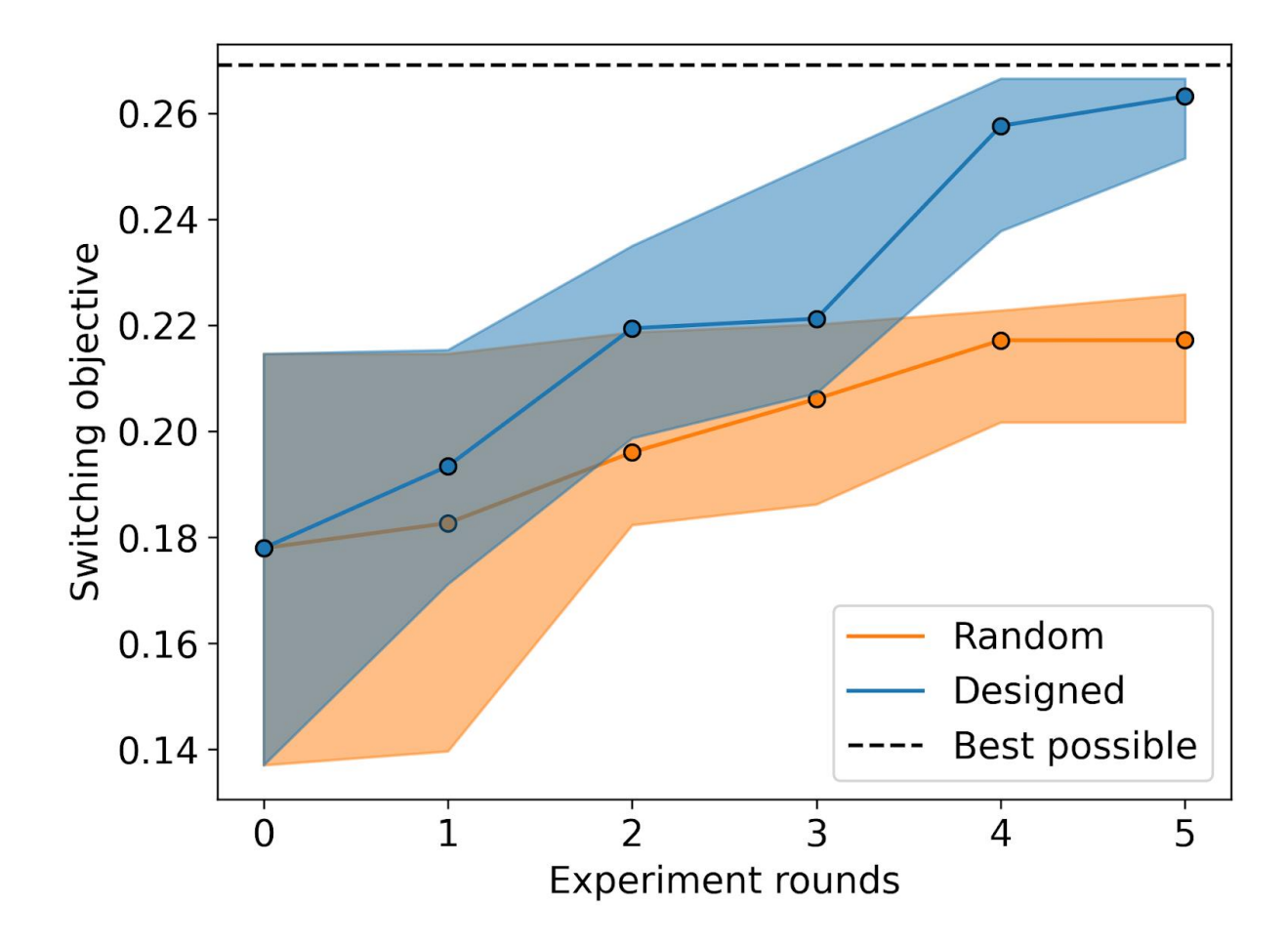


Figure 6. Validation of batch experimental design algorithm using the Bayesian optimization framework. Using simulated experimental data, a neural network was initialized with data from 10 randomly selected light conditions. Using the trained model, a Thompson-sampling Bayesian optimization algorithm was used to select new pairs of light conditions in subsequent experiment rounds. Compared to random selection, the model-guided experimental design algorithm more efficiently identifies conditions with improved switching in induction levels. Solid lines indicate the median performance taken over 10 trials in which the initial set of light conditions was randomly selected and shaded regions represent the interquartile range.

Conclusion:

We characterized a diverse array of blue light-sensitive optogenetic systems, providing a comprehensive foundation for advancing our understanding and manipulation of these crucial biological tools. We described a strategy for dynamic multiplexed control of optogenetic systems

that takes advantage of the native differences in response kinetics between different photoswitches. We used this approach to identify conditions for sequential activation and "switching" between optogenetic systems, enhancing our command over intricate biological processes. We also demonstrated the ability to tune the magnitude of response of an optogenetic system by swapping out the activation domain of the TF, which adds a layer of flexibility for a spectrum of biological applications.

Leveraging the predictive capabilities of a NN model, we harnessed the power of datadriven insights to forecast the response of optogenetic systems to specific light conditions. In a simulated example, we showed that the proposed Bayesian optimization approach could rapidly identify candidate strain and light pairs that optimize switching in relative induction.

In parallel, the implementation of workflow validation with batching represents a strategic leap towards more efficient experimental design. By systematically reducing unnecessary iterations, we have streamlined the process, optimizing experimental efficiency without compromising on data integrity. This methodological innovation promises to be instrumental in the design and execution of future experiments.

While we implemented this strategy for multiplexing optogenetic systems in split TFs here, we propose that this method can be extended to other types of optogenetic switches. For example, this strategy could be applied to characterize and optimize other optogenetic split protein systems, such as split Cas13 systems for regulating RNA in mammalian cells. The strategy could also be applied to multiplex control over optogenetic systems that regulate protein localization or oligomerization. Multiplexed control over optogenetic systems that regulate different types of behavior, such as controlling activity of a split TF and localization of a signaling protein, could be developed. The synergistic integration of high-throughput data

collection from Lustro, NN predictive modeling, and workflow validation techniques offers a potent toolkit for advancing the frontiers of biological control. These multiplexed control strategies could be used to optimize bioproduction processes design engineered living materials, control microbial community structures, or interrogate complex cellular gene expression networks. Combining high-throughput characterization with machine learning to predict and optimize the behavior of biological systems will rapidly accelerate the optogenetic design, build, test cycle for optogenetic systems.

Methods:

Strain Construction and Culture Conditions

Strains used in this study were constructed using standard molecular biology techniques, specifically a modular Type IIS Golden Gate assembly toolkit as previously described. The details of constructs used in this work can be found in Table S3 and Table S5. Part plasmids (Level 0) were created through BsmBI Golden Gate assembly of PCR-amplified products (refer to Table S2 for primer details) or gBlocks (see Table S4) into the yTK entry vector (yTK001). Following this, part plasmids were further combined to form cassette plasmids (Level 1) using BsaI Golden Gate assembly. These cassette plasmids were then integrated into multigene plasmids (Level 2) through BsmBI Golden Gate assembly.

Single-construct strains were generated by introducing multigene plasmids, linearized with NotI-HF, into the genome of *Saccharomyces cerevisiae* strain BY4741 with the genotype MATα HIS3D1 LEU2D0 LYS2D0 URA3D0 GAL80::KANMX GAL4::spHIS5. The transformations followed an established LiAc/SS carrier DNA/PEG protocol⁴. Construct

integration occurred at the URA3 or LEU2 sites, and transformants were selected using SC-Ura or SC-Leu dropout media, respectively. Transformants were further screened using previously established methods².

Overnight yeast cultures were inoculated from colonies on YPD agar plates into 3 mL of liquid SC media overnight at 30 °C with agitation. Post-incubation, the overnight cultures were diluted to an optical density of 700 nm (OD700, to avoid bias from the red fluorescent marker¹², mScarlet-I) of 0.1 in SC media. Subsequently, 200 µL of each culture was dispensed into individual wells of a 96-well glass-bottom plate with black walls (Cat. #P96-1.5H-N).

Lustro

Automated optogenetic experiments were conducted as previously described using a Tecan Fluent Automation Workstation equipped with a Robotic Gripper Arm (RGA) and integrated with an optoPlate and a BioShake 3000-T elm heater shaker designed for well plates, and a Tecan Spark plate reader. The optoPlate was assembled and calibrated in accordance with previously established procedures. Programming of the optoPlate was achieved using scripts available at https://github.com/mccleanlab/Optoplate-96. Throughout the experiments, the Fluent workstation was shielded from ambient light by a blackout curtain. Cellvis 96-well glass bottom plates with #1.5 cover glass (Cat. #P96-1.5H-N) were used for all experiments.

Each 96-well plate, containing cultures diluted to an optical density (OD700) of 0.1, underwent a 5-hour incubation in the dark at 30 °C with continuous shaking. Light induction commenced after this incubation period. For each light induction cycle, the plate was first positioned on the optoPlate for 26.5 minutes at 21 °C. It was then transferred to the plate shaker, where it underwent agitation at 1000 rpm with a 2 mm orbital movement for 1 minute to

resuspend cells. Following this, the plate was moved to the Tecan Spark plate reader for optical density (OD700) and fluorescence measurements (without the lid). Subsequently, the plate was returned to the optoPlate, and this cycle was repeated throughout the experiment. For mScarlet-I¹², fluorescence measurements were recorded with excitation at 563 nm and emission at 606 nm, with an optical gain of 130. For miRFP680¹², fluorescence measurements were recorded with excitation at 652 nm and emission at 697 nm, with an optical gain of 230. The Z-value (vertical distance) was set at 28410 for all fluorescence measurements.

Machine Learning Model

The data and code used for creating the ML model presented in this section can be found at https://github.com/zavalab/ML/tree/master/Optogenetics.

The NN model utilized in this study is designed to predict the relative induction of each strain as a function of a particular light condition. We used a feedforward neural network architecture with a single hidden layer,

$$\hat{y}(u,\theta) = W_{hy} \, \sigma(W_{uh} \cdot u \, + \, b_h) \, + \, b_y$$

where u is a vector defining the light intensity, duty cycle, and the period of the light input and y is a vector of predicted induction levels of each strain. The parameters of the model include the weights and biases, $\theta = \{W_{uh}, W_{hy}, b_h, b_y\}$.

Bayesian Inference and Uncertainty Quantification

We used a Bayesian framework to infer a Gaussian approximation of the NN posterior parameter distribution and an Expectation-Maximization (EM) algorithm to optimize model hyperparameters, with methods adapted from Thompson et al. 2023. Model hyperparameters

include the precision (inverse variance) of the parameter prior and the precision in measurement noise for each strain. The parameter prior is assumed to be a zero mean Gaussian with a precision parameter, α . We assume that error associated with measuring induction levels of m different strains is a zero mean Gaussian random variable with precision β_i for strain j. Given a set of measurements of the induction levels for each strain in response to n different light conditions, $D = \{y(u_1), \dots, y(u_n)\}\$, we define the likelihood of the data as $p(D|\theta) =$ $\prod_{j=1}^{m} N(y_j(u_i) \mid \widehat{y}_j(u_i, \theta), \beta_j^{-1})$. Maximizing the posterior parameter distribution with respect to model parameters is equivalent to maximizing the log of the product of the likelihood and the prior, which gives the maximum a posteriori (MAP) estimate, θ_{MAP} = $argmax_{\theta} \sum_{i=1}^{n} \sum_{j=1}^{m} log N(y_{j}(u_{i}) | \widehat{y}_{j}(u_{i}, \theta), \beta_{j}^{-1}) + log N(\theta | 0, \alpha^{-1}).$ The posterior parameter distribution is approximated as a Gaussian centered at MAP with a covariance matrix given by the inverse of the matrix of second derivatives of the negative log posterior, which we approximate using the outer product, $\Sigma^{-1} = \alpha I_{\theta} + \sum_{i=1}^{n} \sum_{j=1}^{m} \beta_{j} \cdot \nabla_{\theta} \hat{y}_{j}(u_{i}, \theta)$ $\nabla_{\theta} \hat{y}_i(u_i, \theta)^T$ where I_{θ} is the identity matrix with dimension equal to the number of model parameters. The model hyperparameters α and β are optimized using the EM algorithm, which involves maximizing the expectation of the log of the joint probability of the data and the parameter distribution with respect to and, where the expectation is taken with respect to the parameter posterior distribution. Using the updated hyperparameters, inference of the posterior parameter distribution is repeated until convergence of the marginal likelihood.

Experimental Design using Bayesian Optimization

We used a Bayesian optimization algorithm called Thompson sampling to design a batch of experimental conditions predicted to maximize the difference in induction levels between pairs of strains in separate light conditions. To do so, we define the objective function as the negative of the minimum product in the difference between predicted induction for each strain, $J(u_i,u_j,\theta)=-min\left\{\left(\hat{y}_k(u_i,\theta)-\hat{y}_k(u_j,\theta)\right)\cdot\left(\hat{y}_l(u_i,\theta)-\hat{y}_l(u_j,\theta)\right)\;\forall\;k,l\in 1,\ldots,m\right\}.$ We define the experimental design space as all possible pairs of light conditions, $Q=\{(u_i,u_j)\;\forall\;i\neq j\}.$ The Thompson sampling algorithm involves sampling parameter values from the posterior, $\theta^*\sim N(\theta_{MAP},\Sigma)$, and then determining the experimental condition that maximizes the objective, $(u_i,u_j)^*=argmax_{(u_i,u_j)\in Q}\;J(u_i,u_j,\theta^*).$ This process is repeated as many times as necessary to generate the desired number of experimental conditions to be tested in the next experiment.

Materials Availability

Key plasmids have been deposited on Addgene. For all other reagent requests, please contact the corresponding author.

Supporting Information

Additional data and schematics for the experiments described in the text, strains, plasmids, oligos, gene blocks, and optogenetic constructs used in this work

Acknowledgments

This work was supported by National Institutes of Health grant R35GM128873 and National Science Foundation grant 2045493 (awarded to M.N.M.). Megan Nicole McClean, PhD, holds a Career Award at the Scientific Interface from the Burroughs Wellcome Fund.

Z.P.H. was supported by an NHGRI training grant to the Genomic Sciences Training Program 5T32HG002760. We thank Amit Nimunkar and Edvard Grødem for building and modifying the optoPlate. We acknowledge fruitful discussions with McClean lab members, Neydis Moreno for providing feedback on the manuscript, and Stephanie Geller for providing pMM1134 and pMM1137.

Author Contributions

Z.P.H. and M.N.M conceived of the study. J.C.T., D.L.C., and V.M.Z. conceived of the modeling approach. Z.P.H. designed optogenetic parts, performed experiments, and analyzed data. J.C.T. designed the neural network and generated the predictive model. M.N.M. and V.M.Z. provided funding. Z.P.H. and J.C.T. wrote the original draft of the manuscript, and Z.P.H., J.C.T., D.L.C., V.M.Z. and M.N.M wrote, reviewed, and edited the final manuscript.

Conflict of Interest

The authors declare no competing interests.

References:

- (1) Lan, T.-H.; He, L.; Huang, Y.; Zhou, Y. Optogenetics for Transcriptional Programming and Genetic Engineering. *Trends in Genetics* **2022**, *38* (12), 1253–1270. https://doi.org/10.1016/j.tig.2022.05.014.
- Olson, E. J.; Tabor, J. J. Optogenetic Characterization Methods Overcome Key Challenges in Synthetic and Systems Biology. *Nat Chem Biol* **2014**, *10* (7), 502–511. https://doi.org/10.1038/nchembio.1559.
- (3) Pérez, A. L. A.; Piva, L. C.; Fulber, J. P. C.; de Moraes, L. M. P.; De Marco, J. L.; Vieira, H. L. A.; Coelho, C. M.; Reis, V. C. B.; Torres, F. A. G. Optogenetic Strategies for the Control of Gene

- Expression in Yeasts. *Biotechnology Advances* **2022**, *54*, 107839. https://doi.org/10.1016/j.biotechadv.2021.107839.
- (4) An-adirekkun, J. (My); Stewart, C. J.; Geller, S. H.; Patel, M. T.; Melendez, J.; Oakes, B. L.; Noyes, M. B.; McClean, M. N. A Yeast Optogenetic Toolkit (YOTK) for Gene Expression Control in Saccharomyces Cerevisiae. *Biotechnology and Bioengineering* 2020, 117 (3), 886–893. https://doi.org/10.1002/bit.27234.
- (5) Geller, S. H.; Antwi, E. B.; Di Ventura, B.; McClean, M. N. Optogenetic Repressors of Gene Expression in Yeasts Using Light-Controlled Nuclear Localization. *Cell Mol Bioeng* **2019**, *12* (5), 511–528. https://doi.org/10.1007/s12195-019-00598-9.
- (6) Moreno Morales, N.; Patel, M. T.; Stewart, C. J.; Sweeney, K.; McClean, M. N. Optogenetic Tools for Control of Public Goods in Saccharomyces Cerevisiae. *mSphere* 2021, 6 (4), e00581-21. https://doi.org/10.1128/mSphere.00581-21.
- (7) Harmer, Z. P.; McClean, M. N. Lustro: High-Throughput Optogenetic Experiments Enabled by Automation and a Yeast Optogenetic Toolkit. *ACS Synth. Biol.* **2023**. https://doi.org/10.1021/acssynbio.3c00215.
- (8) Scott, T. D.; Sweeney, K.; McClean, M. N. Biological Signal Generators: Integrating Synthetic Biology Tools and in Silico Control. *Current Opinion in Systems Biology* **2019**, *14*, 58–65. https://doi.org/10.1016/j.coisb.2019.02.007.
- (9) Levskaya, A.; Weiner, O. D.; Lim, W. A.; Voigt, C. A. Spatiotemporal Control of Cell Signalling Using A Light-Switchable Protein Interaction. *Nature* 2009, 461 (7266), 997–1001. https://doi.org/10.1038/nature08446.
- (10) Silva, P. M.; Puerner, C.; Seminara, A.; Bassilana, M.; Arkowitz, R. A. Secretory Vesicle Clustering in Fungal Filamentous Cells Does Not Require Directional Growth. *Cell Reports* 2019, 28 (8), 2231-2245.e5. https://doi.org/10.1016/j.celrep.2019.07.062.
- (11) Niopek, D.; Benzinger, D.; Roensch, J.; Draebing, T.; Wehler, P.; Eils, R.; Di Ventura, B. Engineering Light-Inducible Nuclear Localization Signals for Precise Spatiotemporal Control of Protein Dynamics in Living Cells. *Nat Commun* 2014, 5 (1), 4404. https://doi.org/10.1038/ncomms5404.
- (12) Yazawa, M.; Sadaghiani, A. M.; Hsueh, B.; Dolmetsch, R. E. Induction of Protein-Protein Interactions in Live Cells Using Light. *Nat Biotechnol* 2009, 27 (10), 941–945. https://doi.org/10.1038/nbt.1569.

- (13) Chen, S. Y.; Osimiri, L. C.; Chevalier, M.; Bugaj, L. J.; Nguyen, T. H.; Greenstein, R. A.; Ng, A. H.; Stewart-Ornstein, J.; Neves, L. T.; El-Samad, H. Optogenetic Control Reveals Differential Promoter Interpretation of Transcription Factor Nuclear Translocation Dynamics. *Cell Syst* 2020, 11 (4), 336-353.e24. https://doi.org/10.1016/j.cels.2020.08.009.
- (14) Sweeney, K.; McClean, M. N. Transcription Factor Localization Dynamics and DNA Binding Drive Distinct Promoter Interpretations. bioRxiv August 30, 2022, p 2022.08.30.505887. https://doi.org/10.1101/2022.08.30.505887.
- van Bergeijk, P.; Adrian, M.; Hoogenraad, C. C.; Kapitein, L. C. Optogenetic Control of Organelle Transport and Positioning. *Nature* **2015**, *518* (7537), 111–114. https://doi.org/10.1038/nature14128.
- (16) Tague, N.; Coriano-Ortiz, C.; Sheets, M. B.; Dunlop, M. J. Light Inducible Protein Degradation in E. Coli with LOVtag. *bioRxiv* 2023, 2023.02.25.530042. https://doi.org/10.1101/2023.02.25.530042.
- (17) Renicke, C.; Schuster, D.; Usherenko, S.; Essen, L.-O.; Taxis, C. A LOV2 Domain-Based Optogenetic Tool to Control Protein Degradation and Cellular Function. *Chem Biol* **2013**, *20* (4), 619–626. https://doi.org/10.1016/j.chembiol.2013.03.005.
- (18) Dwijayanti, A.; Zhang, C.; Poh, C. L.; Lautier, T. Toward Multiplexed Optogenetic Circuits. *Frontiers in Bioengineering and Biotechnology* **2022**, *9*.
- (19) Harmer, Z. P.; McClean, M. N. High-Throughput Optogenetics Experiments in Yeast Using the Automated Platform Lustro. *JoVE (Journal of Visualized Experiments)* **2023**, No. 198, e65686. https://doi.org/10.3791/65686.
- (20) Benzinger, D.; Ovinnikov, S.; Khammash, M. Synthetic Gene Networks Recapitulate Dynamic Signal Decoding and Differential Gene Expression. *Cell Syst* **2022**, *13* (5), 353-364.e6. https://doi.org/10.1016/j.cels.2022.02.004.
- (21) Bindels, D. S.; Haarbosch, L.; van Weeren, L.; Postma, M.; Wiese, K. E.; Mastop, M.; Aumonier, S.; Gotthard, G.; Royant, A.; Hink, M. A.; Gadella, T. W. J. MScarlet: A Bright Monomeric Red Fluorescent Protein for Cellular Imaging. *Nat Methods* 2017, 14 (1), 53–56. https://doi.org/10.1038/nmeth.4074.
- (22) Taslimi, A.; Zoltowski, B.; Miranda, J. G.; Pathak, G.; Hughes, R. M.; Tucker, C. L. Optimized Second Generation CRY2/CIB Dimerizers and Photoactivatable Cre Recombinase. *Nat Chem Biol* **2016**, *12* (6), 425–430. https://doi.org/10.1038/nchembio.2063.

- (23) Kawano, F.; Suzuki, H.; Furuya, A.; Sato, M. Engineered Pairs of Distinct Photoswitches for Optogenetic Control of Cellular Proteins. *Nat Commun* **2015**, *6* (1), 6256. https://doi.org/10.1038/ncomms7256.
- (24) Benedetti, L.; Marvin, J. S.; Falahati, H.; Guillén-Samander, A.; Looger, L. L.; De Camilli, P. Optimized Vivid-Derived Magnets Photodimerizers for Subcellular Optogenetics in Mammalian Cells. *eLife* **2020**, *9*, e63230. https://doi.org/10.7554/eLife.63230.
- (25) Kennedy, M. J.; Hughes, R. M.; Peteya, L. A.; Schwartz, J. W.; Ehlers, M. D.; Tucker, C. L. Rapid Blue-Light–Mediated Induction of Protein Interactions in Living Cells. *Nat Methods* **2010**, 7 (12), 973–975. https://doi.org/10.1038/nmeth.1524.
- (26) Motta-Mena, L. B.; Reade, A.; Mallory, M. J.; Glantz, S.; Weiner, O. D.; Lynch, K. W.; Gardner, K. H. An Optogenetic Gene Expression System with Rapid Activation and Deactivation Kinetics. Nat Chem Biol 2014, 10 (3), 196–202. https://doi.org/10.1038/nchembio.1430.
- (27) Zoltowski, B. D.; Motta-Mena, L. B.; Gardner, K. H. Blue Light-Induced Dimerization of a Bacterial LOV–HTH DNA-Binding Protein. *Biochemistry* 2013, 52 (38), 6653–6661. https://doi.org/10.1021/bi401040m.
- (28) Pathak, G. P.; Strickland, D.; Vrana, J. D.; Tucker, C. L. Benchmarking of Optical Dimerizer Systems. *ACS Synth Biol* **2014**, *3* (11), 832–838. https://doi.org/10.1021/sb500291r.
- di Pietro, F.; Herszterg, S.; Huang, A.; Bosveld, F.; Alexandre, C.; Sancéré, L.; Pelletier, S.; Joudat, A.; Kapoor, V.; Vincent, J.-P.; Bellaïche, Y. Rapid and Robust Optogenetic Control of Gene Expression in Drosophila. *Developmental Cell* 2021, 56 (24), 3393-3404.e7. https://doi.org/10.1016/j.devcel.2021.11.016.
- (30) Matlashov, M. E.; Shcherbakova, D. M.; Alvelid, J.; Baloban, M.; Pennacchietti, F.; Shemetov, A. A.; Testa, I.; Verkhusha, V. V. A Set of Monomeric Near-Infrared Fluorescent Proteins for Multicolor Imaging across Scales. *Nat Commun* 2020, 11 (1), 239. https://doi.org/10.1038/s41467-019-13897-6.
- (31) Zhao, E. M.; Zhang, Y.; Mehl, J.; Park, H.; Lalwani, M. A.; Toettcher, J. E.; Avalos, J. L. Optogenetic Regulation of Engineered Cellular Metabolism for Microbial Chemical Production. Nature 2018, 555 (7698), 683–687. https://doi.org/10.1038/nature26141.
- (32) Zhao, E. M.; Lalwani, M. A.; Chen, J.-M.; Orillac, P.; Toettcher, J. E.; Avalos, J. L. Optogenetic Amplification Circuits for Light-Induced Metabolic Control. *ACS Synth. Biol.* **2021**, *10* (5), 1143–1154. https://doi.org/10.1021/acssynbio.0c00642.

- (33) Thompson, J. C.; Zavala, V. M.; Venturelli, O. S. Integrating a Tailored Recurrent Neural Network with Bayesian Experimental Design to Optimize Microbial Community Functions. *PLoS Comput Biol* **2023**, *19* (9), e1011436. https://doi.org/10.1371/journal.pcbi.1011436.
- (34) Kandasamy, K.; Krishnamurthy, A.; Schneider, J.; Poczos, B. Parallelised Bayesian Optimisation via Thompson Sampling. In *Proceedings of the Twenty-First International Conference on Artificial Intelligence and Statistics*; PMLR, 2018; pp 133–142.
- (35) Ding, Y.; Tous, C.; Choi, J.; Chen, J.; Wong, W. W. Orthogonal Inducible Control of Cas13 Circuits Enables Programmable RNA Regulation in Mammalian Cells. *bioRxiv* **2023**, 2023.03.20.533499. https://doi.org/10.1101/2023.03.20.533499.
- (36) Bertaux, F.; Sosa-Carrillo, S.; Gross, V.; Fraisse, A.; Aditya, C.; Furstenheim, M.; Batt, G. Enhancing Bioreactor Arrays for Automated Measurements and Reactive Control with ReacSight. *Nat Commun* **2022**, *13* (1), 3363. https://doi.org/10.1038/s41467-022-31033-9.
- (37) Gilbert, C.; Tang, T.-C.; Ott, W.; Dorr, B. A.; Shaw, W. M.; Sun, G. L.; Lu, T. K.; Ellis, T. Living Materials with Programmable Functionalities Grown from Engineered Microbial Co-Cultures. *Nat. Mater.* 2021, 20 (5), 691–700. https://doi.org/10.1038/s41563-020-00857-5.
- (38) Ponomarova, O.; Gabrielli, N.; Sévin, D. C.; Mülleder, M.; Zirngibl, K.; Bulyha, K.; Andrejev, S.; Kafkia, E.; Typas, A.; Sauer, U.; Ralser, M.; Patil, K. R. Yeast Creates a Niche for Symbiotic Lactic Acid Bacteria through Nitrogen Overflow. *Cell Systems* **2017**, *5* (4), 345-357.e6. https://doi.org/10.1016/j.cels.2017.09.002.
- (39) Gutiérrez Mena, J.; Kumar, S.; Khammash, M. Dynamic Cybergenetic Control of Bacterial Co-Culture Composition via Optogenetic Feedback. *Nat Commun* 2022, *13*, 4808. https://doi.org/10.1038/s41467-022-32392-z.
- (40) Lee, M. E.; DeLoache, W. C.; Cervantes, B.; Dueber, J. E. A Highly Characterized Yeast Toolkit for Modular, Multipart Assembly. *ACS Synth. Biol.* **2015**, *4* (9), 975–986. https://doi.org/10.1021/sb500366v.
- (41) Gietz, R. D.; Schiestl, R. H. High-Efficiency Yeast Transformation Using the LiAc/SS Carrier DNA/PEG Method. *Nat Protoc* **2007**, *2* (1), 31–34. https://doi.org/10.1038/nprot.2007.13.
- (42) Hecht, A.; Endy, D.; Salit, M.; Munson, M. S. When Wavelengths Collide: Bias in Cell Abundance Measurements Due to Expressed Fluorescent Proteins. *ACS Synth. Biol.* **2016**, *5* (9), 1024–1027. https://doi.org/10.1021/acssynbio.6b00072.

(43) Bugaj, L. J.; Lim, W. A. High-Throughput Multicolor Optogenetics in Microwell Plates. *Nat Protoc* **2019**, *14* (7), 2205–2228. https://doi.org/10.1038/s41596-019-0178-y.

CHAPTER FIVE: FUTURE DIRECTIONS

Zachary P Harmer

Conclusion:

The advent of optogenetics has propelled biological research into a new era of precision and control. Its impact spans from fundamental discoveries to bioproduction to potential therapeutic interventions. Improving multiplexing strategies for optogenetics expands how much biology can be controlled at once. As the field continues to evolve, the boundaries of what can be achieved through optogenetics will expand, offering exciting possibilities for the future of biology.

Lustro offers dramatically increased throughput for testing optogenetic conditions. Performing optogenetic experiments in a microwell plate format combined with laboratory automation is readily amenable to scaling up and frees up the researcher for other tasks. The ability to assemble optogenetic constructs and rapidly test many different light conditions allows for the formation of data-driven machine learning models. Using the data generated from Lustro, I was able to identify conditions for dynamic multiplexed control and sequential activation of optogenetic systems using only one wavelength of light. These conditions take advantage of the native differences in kinetics between a range of different optogenetic systems. This approach also frees up other wavelengths for fluorescent reporter readout or the use of additional optogenetic systems. These control strategies can be refined and implemented in a wide range of applications, including bioproduction, microbial communities, functional genomics, and medicine.

Challenges and Future Directions:

Optogenetics offers a promising array of future avenues. Expanding beyond conventional model organisms, the field is poised to unlock new biological insights in many non-model organisms. More extensive characterization of optogenetic systems will lead to a better understanding of how to apply them and will offer a deeper understanding of their kinetics and specificity.

Refining multiplexing strategies stands as a key objective, enabling more intricate control over cellular behavior. Further iteration through model prediction and validation will improve the reliability of predictions and the ease of identifying conditions for desired behavior (such as holding activation of one system constant while tuning another). The incorporation of downstream genetic circuits will allow for further processing of the multiplexed control over optogenetic systems. Tuning the outputs of the optogenetic systems to generate multistability will allow for switching between multiple distinct states².

Integration with emerging technologies, including CRISPR-based synthetic biology tools, holds immense potential for groundbreaking discoveries. The split optogenetic TFs used here could be modified to utilize dCas9 (or another deactivated Cas nuclease) as a DNA binding domain. This would allow for a library of targets to be screened with a range of different light conditions for advanced functional genomic screening and characterization. These could also be integrated into biological control circuits.

While Lustro was used to characterize the activity of split optogenetic TFs, this information (and in some cases the approach) can be applied to other circumstances utilizing optical dimerizers. For example, optical dimerizers could be used to reconstitute split proteins, such as dCas13¹¹ or dCas9¹²⁻¹⁴, allowing for regulable control of RNA processing, DNA

transcription, or recruitment of proteins of interest to specific regions in the genome. Optical dimerizers have also been used to control cell signaling pathways.

This opus has focused on the characterization of a suite of CRY2-15-17, EL222-18-19, and VVD-based 28-22 split TFs. However, the inclusion of more optogenetic split TFs with different kinetics will allow for a broader range in selection of behavior. This will likely lead to the identification of better conditions for multiplexing control over optogenetic systems. There are many variants of CRY2-, EL222-, and VVD-based optical dimerizers both in the literature and unexplored variants in native flora, bacteria, and fungi that could be further explored and characterized. Additionally, further blue light-sensitive optical dimerizers, such as the PixD/PixE²² and iLID/Nano²² systems, could be incorporated into this optogenetic split TF architecture and would likely lead to novel kinetic activation profiles.

A crucial step in the implementation of the pipeline and data generated here will be translating these findings into other model and non-model systems. Particularly for the two-component split optogenetic TFs, some tuning of expression levels will likely be required to achieve the same level of control in other eukaryotic cells, such as mammalian cell lines. Lustro could also be used to characterize light response activity in nonconventional organisms useful for a range of bioproduction processes, such as the fungus *Xanthophyllomyces dendrorhous*, which is an attractive target for terpenoid production.

Multiplexed control over optogenetic systems can be used for a wide range of biotechnology applications. For example, it could be used to control microbial community dynamics. Yeast nitrogen overflow can be used to regulate the relative amounts of other microbes in a culture. Dynamic control of these metabolic pathways in yeast could be used to control a three-member microbial consortium. The development of engineered living materials

can be controlled using optogenetic systems²², and the ability to multiplex control over optogenetic systems dramatically expands the design space. Multiplexed control is also of interest in regulating the production of biopharmaceutical compounds (an ongoing collaboration with Ningaloo Biosciences). The fine temporal control offered by optogenetic systems could also be used to optimize bioproduction strategies where sequential activation or multiplexed control is desired.

The capabilities of Lustro can be further enhanced with some instrumentation adjustments or upgrades. The Fluent Automation Workstation's liquid handling capabilities could be used to dilute cell cultures back for long-term experiments. Real-time feedback from the plate reader outputs could be used to dynamically adjust the light input conditions on cell cultures to remain within a desired range, an optimization and control strategy known as cybergenetics. Integration with a CO₂ incubator would allow for culturing mammalian cells for high-throughput optogenetic experiments.

The yeast optogenetic toolkitana (yOTK) for Type IIs molecular cloning assembly used to generate the constructs in this work could be further accelerated. The first two levels of Golden Gate assembly (level 0 and level 1, generation of the part and cassette plasmids) can be performed in parallel and combined. I discovered that the product of the level 0 assembly can be directly incorporated into the next level assembly (using 2 µL of product in a 10 µL reaction), which should be further validated. This allows transformations of level 0 and level 1 plasmids into *Escherichia coli* and sequence verification to occur simultaneously. Additionally, using an assembly strategy developed by Young et al. a., it's possible to design the level 1 cassette plasmids to have short homologous overlap regions, allowing for direct transformation and assembly into yeast. This would require introduction of a few new level 1 vectors into the yeast

toolkit. Combining both of these strategies, it would be possible to shorten the time needed to generate a multigene construct strain requiring new parts from about three weeks to about one week.

References:

- (1) Pérez, A. L. A.; Piva, L. C.; Fulber, J. P. C.; de Moraes, L. M. P.; De Marco, J. L.; Vieira, H. L. A.; Coelho, C. M.; Reis, V. C. B.; Torres, F. A. G. Optogenetic Strategies for the Control of Gene Expression in Yeasts. *Biotechnology Advances* 2022, 54, 107839. https://doi.org/10.1016/j.biotechadv.2021.107839.
- (2) Lan, T.-H.; He, L.; Huang, Y.; Zhou, Y. Optogenetics for Transcriptional Programming and Genetic Engineering. *Trends in Genetics* **2022**, *38* (12), 1253–1270. https://doi.org/10.1016/j.tig.2022.05.014.
- Olson, E. J.; Tabor, J. J. Optogenetic Characterization Methods Overcome Key Challenges in Synthetic and Systems Biology. *Nat Chem Biol* **2014**, *10* (7), 502–511. https://doi.org/10.1038/nchembio.1559.
- (4) Harmer, Z. P.; McClean, M. N. Lustro: High-Throughput Optogenetic Experiments Enabled by Automation and a Yeast Optogenetic Toolkit. ACS Synth. Biol. 2023. https://doi.org/10.1021/acssynbio.3c00215.
- (5) Harmer, Z. P.; McClean, M. N. High-Throughput Optogenetics Experiments in Yeast Using the Automated Platform Lustro. *JoVE (Journal of Visualized Experiments)* **2023**, No. 198, e65686. https://doi.org/10.3791/65686.
- (6) Dwijayanti, A.; Zhang, C.; Poh, C. L.; Lautier, T. Toward Multiplexed Optogenetic Circuits. *Frontiers in Bioengineering and Biotechnology* **2022**, *9*.
- (7) Zhu, R.; del Rio-Salgado, J. M.; Garcia-Ojalvo, J.; Elowitz, M. B. Synthetic Multistability in Mammalian Cells. *Science* 2022, 375 (6578), eabg9765. https://doi.org/10.1126/science.abg9765.
- (8) Polstein, L. R.; Gersbach, C. A. A Light-Inducible CRISPR/Cas9 System for Control of Endogenous Gene Activation. *Nat Chem Biol* 2015, 11 (3), 198–200. https://doi.org/10.1038/nchembio.1753.

- (9) Santos-Moreno, J.; Tasiudi, E.; Stelling, J.; Schaerli, Y. Multistable and Dynamic CRISPRi-Based Synthetic Circuits. *Nat Commun* **2020**, *11* (1), 2746. https://doi.org/10.1038/s41467-020-16574-1.
- (10) Nielsen, A. A.; Voigt, C. A. Multi-Input CRISPR/Cas Genetic Circuits That Interface Host Regulatory Networks. *Mol Syst Biol* **2014**, *10* (11). https://doi.org/10.15252/msb.20145735.
- (11) Ding, Y.; Tous, C.; Choi, J.; Chen, J.; Wong, W. W. Orthogonal Inducible Control of Cas13 Circuits Enables Programmable RNA Regulation in Mammalian Cells. *bioRxiv* **2023**, 2023.03.20.533499. https://doi.org/10.1101/2023.03.20.533499.
- (12) Zetsche, B.; Volz, S. E.; Zhang, F. A Split-Cas9 Architecture for Inducible Genome Editing and Transcription Modulation. *Nat Biotechnol* 2015, 33 (2), 139–142. https://doi.org/10.1038/nbt.3149.
- (13) Huang, X.; Zhou, Q.; Wang, M.; Cao, C.; Ma, Q.; Ye, J.; Gui, Y. A Light-Inducible Split-DCas9 System for Inhibiting the Progression of Bladder Cancer Cells by Activating P53 and E-Cadherin. *Frontiers in Molecular Biosciences* **2021**, 7.
- (14) Ma, D.; Peng, S.; Xie, Z. Integration and Exchange of Split DCas9 Domains for Transcriptional Controls in Mammalian Cells. *Nat Commun* 2016, 7 (1), 13056. https://doi.org/10.1038/ncomms13056.
- (15) Kennedy, M. J.; Hughes, R. M.; Peteya, L. A.; Schwartz, J. W.; Ehlers, M. D.; Tucker, C. L. Rapid Blue-Light–Mediated Induction of Protein Interactions in Living Cells. *Nat Methods* 2010, 7 (12), 973–975. https://doi.org/10.1038/nmeth.1524.
- (16) Pathak, G. P.; Strickland, D.; Vrana, J. D.; Tucker, C. L. Benchmarking of Optical Dimerizer Systems. *ACS Synth Biol* **2014**, *3* (11), 832–838. https://doi.org/10.1021/sb500291r.
- (17) Taslimi, A.; Zoltowski, B.; Miranda, J. G.; Pathak, G.; Hughes, R. M.; Tucker, C. L. Optimized Second Generation CRY2/CIB Dimerizers and Photoactivatable Cre Recombinase. *Nat Chem Biol* **2016**, *12* (6), 425–430. https://doi.org/10.1038/nchembio.2063.
- (18) Benzinger, D.; Khammash, M. Pulsatile Inputs Achieve Tunable Attenuation of Gene Expression Variability and Graded Multi-Gene Regulation. *Nat Commun* **2018**, *9* (1), 3521. https://doi.org/10.1038/s41467-018-05882-2.
- (19) Benzinger, D.; Ovinnikov, S.; Khammash, M. Synthetic Gene Networks Recapitulate Dynamic Signal Decoding and Differential Gene Expression. *Cell Syst* **2022**, *13* (5), 353-364.e6. https://doi.org/10.1016/j.cels.2022.02.004.

- (20) di Pietro, F.; Herszterg, S.; Huang, A.; Bosveld, F.; Alexandre, C.; Sancéré, L.; Pelletier, S.; Joudat, A.; Kapoor, V.; Vincent, J.-P.; Bellaïche, Y. Rapid and Robust Optogenetic Control of Gene Expression in Drosophila. *Developmental Cell* 2021, 56 (24), 3393-3404.e7. https://doi.org/10.1016/j.devcel.2021.11.016.
- (21) Benedetti, L.; Marvin, J. S.; Falahati, H.; Guillén-Samander, A.; Looger, L. L.; De Camilli, P. Optimized Vivid-Derived Magnets Photodimerizers for Subcellular Optogenetics in Mammalian Cells. *eLife* **2020**, *9*, e63230. https://doi.org/10.7554/eLife.63230.
- (22) Kawano, F.; Suzuki, H.; Furuya, A.; Sato, M. Engineered Pairs of Distinct Photoswitches for Optogenetic Control of Cellular Proteins. *Nat Commun* **2015**, *6* (1), 6256. https://doi.org/10.1038/ncomms7256.
- (23) Masuda, S.; Nakatani, Y.; Ren, S.; Tanaka, M. Blue Light-Mediated Manipulation of Transcription Factor Activity In Vivo. ACS Chem. Biol. 2013, 8 (12), 2649–2653. https://doi.org/10.1021/cb400174d.
- (24) Guntas, G.; Hallett, R. A.; Zimmerman, S. P.; Williams, T.; Yumerefendi, H.; Bear, J. E.; Kuhlman, B. Engineering an Improved Light-Induced Dimer (ILID) for Controlling the Localization and Activity of Signaling Proteins. *Proc Natl Acad Sci U S A* **2015**, *112* (1), 112–117. https://doi.org/10.1073/pnas.1417910112.
- (25) Kucsera, J.; Pfeiffer, I.; Takeo, K. Biology of the Red Yeast Xanthophyllomyces Dendrorhous (Phaffia Rhodozyma). *Mycoscience* **2000**, *41* (3), 195–199. https://doi.org/10.1007/BF02489671.
- (26) Tobin, E. E.; Collins, J. H.; Marsan, C. B.; Nadeau, G. T.; Mori, K.; Lipzen, A.; Mondo, S.; Grigoriev, I. V.; Young, E. M. Transcriptomics Elucidates Metabolic Regulation and Functional Promoters in the Basidiomycete Red Yeast Xanthophyllomyces Dendrorhous CBS 6938. bioRxiv July 31, 2023, p 2023.07.31.551333. https://doi.org/10.1101/2023.07.31.551333.
- (27) Ponomarova, O.; Gabrielli, N.; Sévin, D. C.; Mülleder, M.; Zirngibl, K.; Bulyha, K.; Andrejev, S.; Kafkia, E.; Typas, A.; Sauer, U.; Ralser, M.; Patil, K. R. Yeast Creates a Niche for Symbiotic Lactic Acid Bacteria through Nitrogen Overflow. *Cell Systems* **2017**, *5* (4), 345-357.e6. https://doi.org/10.1016/j.cels.2017.09.002.
- (28) Gilbert, C.; Tang, T.-C.; Ott, W.; Dorr, B. A.; Shaw, W. M.; Sun, G. L.; Lu, T. K.; Ellis, T. Living Materials with Programmable Functionalities Grown from Engineered Microbial Co-Cultures. *Nat. Mater.* **2021**, *20* (5), 691–700. https://doi.org/10.1038/s41563-020-00857-5.

- (29) Gutiérrez Mena, J.; Kumar, S.; Khammash, M. Dynamic Cybergenetic Control of Bacterial Co-Culture Composition via Optogenetic Feedback. *Nat Commun* 2022, *13*, 4808. https://doi.org/10.1038/s41467-022-32392-z.
- (30) Khammash, M. H. Cybergenetics: Theory and Applications of Genetic Control Systems. *Proceedings of the IEEE* **2022**, *110* (5), 631–658. https://doi.org/10.1109/JPROC.2022.3170599.
- (31) Lee, M. E.; DeLoache, W. C.; Cervantes, B.; Dueber, J. E. A Highly Characterized Yeast Toolkit for Modular, Multipart Assembly. *ACS Synth. Biol.* **2015**, *4* (9), 975–986. https://doi.org/10.1021/sb500366v.
- (32) An-adirekkun, J. (My); Stewart, C. J.; Geller, S. H.; Patel, M. T.; Melendez, J.; Oakes, B. L.; Noyes, M. B.; McClean, M. N. A Yeast Optogenetic Toolkit (YOTK) for Gene Expression Control in *Saccharomyces Cerevisiae*. *Biotechnology and Bioengineering* **2020**, *117* (3), 886–893. https://doi.org/10.1002/bit.27234.
- Young, E. M.; Zhao, Z.; Gielesen, B. E. M.; Wu, L.; Benjamin Gordon, D.; Roubos, J. A.; Voigt, C. A. Iterative Algorithm-Guided Design of Massive Strain Libraries, Applied to Itaconic Acid Production in Yeast. *Metabolic Engineering* 2018, 48, 33–43. https://doi.org/10.1016/j.ymben.2018.05.002.

APPENDIX A: HIGH-THROUGHPUT OPTOGENETICS EXPERIMENTS IN YEAST USING THE AUTOMATED PLATFORM LUSTRO

Zachary P. Harmer¹ and Megan N. McClean^{1,2,*}

Department of Biomedical Engineering, University of Wisconsin-Madison, Madison,

WI USA

² University of Wisconsin Carbone Cancer Center, University of Wisconsin School of Medicine and Public Health, Madison, WI USA

*Email: mmcclean@wisc.edu

Published in Journal of Visualized Experiments

SUMMARY:

This protocol describes how to use the automated platform Lustro for the high-throughput characterization of optogenetic systems in yeast.

ABSTRACT:

Optogenetics provides precise control of cellular behavior through genetically encoded light-sensitive proteins. However, optimizing these systems to achieve the desired range of functionality often requires many design-build-test cycles, which is time-consuming and labor-intensive. To address this, we designed Lustro, a platform which integrates light stimulation with laboratory automation to enable high-throughput screening and characterization of optogenetic systems. Lustro utilizes an automation workstation equipped with an illumination device, a shaking device, and a plate reader. A robotic arm is programmed to move a microwell plate between the devices to stimulate optogenetic strains and measure their response. Here we present

a protocol for using Lustro to characterize optogenetic systems for gene expression control in the budding yeast *Saccharomyces cerevisiae*. The protocol describes how to set up the components of Lustro, integrating an illumination device with an automation workstation, and provides instruction for programming the illumination device, plate reader, and robot.

INTRODUCTION:

Optogenetics is a powerful technique that uses light-sensitive proteins to control the behavior of cells with high precision. However, prototyping optogenetic constructs and identifying optimal illumination conditions can be time consuming, which makes it difficult to optimize optogenetic systems. High-throughput methods to rapidly screen and characterize the activity of optogenetic systems can accelerate the design-build-test cycle for prototyping constructs and exploring their function.

We therefore developed Lustro, a laboratory automation technique designed for high-throughput screening and characterization of optogenetic systems that integrates a microplate reader, illumination device, and shaking device with an automation workstation. Lustro combines automated culturing and light stimulation of cells in microwell plates (Figure 1), allowing for the rapid screening and comparison of different optogenetic systems. The Lustro platform is highly adaptable and can be generalized to work with other laboratory automation robots, illumination devices, plate readers, cell types, and optogenetic systems, including those responsive to different wavelengths of light.

In this protocol, we demonstrate how to set up Lustro and use it to characterize an optogenetic system. We use optogenetic control of split transcription factors in yeast as an example system to illustrate the function and utility of the platform by probing the relationship

between light inputs and the expression of a fluorescent reporter gene, mScarlet-I₂. By following this protocol, researchers can streamline the optimization of optogenetic systems and accelerate the discovery of new strategies for the dynamic control of biological systems.

PROTOCOL:

1. Set up the automation workstation.

- a) Equip the automated workstation with a Robotic Gripper Arm (RGA) capable of moving microwell plates (see Figure 1).
- b) Install a microplate heater shaker into the automated workstation (Figure 1.1) with an automatic plate locking mechanism that allows access to the RGA.
- c) Secure a microplate reader adjacent to the automated workstation (Figure 1.2) that allows access to the RGA.
- d) Install a microplate illumination device (Figure 1.3) that allows easy access to the RGA, such as the optoPlate^a (as used here) or LITOS^a.

2. Prepare the illumination device.

- b) Use an adaptor on the illumination device that allows access to the RGA.
- c) Program the optoPlate from a spreadsheet input¹⁰ (or via a graphical interface¹²).

 Considerations for programming light stimulation programs are detailed below.
- 3. **Design a light stimulation program.** Determine the light conditions that will be used for the sample plate and flash (load) them onto the illumination device.

- a) Enter desired light conditions (including light intensity, light start time, pulse length, pulse number, and interpulse duration) into a spreadsheet and flash onto the optoPlate (as described in the following github repository: github.com/mccleanlab/Optoplate-96). Note when programming the light conditions into the illumination device that the sample plate will not receive illumination while in the microplate reader or on the heater shaker. The duration and frequency of these events may need to be optimized for specific experimental needs.
- b) Include dark conditions for each strain for proper background measurements to be taken.
- c) Use high light intensity for initial characterization experiments to determine functionality of transformants. Note that light intensity should be optimized for more sensitive experiments as excessive light is phototoxic to yeast.
- 4. Prepare the microplate reader. Configure the microplate reader to measure the quantity of interest prior to performing experiments. In the example presented here, we configure the microplate reader to measure the amount of fluorescence from a reporter expressed by the strain of interest. Outputs such as luminescence or optical density can also be used, depending on experimental needs.
 - a) Grow the strain of interest (and a nonfluorescent control) in synthetic complete (SC) media¹⁴ (or another low fluorescence media) to the highest cell density that will be measured, pipette into a glass-bottom black-walled microwell plate, and measure to determine optimal microplate reader settings. Verify the plate dimensions are correctly

- entered to ensure accurate readings are taken. Measure the plate from below to ensure accuracy.
- b) Consult fpbase.org to determine approximate absorption and emission spectra of the target fluorescent protein.¹⁵.
- c) Determine the z-value (the distance between the plate and reader) for the plate by performing a z-scan on wells with the fluorescent strain and well with the nonfluorescent strain. Select the z-values that yield the highest signal-to-noise ratio.
- d) Optimize absorption and emission spectra by using the absorption scan and emission scan on the fluorescent and nonfluorescent strains to determine the optimal signal-to-noise ratio.
- e) Measure the fluorescent strain with the gain set to optimal to determine the highest optical gain that can be used without returning an overflow measurement error. This optical gain should be manually set across experiments with a given strain to ensure consistency in results.
- f) Prepare a measurement script (see Figure 2) in the microplate reader software. This measurement script configures the instrument to measure the optical density of the cultures and fluorescence spectra of any fluorescent proteins to be measured. Measure optical density of strains at 600 nm unless they produce red fluorescent proteins. If the strains express a red fluorescent protein, measure optical density at 700 nm to avoid bias¹⁶.
- g) Set the script to maintain an internal incubation temperature during measurements of 30 °C.

- Set the measurement script to export the data into a spreadsheet (or ASCII files, if desired).
- 5. **Program the robot.** Set up the worktable definition in the automated workstation software according to the physical layout of the carriers (e.g., heater shakers, nest platforms, illumination devices, etc.) and the labware (i.e., the 96-well plate). Prepare a script on the automation workstation software to perform light induction and measurement (see Figure 3) as follows.
 - a) Turn off any internal sources of illumination to avoid background activation of optogenetic systems.
 - b) Set the heater shaker to 30 °C. The plate will be at ambient temperature (22 °C) while not on the heater shaker.
 - c) Use loops, a timer, and a loop counting variable to repeat the steps of inducing and measuring the cells over regular intervals.
 - d) Prior to recording any measurements, shake the sample plate to ensure all cells are suspended (60 s at 1,000 rpm with a 2 mm orbital is sufficient to resuspend S288C *S. cerevisiae* cells) to avoid bias in measurement.
 - e) The robot arm then moves the sample plate to the microplate reader and removes the lid (to avoid bias in optical density measurement). Control software will automatically remove (and replace) the lid to the designated position if the microplate reader carrier is defined as not allowing lids.
 - f) Run the microplate reader measurement script (described in step 4).
 - g) The robot arm then replaces the lid to the sample plate and moves the plate to the illumination device.

- h) Set the script to wait until the timer reaches 30 min (multiplied by the loop counting variable), and then repeat the whole loop 48 times (for a 24-hour experiment).
- i) Run an empty plate through the steps of the script loop described above several times to troubleshoot potential errors and ensure that the carrier and labware definitions are set properly and that the RGA can correctly and precisely pick up and place the plate at each carrier site.
- j) Set up user alerts to notify the user in the case of any instrument state changes (such as errors).
- 6. **Set up the sample plate.** Grow up the strains of interest and load them into a glass-bottom black-walled 96-well plate.
 - a) Grow yeast strains on rich media plates, such as YPD
 ¹² agar. Include a nonfluorescent (negative) control. Yeast strains used here (see Table of Materials) grow well between 22
 °C 30 °C and in a range of standard yeast media.
 - b) Pick colonies from these plates and grow them overnight in 3 mL SC¹⁴ (or another low fluorescence media, such as LFM¹⁸) at 30 °C on a roller drum. Keep cultures in the dark (or under a non-responsive wavelength of light, such as red light for blue light-responsive systems) during incubation and for downstream processing steps.
 - c) Measure the optical density of the overnight cultures by diluting $200~\mu L$ of each into 1 mL (final volume) SC and measuring the optical density at 600~nm (OD₆₀₀) with a spectrophotometer or microplate reader.
 - d) Dilute each overnight culture to OD₆₀₀=0.1 in glass culture tubes. Where higher straintesting throughput is desired, automated dilutions can be performed in microwell plates.

- e) Pipette the diluted cultures into the 96-well plate. Perform each condition in triplicate (i.e., three identical wells with the same strain and light condition) to determine technical variation. Include blank media and nonfluorescent cells as negative controls for determining background fluorescence and optical density.
- f) Incubate the plate at 30 °C, shaking for 5 hours before beginning the light induction experiment. Dilution amounts and incubation times may need to be optimized for specific strains and experimental conditions.

7. Perform the experiment.

- a) Load the sample plate onto the heater shaker and start the automation script (described in step 5).
- b) Start the light stimulation program (described in step 3) once the first measurement on the plate reader has been taken.
- c) If the automation workstation isn't located in a dark room, cover it in a blackout curtain to prevent background illumination.
- 8. **Analyze the data.** Use Python or another programming language to process the data exported by the microplate reader during the experiment.
 - a) Prepare a spreadsheet map for the experiment. This map should correspond to the 8x12 layout of the 96-well plate and include the names of the strains being measured in one grid and descriptions of the light conditions used in another grid.
 - b) Use a Python script (or other preferred coding language) to analyze the data. Read the map spreadsheet into an array with the strain names and condition names for each well of the plate. Find sample code here: https://github.com/mccleanlab/Lustro. Alternatively, use an app that can parse data from a variety of plate readers.

- c) Read the data from the experiment spreadsheet export into another array.
- d) Plot the optical density values and fluorescence values of each strain and condition versus time (as shown in Figure 4).
- e) Use the optical density plots to determine when cultures are in the exponential growth phase or reach saturation and can thus be used to select appropriate timepoints for comparing fluorescence measurements between strains or conditions (see Figure 5).

REPRESENTATIVE RESULTS:

Figure 4A shows the fluorescence values recorded over time from an optogenetic strain (with the expression of a fluorescent reporter driven by a light-inducible split transcription factor) induced by different light conditions. The duty cycle (percentage of the time the light is on) of the light stimulation is proportional to the overall level of fluorescence measured. Figure 4B shows the corresponding OD₇₀₀ values for the same experiment. The consistency of the optical density readings between different light conditions indicates that the experimental technique does not result in significant differences in growth rate between different light conditions. Measuring fluorescence and optical density over time can lend more insight into how optogenetic systems respond to different light stimulation programs compared to techniques that only record the output at a single time point. This time-course data can also be used to inform which time point measurements should be used for comparing different strains and conditions. Figure 5 shows a single time point (measured at 10 hours into light induction) comparing two different optogenetic strains induced by different light stimulation programs. These strains use a light-inducible split transcription factor to drive expression of a fluorescent reporter. Varying light pulse intensity, period, and duty cycle elicit different responses in the strains.

FIGURE AND TABLE LEGENDS:

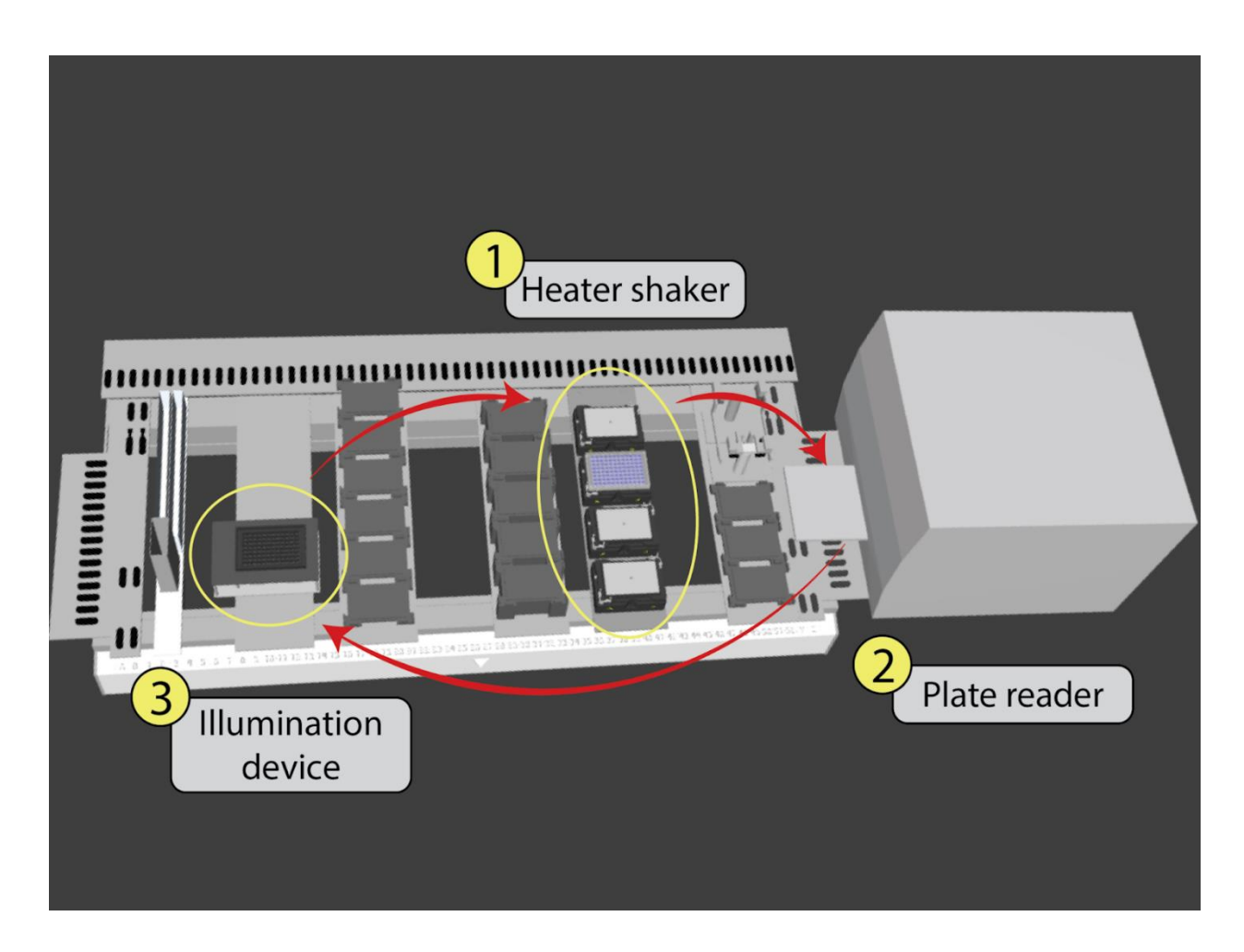


Figure 1. Worktable layout and experimental workflow. Screenshot of a sample worktable layout, denoting the movement of the sample plate in Lustro. The plate is moved by the robotic arm from a heater shaker (1) to the microplate reader (2), and then to the illumination device (3). Photographs are included in Supplementary Figure 1.

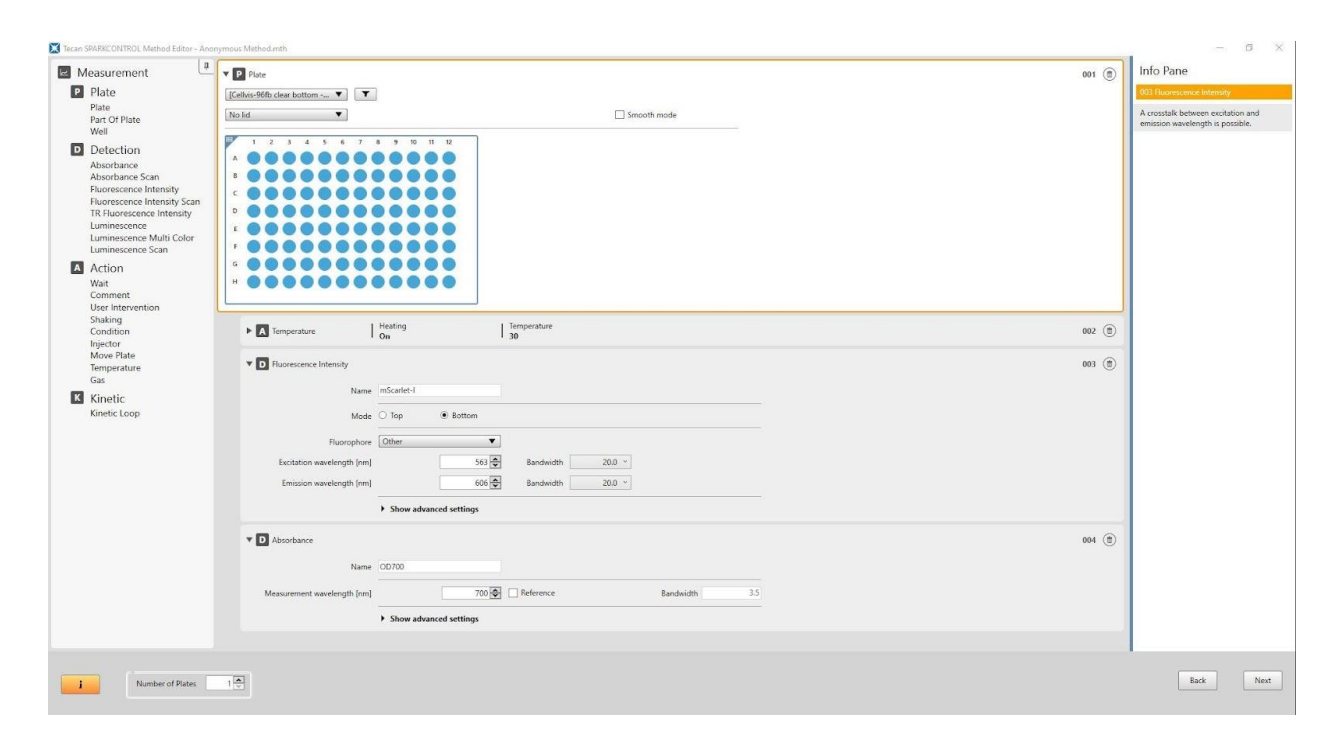


Figure 2. Plate reader measurement script. Sample screenshot of a plate reader script setting the microplate reader to incubate at 30 $^{\circ}$ C and record fluorescence and optical density measurements.

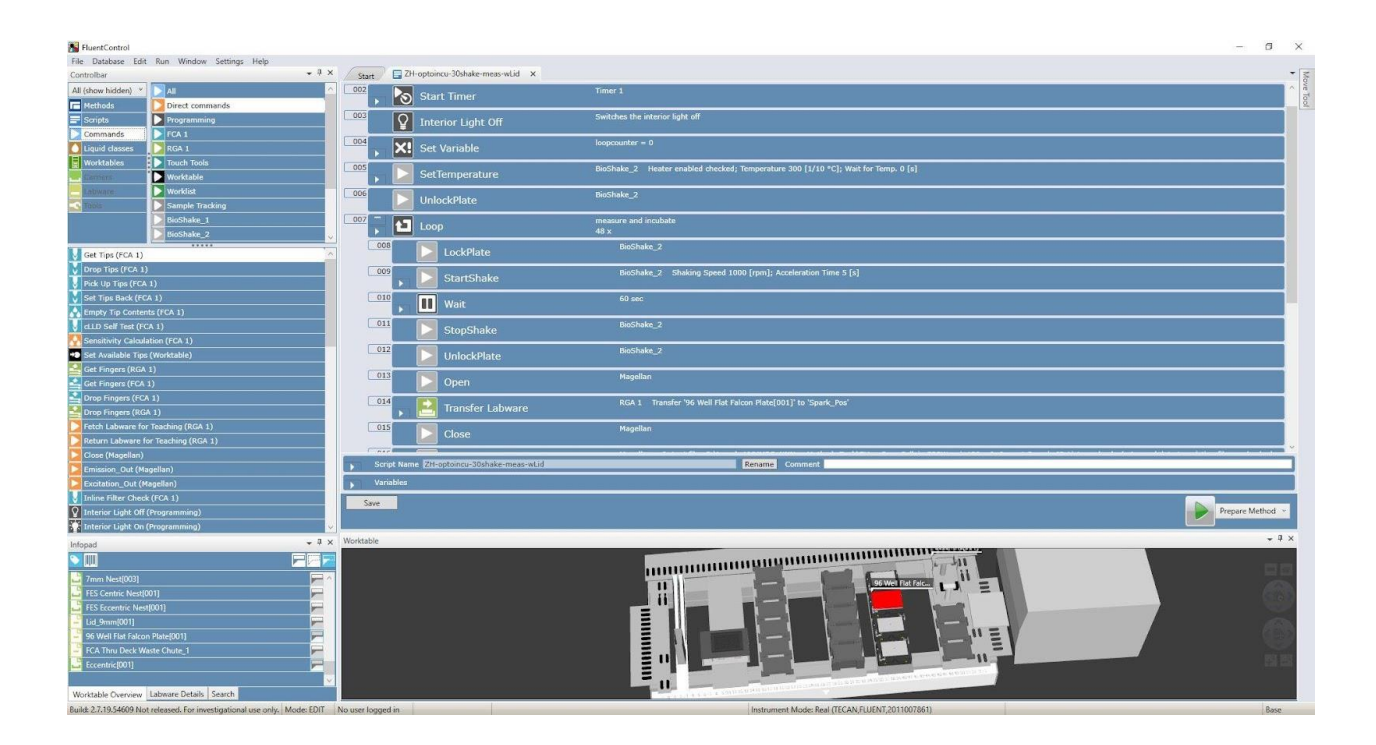


Figure 3. Automated workstation script. Sample screenshot of an automated workstation script for Lustro. The script starts a timer, ensures the interior light is turned off, sets a loop counting variable to an initial value of 0, and sets the heater shaker to incubate at 30 °C. Within each loop, the plate is locked, shaken for 1 minute, moved to the plate reader and measured, then moved to the illumination device and the robot is set to wait for the remainder of the 30-minute loop interval. At the end of this time, the loop counter variable is increased by one and the loop is repeated.

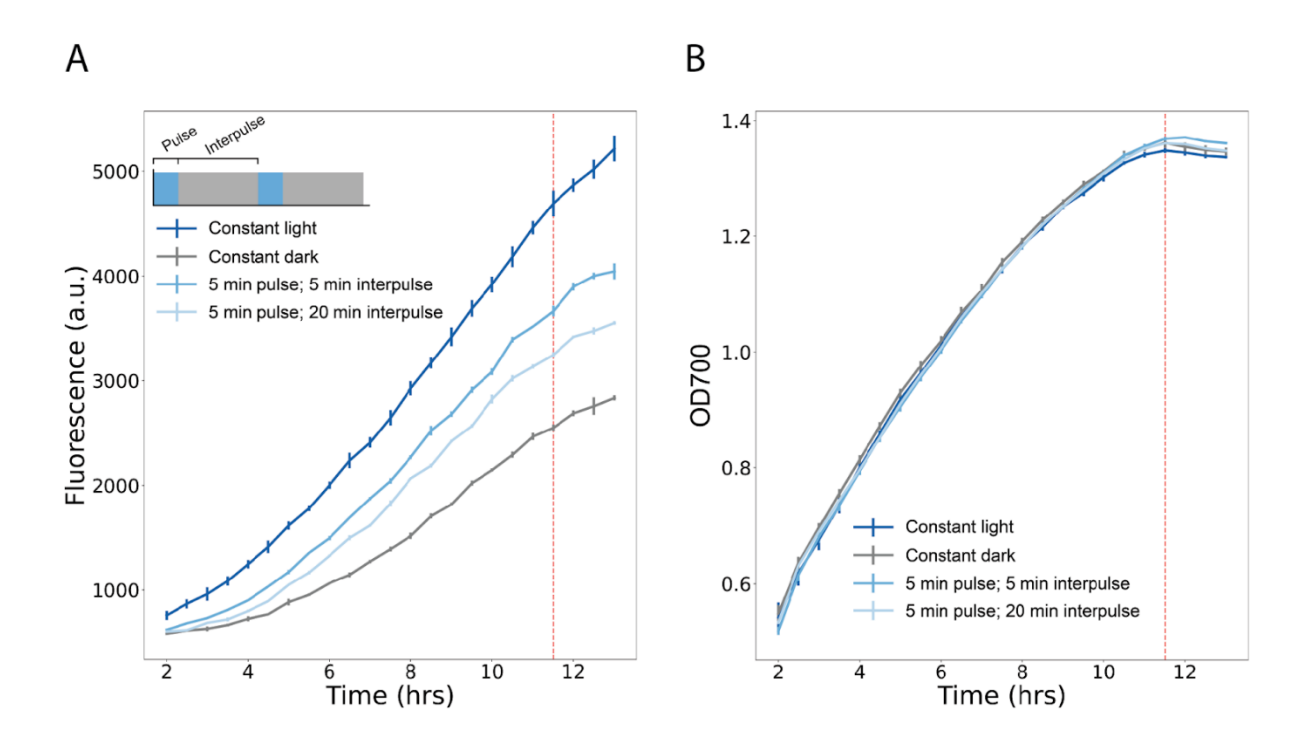


Figure 4. Induction time course. Sample light induction time course data from a Gal4BD-eMagA/eMagB-Gal4AD split transcription factor strain with a pGAL1-mScarlet-I reporter (yMM1734ε). Fluorescence of mScarlet-I₂ is measured at 563 nm excitation and 606 nm emission with an optical gain of 130. Light intensity is 125 μW/cm² and error bars represent standard error of triplicate samples. Vertical red dotted line shows when cultures reach saturation. (A) Fluorescence values from the strain over time. Light patterns (as indicated) were repeated for the full duration of the experiment shown. Inset shows that light pulse times are interspersed with dark interpulse times, repeated over the course of the experiment. (B) Optical density (measured at 700 nm) values for the experiment shown in (A).

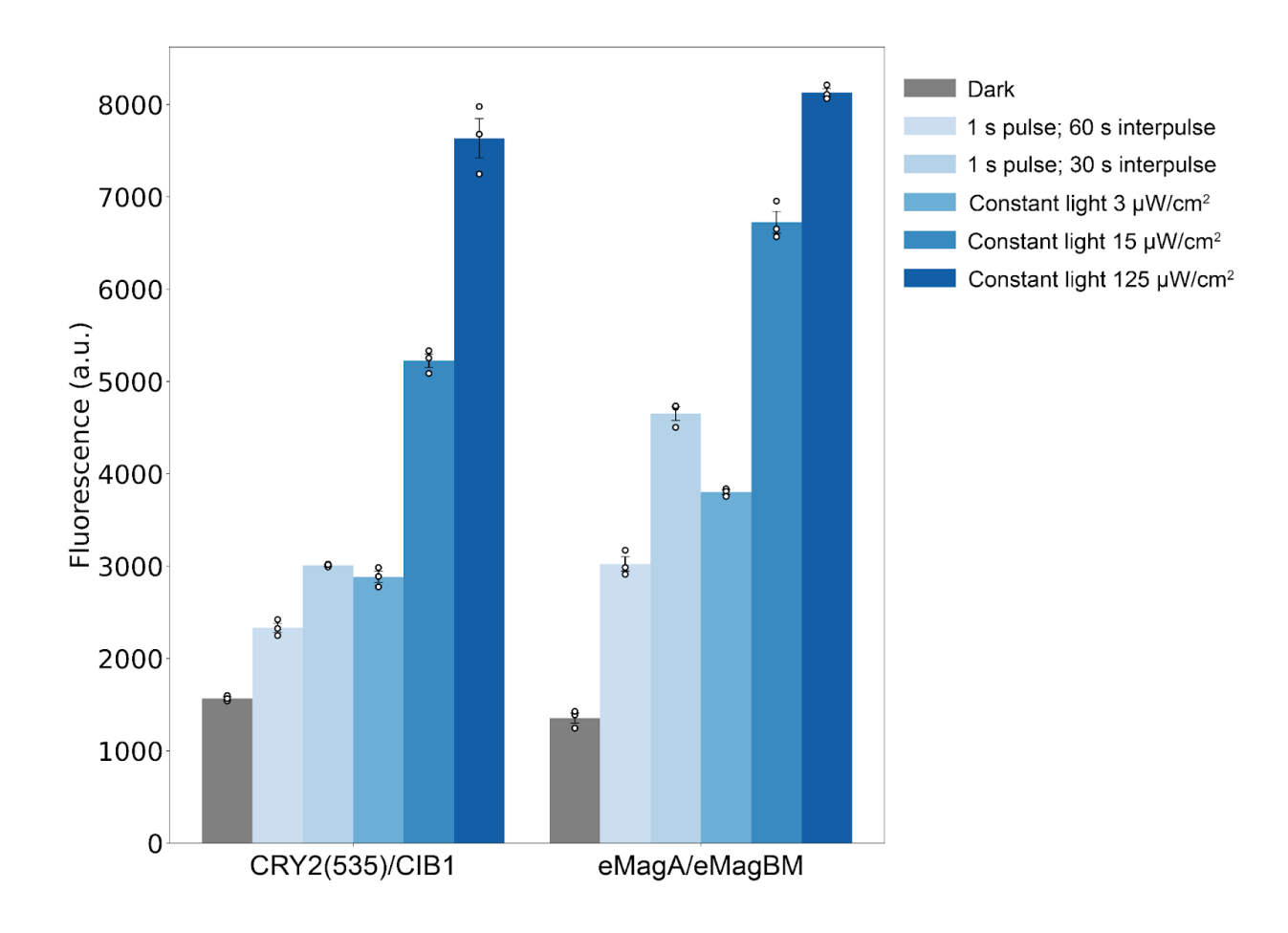
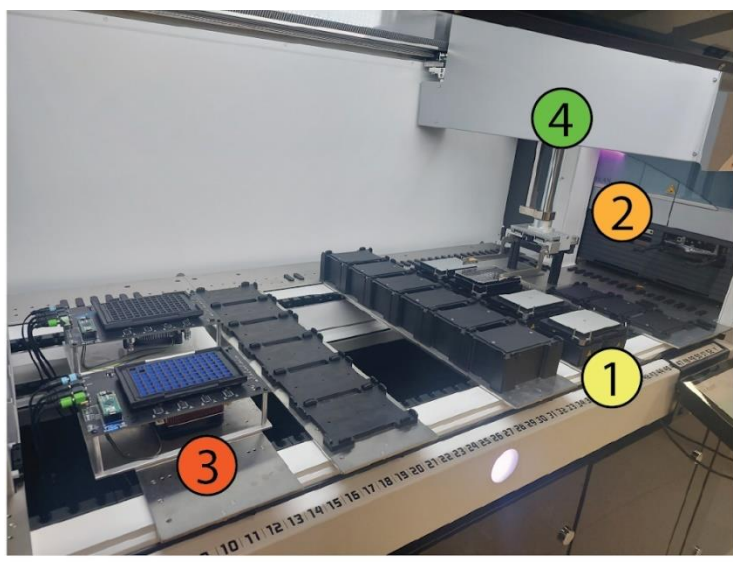
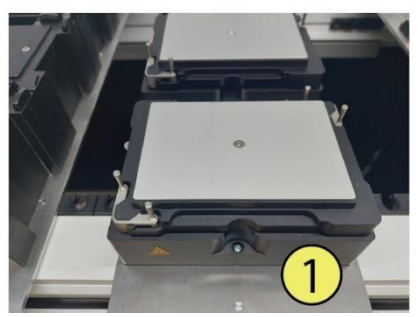


Figure 5. Comparison of different optogenetic systems. Comparison of different light induction programs between CRY2(535)/CIB1 and eMagA/eMagBM split transcription factor strains with pGAL1-mScarlet-I reporters (yMM1763 and yMM1765 $^{\rm s}$, respectively). Fluorescence of mScarlet-I $^{\rm z}$ is measured at 563 nm excitation and 606 nm emission with an optical gain of 130. Light intensity used is 125 μ W/cm $^{\rm z}$, except where otherwise noted. Error bars represent standard error of triplicate samples (indicated as dots). Fluorescence values shown were recorded 10 hours into induction.



- 1 Heater shaker
- 2 Plate reader
- 3 Illumination device
- 4 Robotic arm







Supplementary Figure 1. Representative images of the devices used in Lustro. Picture of the Lustro setup and zoomed-in images of the devices used. The robotic arm moves the sample plate from the heater shaker to the plate reader, and then to the illumination device in a cycle over the course of the experiment. Components are numbered with a legend on the side.

| Material | Source | Catalog # |
|--|--------------|----------------|
| 96-well glass bottom plate with #1.5 cover glass | Cellvis | P96- 1.5H-N |
| BioShake 3000-T elm (heater shaker) | QINSTRUMENTS | |
| Fluent Automation Workstation | Tecan | |

| LITOS (alternative illumination device) | Hohener, et al. Scientific Reports. 2022 | |
|---|--|-------|
| optoPlate-96 (illumination device) | Bugaj, et al. Nature Protocols. 2019 | |
| Spark (plate reader) | Tecan | |
| Synthetic Complete media | SigmaAldrich | Y1250 |
| Tecan Connect (user alert app) | Tecan | |
| yMM1734 (BY4741 Matα ura3Δ0::5' Ura3 homology, pRPL18B-Gal4DBD-eMagA-tENO1, pRPL18B-eMagB- Gal4AD-tENO1, pGAL1-mScarlet-I-tENO1, Ura3, Ura 3' homology his3D1 leu2D0 lys2D0 gal80::KANMX gal4::spHIS5) | Harmer, et al. ACS Syn Bio. 2023 | |
| yMM1763 (BY4741 Matα ura3Δ0::5' Ura3 homology, pRPL18B-Gal4DBD-CRY2(535)-tENO1, pRPL18B-Gal4AD- CIB1-tENO1, pGAL1-mScarlet-I-tENO1, Ura3, Ura 3' homology his3D1 leu2D0 lys2D0 gal80::KANMX gal4::spHIS5) | Harmer, et al. ACS Syn Bio. 2023 | |
| yMM1765 (BY4741 Matα ura3Δ0::5' Ura3 homology, pRPL18B-Gal4DBD-eMagA-tENO1, pRPL18B-eMagBM-Gal4AD-tENO1, pGAL1-mScarlet-I-tENO1, Ura3, Ura 3' homology his3D1 leu2D0 lys2D0 gal80::KANMX gal4::spHIS5) | Harmer, et al. ACS Syn Bio. 2023 | |
| YPD Agar | SigmaAldrich | Y1500 |

Table of Materials.

DISCUSSION:

The Lustro protocol provided here automates culturing, illumination, and measurement to allow for high-throughput screening and characterization of optogenetic systems. This is accomplished by integrating an illumination device, microplate reader, and shaking device in an

automation workstation. In this protocol we specifically demonstrate the utility of Lustro for screening different optogenetic constructs integrated into the yeast *S. cerevisiae* and comparing light induction programs.

This protocol emphasizes several crucial steps that are integral to the effective utilization of Lustro. It is essential to carefully design customized light programs that align with the specific kinetics of the optogenetic construct under investigation. Additionally, precise calibration of the plate reader to achieve the desired output is necessary to obtain reliable measurements. Thorough dry runs of the experiments on the robot, including adjusting the timings as necessary to ensure proper synchronization with the light programs, are critical to ensure the script runs properly.

The sample protocol detailed here describes comparing a light-inducible split transcription factor driving expression of a fluorescent reporter to a nonfluorescent control over a range of light stimulation conditions. We measure fluorescence from each well in the plate at 30-minute intervals with one minute on the heater shaker prior to measurement. As described and implemented in this protocol, Lustro is suitable for use directly with blue light-responsive optogenetic systems integrated into many non-adherent cell types, including bacteria and other yeasts. However, the protocol is easily extended to different cell types, optogenetic systems, and experimental designs with small modifications. Minor changes to the plate reader settings would allow measurement of outputs other than fluorescence, such as bioluminescence. Measurements could be taken more frequently where finer temporal resolution is needed. Incubation on the heater shaker could be repeated more frequently as needed for specific cell types where shaking and temperature control are critical. Gas and environmental control, for example through an incubated hotel, would allow incorporation of mammalian cell lines. The iteration of Lustro described here uses specific instrumentation; however, the Lustro platform can be easily adapted

to work with other laboratory automation robots or microplate readers. Illumination devices, such as the LPA26 or LITOS2, could be substituted for the optoPlate to stimulate different optogenetic systems. A particularly exciting future modification of the Lustro platform would be to incorporate liquid handling to facilitate automated dilutions for continuous culture applications. This would also allow Lustro to be adapted for cybergenetic feedback control, where real-time measurements inform changes in light or culture conditions to reach or maintain a desired responses.21.22.

High-throughput techniques are important for optimizing and taking advantage of the dynamic nature of optogenetic systems. Lustro overcomes many of the limitations of existing protocols. For example, while bioreactor-based optogenetics techniques allow for constant readout and culturing conditions, they are limited by low throughput22-26. The optoPlateReader22 device shows great promise for performing real-time optogenetics experiments in microwell plates, but currently suffers from low throughput due to the high number of replicates needed to obtain reliable results and doesn't provide access to continuous culturing. Lustro is able to perform high-throughput screening of optogenetic systems to characterize their dynamic activity. Nevertheless, some limitations of the Lustro protocol remain. Intermittent shaking in Lustro does cause a small lag in growth for yeast cells, but that could be remedied by adapting an illumination device to shake. An additional limitation of the Lustro system is that the sample plate is not incubated while on the illumination device and is maintained at ambient temperature (22 °C). While the small volume of each sample allows for high-throughput screens to be performed, it is possible that additional optimization of the illumination steps would need to be undertaken when scaling to larger reaction volumes for bioproduction or other applications^{28, 29}.

Overall, Lustro enables the rapid development and testing of optogenetic systems through high-throughput screening and precise light control. This automated approach allows for efficient characterization and comparison of different optogenetic constructs under various induction conditions, leading to faster iteration and refinement of these systems. With its adaptability to different cell types, optogenetic tools, and automation setups, Lustro paves the way for advancements in the field of optogenetics, facilitating the exploration of dynamic gene expression control and expanding possibilities for studying biological networks and engineering cellular behavior.

ACKNOWLEDGMENTS:

This work was supported by National Institutes of Health grant R35GM128873 and National Science Foundation grant 2045493 (awarded to M.N.M.). Megan Nicole McClean, PhD holds a Career Award at the Scientific Interface from the Burroughs Wellcome Fund. Z.P.H. was supported by an NHGRI training grant to the Genomic Sciences Training Program 5T32HG002760. We acknowledge fruitful discussions with McClean lab members and in particular we are grateful to Kieran Sweeney for providing comments on the manuscript.

DISCLOSURES:

The authors have nothing to disclose.

REFERENCES:

1. Pérez, A.L.A. *et al.* Optogenetic strategies for the control of gene expression in yeasts. *Biotechnology Advances*. **54**, 107839, doi: 10.1016/j.biotechadv.2021.107839 (2022).

- 2. Lan, T.-H., He, L., Huang, Y., Zhou, Y. Optogenetics for transcriptional programming and genetic engineering. *Trends in Genetics*. **38** (12), 1253–1270, doi: 10.1016/j.tig.2022.05.014 (2022).
- 3. Olson, E.J., Tabor, J.J. Optogenetic characterization methods overcome key challenges in synthetic and systems biology. *Nature Chemical Biology*. **10** (7), 502–511, doi: 10.1038/nchembio.1559 (2014).
- 4. Hallett, R.A., Zimmerman, S.P., Yumerefendi, H., Bear, J.E., Kuhlman, B. Correlating in vitro and in vivo Activities of Light Inducible Dimers: a Cellular Optogenetics Guide. *ACS synthetic biology*. **5** (1), 53–64, doi: 10.1021/acssynbio.5b00119 (2016).
- 5. Scott, T.D., Sweeney, K., McClean, M.N. Biological signal generators: integrating synthetic biology tools and in silico control. *Current Opinion in Systems Biology*. **14**, 58–65, doi: 10.1016/j.coisb.2019.02.007 (2019).
- Harmer, Z.P., McClean, M.N. Lustro: High-Throughput Optogenetic Experiments Enabled by Automation and a Yeast Optogenetic Toolkit. ACS Synthetic Biology. doi: 10.1021/acssynbio.3c00215 (2023).
- 7. Bindels, D.S. *et al.* mScarlet: a bright monomeric red fluorescent protein for cellular imaging. *Nature Methods*. **14** (1), 53–56, doi: 10.1038/nmeth.4074 (2017).
- 8. Bugaj, L.J., Lim, W.A. High-throughput multicolor optogenetics in microwell plates. *Nature Protocols*. **14** (7), 2205–2228, doi: 10.1038/s41596-019-0178-y (2019).
- 9. Höhener, T.C., Landolt, A.E., Dessauges, C., Hinderling, L., Gagliardi, P.A., Pertz, O. LITOS: a versatile LED illumination tool for optogenetic stimulation. *Scientific Reports*. **12** (1), 13139, doi: 10.1038/s41598-022-17312-x (2022).
- 10. Grødem, E.O., Sweeney, K., McClean, M.N. Automated calibration of optoPlate LEDs to reduce light dose variation in optogenetic experiments. *BioTechniques*. **69** (4), 313–316, doi: 10.2144/btn-2020-0077 (2020).
- 11. Dunlop, M.J. A Supplemental Guide to Building the optoPlate-96. at https://www.protocols.io/view/a-supplemental-guide-to-building-the-optoplate-96-b2vwqe7e (2021).
- 12. Thomas, O.S., Hörner, M., Weber, W. A graphical user interface to design high-throughput optogenetic experiments with the optoPlate-96. *Nature Protocols*. **15** (9), 2785–2787, doi: 10.1038/s41596-020-0349-x (2020).

- 13. Robertson, J.B., Davis, C.R., Johnson, C.H. Visible light alters yeast metabolic rhythms by inhibiting respiration. *Proceedings of the National Academy of Sciences of the United States of America*. **110** (52), 21130–21135, doi: 10.1073/pnas.1313369110 (2013).
- 14. Synthetic Complete (SC) Medium. *Cold Spring Harbor Protocols*. **2016** (11), pdb.rec090589, doi: 10.1101/pdb.rec090589 (2016).
- 15. Lambert, T.J. FPbase: a community-editable fluorescent protein database. *Nature Methods*. **16** (4), 277–278, doi: 10.1038/s41592-019-0352-8 (2019).
- 16. Hecht, A., Endy, D., Salit, M., Munson, M.S. When Wavelengths Collide: Bias in Cell Abundance Measurements Due to Expressed Fluorescent Proteins. *ACS Synthetic Biology*. **5** (9), 1024–1027, doi: 10.1021/acssynbio.6b00072 (2016).
- 17. YPD media. *Cold Spring Harbor Protocols*. **2010** (9), pdb.rec12315, doi: 10.1101/pdb.rec12315 (2010).
- 18. Low-Fluorescence Yeast Nitrogen Base without Riboflavin and Folic Acid Medium (LFM) (10×). *Cold Spring Harbor Protocols.* **2016** (11), pdb.rec090662, doi: 10.1101/pdb.rec090662 (2016).
- 19. Csibra, E., Stan, G.-B. *Parsley: a web app for parsing data from plate readers*. doi: 10.5281/zenodo.8072500. Zenodo. (2023).
- 20. Gerhardt, K.P. *et al.* An open-hardware platform for optogenetics and photobiology. *Scientific Reports*. **6** (1), 35363, doi: 10.1038/srep35363 (2016).
- 21. Gutiérrez Mena, J., Kumar, S., Khammash, M. Dynamic cybergenetic control of bacterial co-culture composition via optogenetic feedback. *Nature Communications*. **13**, 4808, doi: 10.1038/s41467-022-32392-z (2022).
- 22. Milias-Argeitis, A. *et al.* In silico feedback for in vivo regulation of a gene expression circuit. *Nature Biotechnology.* **29** (12), 1114–1116, doi: 10.1038/nbt.2018 (2011).
- 23. Milias-Argeitis, A., Rullan, M., Aoki, S.K., Buchmann, P., Khammash, M. Automated optogenetic feedback control for precise and robust regulation of gene expression and cell growth. *Nature Communications*. **7**, 12546, doi: 10.1038/ncomms12546 (2016).
- 24. Bertaux, F. *et al.* Enhancing bioreactor arrays for automated measurements and reactive control with ReacSight. *Nature Communications.* **13** (1), 3363, doi: 10.1038/s41467-022-31033-9 (2022).

- 25. Benisch, M., Benzinger, D., Kumar, S., Hu, H., Khammash, M. Optogenetic closed-loop feedback control of the unfolded protein response optimizes protein production. *Metabolic Engineering*. doi: 10.1016/j.ymben.2023.03.001 (2023).
- 26. Melendez, J., Patel, M., Oakes, B.L., Xu, P., Morton, P., McClean, M.N. Real-time optogenetic control of intracellular protein concentration in microbial cell cultures. *Integrative Biology*. **6** (3), 366–372, doi: 10.1039/c3ib40102b (2014).
- 27. Datta, S. *et al.* High-throughput feedback-enabled optogenetic stimulation and spectroscopy in microwell plates. 2022.07.13.499906, doi: 10.1101/2022.07.13.499906 (2022).
- 28. Pouzet, S. *et al.* Optogenetic control of beta-carotene bioproduction in yeast across multiple labscales. *Frontiers in Bioengineering and Biotechnology*. **11**, 1085268, doi: 10.3389/fbioe.2023.1085268 (2023).
- 29. Pouzet, S., Banderas, A., Le Bec, M., Lautier, T., Truan, G., Hersen, P. The Promise of Optogenetics for Bioproduction: Dynamic Control Strategies and Scale-Up Instruments. *Bioengineering*. **7** (4), 151, doi: 10.3390/bioengineering7040151 (2020).

APPENDIX B: ENHANCING HIGH-THROUGHPUT OPTOGENETICS: INTEGRATION OF LITOS WITH LUSTRO ENABLES SIMULTANEOUS LIGHT STIMULATION AND SHAKING

Zachary P Harmer^{1,2}, Thomas Höhener^{2,2}, Alex Landolt^{2,2}, Claire Mitchell¹, and Megan N

McClean^{1,3,4}

- Department of Biomedical Engineering, University of Wisconsin-Madison, Madison, Wisconsin 53706, United States
 - ² Institut für Zellbiologie, Universität Bern, Bern, Switzerland
- ³ University of Wisconsin Carbone Cancer Center, University of Wisconsin School of Medicine and Public Health, Madison, Wisconsin 53706, United States

These authors contributed equally to this work

[†]Email: mmcclean@wisc.edu

Submitted to *Micropublication*

Abstract:

Optogenetics is a powerful tool that uses light to control cellular behavior. Here we enhance high-throughput characterization of optogenetic experiments through the integration of the LED Illumination Tool for Optogenetic Stimulation (LITOS) with the previously published automated platform Lustro. Lustro enables efficient high-throughput screening and characterization of optogenetic systems. The initial iteration of Lustro used the optoPlate illumination device for light induction, with the robot periodically moving the plate over to a shaking device to resuspend cell cultures. Here, we designed a 3D-printed adaptor, rendering LITOS compatible with the BioShake 3000-T ELM used in Lustro. This novel setup allows for

concurrent light stimulation and culture agitation, streamlining experiments. Our study demonstrates comparable growth rates between constant and intermittent shaking of *Saccharomyces cerevisiae* liquid cultures. While the light intensity of the LITOS is not as bright as the optoPlate used in the previous iteration of Lustro, the constant shaking increased the maturation rate of the mScarlet-I fluorescent reporter used. Only a marginal increase in temperature was observed when using the modified LITOS equipped with the 3D-printed adaptor. Our findings show that the integration of LITOS onto a plate shaker allows for constant culture shaking and illumination compatible with laboratory automation platforms, such as Lustro..

Introduction:

Optogenetics has transformed the field of cellular biology by using light-sensitive proteins to precisely control cellular processes. The light-induced conformational change of the optogenetic protein can alter the protein's binding activity or localization, which can be used to control gene expression, signaling pathways, and other biological behavior. In our previous work, we integrated optogenetics in an automation platform to make the Lustro platform (Harmer & McClean, 2023b, 2023a). Performing optogenetic experiments with automation platforms like Lustro has the potential to significantly accelerate experimental workflows, providing researchers with a powerful tool for dynamic gene expression control.

Lustro comprises an illumination device, a shaking device, and a plate reader, all integrated with a Tecan Fluent Automation Workstation. The platform's robotic gripper arm facilitates the transfer of microwell plates between these components, following a programmed schedule. Lustro uses the optoPlate, designed by Bugaj and colleagues (Bugaj & Lim, 2019) for

powerful illumination of cell cultures in microwell plates. Cell cultures are placed in the microplate, and after a period of light induction through individually programmable LEDs (using the optoPlate), the plate is moved to the shaking device to resuspend the cultures. However, due to the size and weight of the optoPlate, the shaking step must be performed separately because it exceeds the maximum capacity of the BioShakes. The plate is then moved to the plate reader to measure optical density and fluorescence, enabling frequent and reliable data collection. This automated process greatly expedites the prototyping and testing of optogenetic systems.

In this work, we substituted the optoPlate LED device with LITOS, an illumination system featuring an individually programmable LED matrix, rendering it compatible with multiple microplate formats (Höhener et al., 2022). Thanks to its low cost, and ease-of-use, LITOS is a versatile tool for various optogenetics applications. Its lightweight and compact design permits seamless adaptation to cell culture shaking devices, facilitating concurrent illumination and agitation, thereby simplifying and optimizing the experimental process.

Adapting the LITOS to securely fit on the shaking device with a 3D-printed bottom adapter and top mask allows for simultaneous light stimulation and shaking. This reduces the amount of time the sample plate needs to be in the dark to take measurements, and allows light programs to be more continuously applied throughout an experiment (albeit at a lower light intensity). The constant shaking also improves fluorescent protein maturation rates, likely due to increased oxygenation rates (Hebisch et al., 2013).

Results:

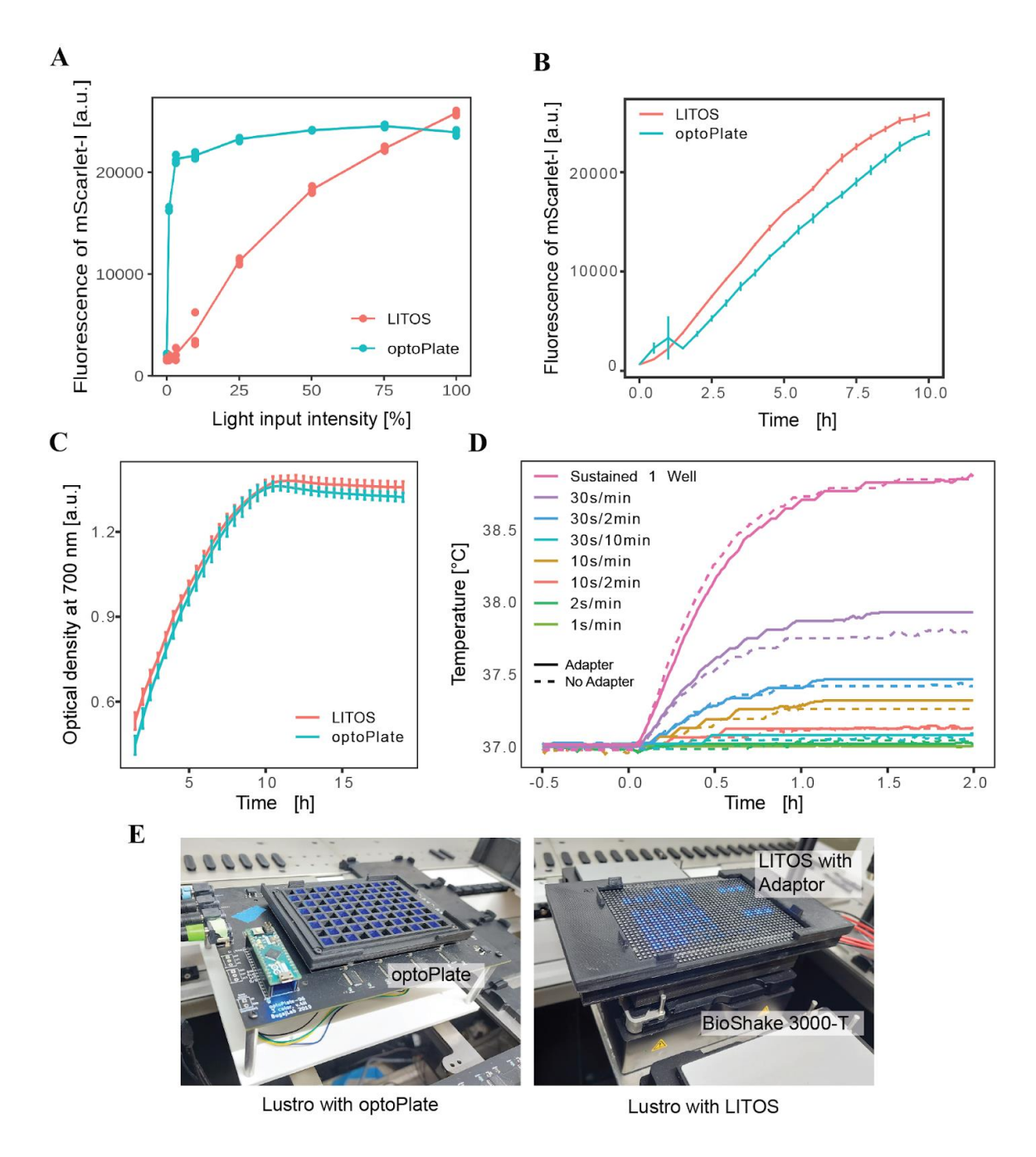


Figure 1: A) A strain with a CRY2PHR/CIB1 optogenetic split transcription factor driving expression of mScarlet-I (yMM1731) is induced on the optoPlate (with intermittent shaking) or on the LITOS (with constant shaking) under a range of programmed light intensities (in 200 μL volumes). 100% intensity corresponds to 1500 $\mu W/cm2$ on the optoPlate and 20 $\mu W/cm2$ on the LITOS. Fluorescence shown was measured at 10 hours into induction. B) Fluorescence over time for the maximum light intensity conditions of the strain on the LITOS (constant shaking) and optoPlate (intermittent shaking). C) Optical densities of a strain grown with intermittent shaking on the optoPlate or constant shaking on the LITOS mounted on the BioShake 3000-T ELM. D) Temperature of the LITOS with the adapter (solid lines) and without the adapter (dotted lines) for different light pulsing

conditions over two hours. E) Photos of the Lustro setup using either the optoPlate or LITOS (mounted on the BioShake shaker).

We induced a strain with an optogenetic split transcription factor driving expression of a fluorescent protein (mScarlet-I). The optogenetic split transcription factor incorporates an optical dimerizer pair fused to a DNA-binding domain and an activation domain. The optical dimerizers bind each other upon blue light induction, reconstituting the split transcription factor and resulting in expression of the gene of interest. Induction was performed using either the optoPlate (with intermittent shaking) or the LITOS (adapted for use on the BioShake with constant shaking) with constant blue light illumination and different set intensities. The induction of the mScarlet-I reporter was measured every 30 minutes for 18 hours. A CRY2PHR/CIB1 split transcription factor strain (yMM1731) was selected, as it's known to be sensitive to low light intensities(Figure 1A)(Harmer & McClean, 2023b). While the LITOS exhibited lower brightness compared to the optoPlate, it remained effective for inducing CRY2PHR/CIB1 and is compatible with the plate shaker. The sample induced on the LITOS (with constant shaking) increased in fluorescence more quickly than the sample on the optoPlate (with intermittent shaking), likely due to faster fluorescent protein maturation time with higher oxygen availability (Figure 1B)(Hebisch et al., 2013).

We then wanted to check whether the growth rate differs between illumination and shaking conditions. Therefore, we compared the growth rate of yeast cells grown with intermittent shaking (1 minute of shaking every 30 minutes) (Harmer & McClean, 2023b) to that of yeast cells shaken constantly on the LITOS with the BioShake, by measuring the optical density (OD) at 700 nm (to avoid bias from the red fluorescent reporter). Growth rates under constant and intermittent shaking were comparable, with slightly faster growth under constant agitation (Figure 1C).

Since we added 3D-printed adapters to the LITOS, we examined whether this would change the thermal equilibrium of the setup while it is running. Therefore, the temperature of samples on the device was measured over time, both with and without the mask. Temperatures in the modified LITOS with 3D-printed adapters were consistent with the original system, showing only marginal increases (Figure 1D).

Discussion:

The integration of LITOS with Lustro represents an important advancement in optogenetic research for cell types grown in suspension. This combined platform allows for concurrent light stimulation and culture agitation, streamlining experiments and providing valuable insights into cellular responses. Our findings suggest that both constant and intermittent shaking patterns are suitable for optogenetic studies. While LITOS may not match the brightness of the optoPlate, it remains effective for a range of optogenetic applications, particularly where performing optogenetic stimulation with shaking is desired in a laboratory automation context. The consistent temperature profiles in the modified LITOS with adapters demonstrate the robustness of this integrated system. Additionally, the versatile nature of this platform allows for further customization and integration with other experimental setups, opening doors to novel research avenues in dynamic gene expression control.

Methods:

Integration of LITOS with Lustro:

To attach LITOS to the BioShake 3000-T ELM shaker used in Lustro, 3D-printed adapters were designed (.stl files are in the Extended Data section or available on the LITOS GitHub page). The adapter consists of a top and a bottom part enclosing the LED matrix. This allowed it to be shaken vigorously enough to suspend yeast cells in liquid media (1000 rpm with 2 mm orbital), and to interface with the robotic gripper arm of the Fluent Automation Workstation. The shaking device clamps onto the base of the LITOS adapter to hold it in place. Fluorescence of mScarlet-I in the yeast cultures was read with a Tecan Spark plate reader. Light intensity was measured 1 cm above the bottom of the plate using a Thorlabs S120VC photodiode.

Comparative Growth Analysis:

Cultures were grown under constant and intermittent shaking conditions. Shaking was performed at 1000 rpm with 2 mm orbital on a BioShake 3000-T ELM. Intermittent shaking was performed for 1 minute, repeated every 30 minutes. Optical densities (ODs) were measured at 700 nm (to avoid bias from the red mScarlet-I fluorescent protein) on a Tecan Spark plate reader to assess growth rates and the impact of agitation patterns. Strains used in this work were previously published (Harmer & McClean, 2023b).

Temperature Measurements:

The effect of the 3D adapters on the heating of the medium in a well plate was determined by using an Arduino device equipped with multiple digital DS18B20 waterproof temperature sensors (as detailed in Höhener et al., 2022). The LITOS systems with and without the attached adapters were measured in parallel.

Materials Availability

3D-printing files for the LITOS adapters can be found on GitHub: https://github.com/pertzlab/LITOS

Acknowledgments

This work was supported by National Institutes of Health grant R35GM128873 and National Science Foundation grant 2045493 (awarded to M.N.M.). Megan Nicole McClean, PhD, holds a Career Award at the Scientific Interface from the Burroughs Wellcome Fund.

Z.P.H. was supported by an NHGRI training grant to the Genomic Sciences Training Program 5T32HG002760.

Author Contributions

Z.P.H. and M.N.M conceived of the study. Z.P.H. designed optogenetic parts and performed optogenetic experiments. A.E.L. and T.C.H. performed temperature testing. C.M. explored parameters for shaking an illumination device. C.M., T.C.H., A.E.L., and Z.P.H. designed .stl files. M.N.M. provided funding. Z.P.H., T.C.H., and A.E.L. wrote the original draft of the manuscript, and Z.P.H., T.C.H., A.E.L., and M.N.M wrote, reviewed, and edited the final manuscript.

Conflict of Interest

The authors declare no competing interests.

References:

Bugaj, L. J., & Lim, W. A. (2019). High-throughput multicolor optogenetics in microwell plates.

Nature Protocols, 14(7), 2205–2228. https://doi.org/10.1038/s41596-019-0178-y

Harmer, Z. P., & McClean, M. N. (2023a). High-Throughput Optogenetics Experiments in Yeast Using the Automated Platform Lustro. *JoVE (Journal of Visualized Experiments)*, 198, e65686. https://doi.org/10.3791/65686

Harmer, Z. P., & McClean, M. N. (2023b). Lustro: High-Throughput Optogenetic Experiments Enabled by Automation and a Yeast Optogenetic Toolkit. *ACS Synthetic Biology*. https://doi.org/10.1021/acssynbio.3c00215

Hebisch, E., Knebel, J., Landsberg, J., Frey, E., & Leisner, M. (2013). High Variation of Fluorescence Protein Maturation Times in Closely Related Escherichia coli Strains. *PLoS ONE*, 8(10). https://doi.org/10.1371/journal.pone.0075991

Höhener, T. C., Landolt, A. E., Dessauges, C., Hinderling, L., Gagliardi, P. A., & Pertz, O. (2022). LITOS: A versatile LED illumination tool for optogenetic stimulation. *Scientific Reports*, *12*(1), 13139. https://doi.org/10.1038/s41598-022-17312-x